CYCLIC BEHAVIOUR AND DYNAMIC PROPERTIES OF SOILS: A CASE OF JIMMA TOWN

TESHOME BIRHANU KEBEDE

MASTER OF SCIENCE

ADDIS ABABA SCIENCE AND TECHNOLOGY UNIVERSITY

JANUARY 2019

CYCLIC BEHAVIOUR AND DYNAMIC PROPERTIES OF SOILS: A CASE OF JIMMA TOWN

By

TESHOME BIRHANU KEBEDE

A Thesis Submitted to the Department of Civil Engineering for the Partial Fulfillment of the Requirements for the Degree of Master of Science in Civil Engineering

(Geotechnical Engineering)

ADDIS ABABA SCIENCE AND TECHNOLOGY UNIVERSITY

JANUARY 2019

Declaration

I hereby declare that this thesis entitled **"CYCLIC BEHAVIOUR AND DYNAMIC PROPERTIES OF SOILS: A CASE OF JIMMA TOWN"** was composed by myself, with the guidance of my advisor, that the work contained herein is my own except where explicitly stated otherwise in the text, and that this work has not been submitted, in whole or in part, for any other degree or professional qualification.

Name: Signature, Date:

Certificate

This is to certify that the thesis prepared by **Mr. Teshome Birhanu Kebede entitled "Cyclic Behaviour and Dynamic Properties Of Soils: A Case of Jimma Town"** and submitted in fulfillment of the requirements for the Degree of Master of Science complies with the regulations of the University and meets the accepted standards with respect to originality and quality.

Singed by Examining Board:

Examiner:	Signature, Date:
Examiner:	Signature, Date:
Thesis Advisor:	Signature, Date:
Thesis Co-Advisor:	Signature, Date:

Abstract

The objective of the research is to investigate the dynamic properties of typical soils found in Jimma town. To meet its objective samples from different parts of the city were collected and laboratory tests were done on the collected samples. From the index property test silty and clayey soils dominate the area, having the liquid limit value ranging from 67% to 84% and plasticity index value of 31% to 46%. The specific gravity value ranges from 2.53 to 2.72. Cyclic simple shear test were conducted at cyclic shear strain of 0.01%, 0.1%, 1%, 2.5% and 5% under axial stress of 100 kPa, 250 kPa and 400 kPa. The value of shear modules found in the laboratory ranges from 0.33 to 7.01 MPa and damping ratio values from 2.03 to 22.98%. The shear modulus values were used to calculate the normalized shear modulus (G/Gmax) value which is used for comparison with previous studies. The results have shown that the obtained (G/Gmax) values have good agreement with curve developed by previous researchers but at lower strains the obtained result was lower. For higher strains the obtained (G/Gmax) values agree with those suggested in literature. This shows that testing conditions, sample preparation and type of soil sample have significant effect on the shear modulus values and damping characteristics, especially at small strain levels.

Key words: - Cyclic simple shear test, Damping ratio, Dynamic properties, Normalized shear modulus, Shear modulus and shear strain.

.

Acknowledgements

I am thankful to God as He has been grateful to me much more than I deserve and to my all teachers from school level to university level. Besides, I would like to thank my Dad, Mom and Sister for being by my side in every challenges and difficulties I faced.

I’m also greatly indebted to the people and institution that made the writing of this project successful. Special thanks go to my supervisor, Dr. Yoseph Birru for his invaluable guidance, continuous assistance and encouragement throughout the writing of this thesis.

Table of Contents

LIST OF TABLES

LIST OF FIGURES

ABBREVIATIONS

a	Parameter related to plastic index
ASTM	American Society for Testing Materials standard
Aloop	Loop area
D	Damping ratio
e	Void ratio
Eq	Equation
G	Dynamic shear modulus
Gmax	Maximum Dynamic shear modulus
Gs	Specific gravity of soil
Ko	Coefficient of lateral earth pressure at rest
LL	Liquid limit
Lvdt	Linear variable differential transducer
Pc	Pre-consolidation pressure
PI	Plastic index
PL	Plastic Limit
OCR	Over consolidation ratio
MH	silty clay
TP	Test pit
W_D	energy dissipated in one cycle of loading
W_S	Maximum strain energy stored during the cycle
v_s	Shear wave velocity
γ	Shear strain
ρ	Density of soil
σ	Normal stress
$\sigma'o$	Effective confining stress
$\sigma'v$	Effective vertical stress
τ	Shear stress

CHAPTER ONE

INTRODUCTION

1.1 Background

Geotechnical investigation which determines the dynamic loading effect is very essential. Among the dynamic loading earthquake is one of the natural hazards that destroys billions of dollars properties and kills countless lives annually.

The town of Jimma is found in southwest part of Ethiopia at 354 km distance from the capital Addis Ababa. Currently there is a dramatic increase of population growth and industrialization with infrastructures like high rise building, residence houses, bridges, airport, Industry Park and dams near and in the city .Additionally, the railway project which will connect south Sudan to the capital will be part of the city. On December 19, 2010 earth quake occurred near Hosanna town 70miles East of Jimma town with a magnitude of 5.2 mb. It caused significant damage on several buildings in Hosanna and the shaking was felt from Mizan town in the south as far as Addis Ababa in the north. It was also strongly felt in Jimma town and over 26 Jimma University students were injured those accommodated in dormitory buildings. There also damages to reinforced concrete frame and slab of dormitory buildings was observed. Even if the city has the above infrastructures and record of seismic hazard, the dynamic properties of soil in the vicinity have not been investigated so far.

In this study presents result of representative samples from the excavated pits collected and tested for the determination of field test, index properties test and cyclic simple shear test. The behavior of soils is described and the implications of the test results with

published data are discussed. The dynamic soil properties can be used as input parameters for the design of foundations for machinery and vibrating equipment, analysis of slope stability of embankments under earthquake loading conditions and also used to model soil behavior under dynamic loading.

1.2 Objective of the study

1.2.1 General objective

The major objective of this research is to determine the dynamic shear modulus and Damping ratio values of typical soils found in Jimma town.

1.2.2 Specific objective

- To determine the index properties and classify the soil.
- To determine bulk density of the soil using core cutter method.
- To determine shear modulus and damping ratio using cyclic simple shear tests.

1.3 Methodology

To meet the above objectives, typical soil samples were collected from four pits excavated up to 3.0 m depth each for the investigation which are representative to characterize the dominant soils in the study area. Cyclic simple shear tests were then performed, to determine the stiffness and damping characteristics of the soil samples.

In addition to meet this goal the following laboratory tests were conducted:

- In-situ density and moisture content
- Particle size analysis
- Specific gravity
- Consolidation tests

1.4 Scope and limitation of the study

The dynamic properties of soil are influenced by soil type and specific location of where the soil sample is collected. The collected samples may not fully represent all the soil profile in Jimma town as it is limited to four pits and the samples were taken from the depth of only three meters despite the fact that seismic related ground response behavior significantly affected by 30 m loose layer. In addition to sampling limitation the tests were conducted using cyclic simple shear testing equipment due to unavailability of more sophisticated facilities.

1.5 Organization of the thesis

The study consists of six Chapters and appendixes. The background information is presented under Chapter one which mainly focus on introduction, objective, and scope and limitation of the thesis. Literature review is mainly presented in second Chapter which includes index property and dynamic properties of soils. Chapter three discusses about study area, geology and formation of soil found in Jimma. The sample collection, sample preparation, overview of cyclic simple shear apparatus, experimental programme and calculations are discussed in chapter four. In fifth chapter discussion of test results and some comparison with previous study is presented. The sixth Chapter is conclusion and recommendation of the thesis.

CHAPTER TWO

LITERATURE REVIEW

2.1 Introduction

The geological conditions, topographic characteristics and climatic conditions play a vital role in the formation of soil in any region. Soil is generally considered as a three-phase system (air, water and solid) causing significant changes in the system characteristics due to interaction of these phases under applied static and/or dynamic load. Static loads remain unchanged over space and time, while dynamic load represents loading conditions which vary both in their direction/position and/or magnitude (Shankar et al., 2013). Several researchers have been involved in exploring the complex behavior of soils under various types of loading conditions.

As Thirugnanasampanther (2012) have demonstrated soils are subjected to cyclic loading during earthquakes and consequently it might lose their shear strength partially or completely .As a result, natural and man-made structures founded on soils will be exposed to stability problems such as unpredicted deformations, settlement or catastrophic collapse due to dynamic loading of earthquakes, operation of machinery, bomb blasting, wind or wave action of water, construction operation, fast moving transportation media and others. Therefore, an assessment of the loading conditions and a better understanding of the dynamic properties of soils will help in the design of seismic resistant earth structures such as foundations, dams, bridges, and retaining structures. Further, evaluation of liquefaction is very vital in sites located within earthquake prone regions or heavily populated areas.

Dynamic properties of soils are used to evaluate the dynamic response of soils at different strain levels in geotechnical engineering. Shear modulus and material damping ratio are the most important dynamic properties of soils (Moayerian, 2012) and determination of these properties is an utmost critical and important aspect of geotechnical engineering problems.

2.2 Dynamic soil properties

The response of soil which is subjected to dynamic loads is governed by dynamic soil properties. To determine these properties the response obtained after different loading case need to be analyzed. A typical soil subjected to cyclic loading exhibits hysteresis response. The hysteresis loop produced from the cyclic loading of a typical soil can be described by the path of the loop itself or by two parameters that describe its general shape. These parameters are the inclination and the breath of the hysteresis loop, shear modulus and damping ratio (Luna and Jadi, 2000). As the strain amplitude of cyclic loading is varied, different size of loops will be developed (Shankar et al., 2013).

2.2.1 Damping ratio

The material damping represents the dissipation of strain energy during cyclic loading (Kramer, 1996) but Moayerian (2012) defined as the ratio between the system damping and the critical damping (no oscillatory movement involved). As the soil element loose stiffness with the amplitude of strain, its ability to dampen dynamic forces to increase. This is due to energy dissipated in the soil by friction, heat or plastic yielding .The damping ratio is proportional to the area inside the hysteretic loop (Abu, 2011). It is readily apparent that each of these properties will depend on the magnitude of the strain for which the hysteresis loop is determined (Figure 2.1) and thus both shear moduli and

damping factors must be determined as functions of the induced strain in a soil specimen or soil deposit (Abraham,2014).

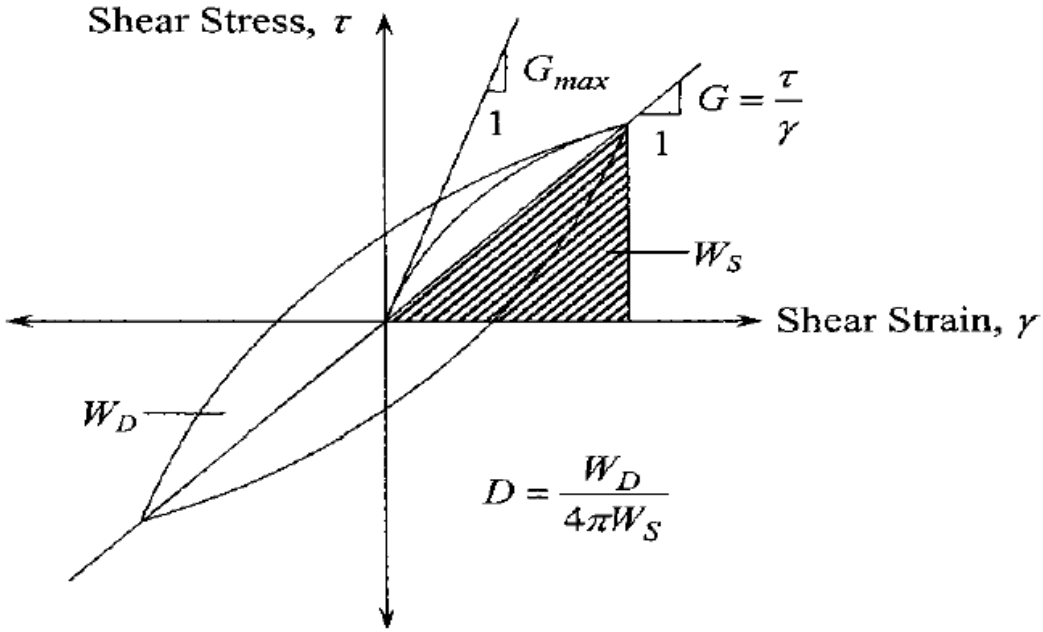

Figure 2. 1: Hysteretic loop for one cycle of loading showing Gmax, G, and D (Seed & Idriss, 1970**)**

Damping ratio can be obtained by:-

$$D = \frac{W_D}{4*\pi*W_S} = \frac{Area\ of\ hystersis\ loop}{2\pi*G*\gamma^2} - - - - - - - - \quad (2.1)$$

Where, W_D = energy dissipated in one cycle of loading

W_S = maximum strain energy stored during the cycle.

2.2.2 Shear modulus

Shear modulus, G, is generally defined as the slope of the line connecting two extreme points on the hysteresis loop at a certain shear strain. (Fig.2.1). Also G can be expressed as ratio of cyclic shear stress (τ) and corresponding cyclic strain (γ).

$$G = \frac{\tau}{\gamma} \quad \ldots\ldots\ldots\ldots\ldots\ldots\ldots\ldots 2.2$$

2.2.3 Maximum Shear Modulus (G_{max})

Maximum shear modulus is obtained at small strain range of amplitude. This parameter is used to normalize the shear modulus G by dividing it by G_{max}. A plot of the variation of G/G_{max} with γ is called a normalized modulus reduction curve.

The maximum shear modulus, G_{max} which corresponds to very low strain levels cannot be determined from simple shear tests. So, seismic geophysical tests which induce shear strains lower than about $3*10^{-4}$ % is used for computation (Luna and Jadi 2000).

$$G_{max} = \rho*(V_S)^2 \ldots\ldots\ldots\ldots\ldots\ldots\ldots\ldots\ldots\ldots\ldots\ldots 2.3.$$

. Where: ρ = the density of the soil deposit and

V_S = shear wave velocity

The in situ measured shear wave velocity is the most reliable means of obtaining G_{max} for particular soil deposit. Hardin (1972) published that for undisturbed cohesive soils, as well as sands, G_{max} can be calculated from:

$$G_{max} = 1230 * \frac{(2.973-e)^2 * (OCR)^a * (\sigma'_m)^{0.5}}{1+e} \quad \text{.....2.4}$$

Where: OCR = over consolidation ratio, $\frac{P_r}{P_o}$

e = void ratio of the soil

σ'_m = mean effective confining stress,

K = 0.5, is the coefficient of lateral pressure at rest

a = parameter that depends on the plasticity index of the soil

The value of a can be obtained from the following table:

Table 2. 1: Value of a with respect to plasticity index (Hardin, 1972)

PI	a
0	0
20	0.18
40	0.30
60	0.41
80	0.48
≥100	0.50

2.3 Methods of Determining Shear Modules and Damping Characteristics

For field and laboratory tests, various test procedures have been used to determine shear moduli and damping characteristics (Girmachew, 2010). The main procedures can be summarized as follows:

2.3.1 Direct determination of stress-strain relationships

Hysteretic stress-strain relationships of the type shown in Figure 2.1 may be determined in the laboratory by means of triaxial compression tests, simple shear tests or torsional shear tests conducted under cyclic loading conditions. Seed and Edriss (1970) studied these procedures are useful for measuring shear modules and damping factors under moderate to relatively high strains ($0.01<\gamma<5\%$). In this paper the test was performed using simple shear test among the given method above.

2.3.2 Forced vibration tests

Forced vibration tests, involving the determination of resonant frequencies and measurement of response with different frequencies have been used to determine both shear modules and damping factors. Test conditions in the laboratory have included the application of longitudinal vibrations and tensional vibrations to cylindrical samples or shear vibrations to layers of soil placed on a shaking table. As studied by Seed and Edriss (1970) these procedures are useful for determining properties at relatively low to moderate strain levels ($10^{-4} < \gamma < 10^{-2}\%$).

2.3.3 Free vibration tests

Free vibration tests, in which measurements are made of the decay in response of a soil sample or soil deposit, have been used to measure both shear modules and damping factors for soils. Seed and Edriss (1970) published that methods of excitation are essentially similar to those used for forced vibration tests, but the procedures can be used for measurement of soil characteristics at relatively low to moderately high strain levels ($10^{-3}< \gamma <1\%$).

2.3.4 Field measurement of wave velocities

Field tests have been used to measure the velocity of propagation of compression waves, shear waves, and Rayleigh waves from which values of soil modulus can readily be determined for low strain ($\gamma \leq 10^{-4}$ %) conditions. These procedures have not provided values of damping factors (Seed and Edriss, 1970).

The different test procedures for measuring moduli and damping characteristics and the approximate ranges of strain within which they have been used are summarized below in Table 2.2.

Table 2. 2: Test procedures for measuring moduli and damping characteristics (Seed & Idriss, 1970)

General Procedure	Test condition	Approximate strain range (γ)	Properties that may be determined
Determination of Hysteretic stress strain Relationships	Tri-axial compression	10^{-2} to 5%	Modulus; Damping
	Simple shear	10^{-2} to 5%	Modulus; Damping
	Torsional shear	10^{-2} to 5%	Modulus; Damping
Forced vibration	Longitudinal Vibrations	10^{-4} to 10^{-2}%	Modulus; Damping
	Torsional vibrations	10^{-4} to 10^{-2}%	Modulus; Damping

	Shear vibrations-lab	10^{-4} to 10^{-2}%	Modulus; Damping
	Shear vibrations-field	10^{-4} to 10^{-2}%	Modulus
Free vibration tests	Longitudinal Vibrations	10^{-3} to 1%	Modulus; Damping
	Torsional vibrations	10^{-3} to 1%	Modulus; Damping
	Shear vibrations-lab	10^{-3} to 1%	Modulus; Damping
	Shear vibrations-field	10^{-3} to 1%	Modulus
Field wave velocity Measurements	Compression waves	~5x10^{-4}%	Modulus
	Shear waves	~5x10^{-4}%	Modulus

2.4 Parameters Affecting dynamic soil properties

When a soil is subjected to earthquake or cyclic loading, the shear modulus and damping ratio of the soil are influenced by many factors. Those parameters which have influence on shear modulus and damping characteristic are like: Strain amplitude, void ratio, effective confining stress, effect of soil plasticity, number of loading cycles, over consolidation ratio, degree of saturation, effect of non-plastic fines and effect of frequency. This paper presents a review on the dynamic soil properties and their influencing parameters.

2.4.1 Effect of non-plastic fine Materials

The role of non-plastic fines in large-strain phenomenon such as Liquefaction has been studied extensively. Yamamuro and Lade (1998) discussed that, the induction of liquefaction can be described in terms of particle contacts shearing against each other in the small to intermediate strain range even if liquefaction itself results in large strains in the soil.

Figure 2.2 demonstrates that soil deposited in the loose state will have silt grains at or near the contact points between the larger grains. If the soil only has a moderate amount of fines, initial shearing causes the finer particles to fill the voids between the larger grains and the contacts of the larger particles dominates the behavior of the soil. This response continues until the voids of the larger particles are completely filled with finer material.

Additional fines push the larger particles apart and the contacts of the fines increasingly dominate the behavior of the soil. Initial shearing of silty sand may push the fines into the void spaces of the sand, leading to a high initial contractive tendency which may cause static liquefaction at low confining pressures. Higher confining pressures push the sand particles into better contact, increasing the dilative tendencies of the soil and leading to higher liquefaction resistance (Umberg, 2012).

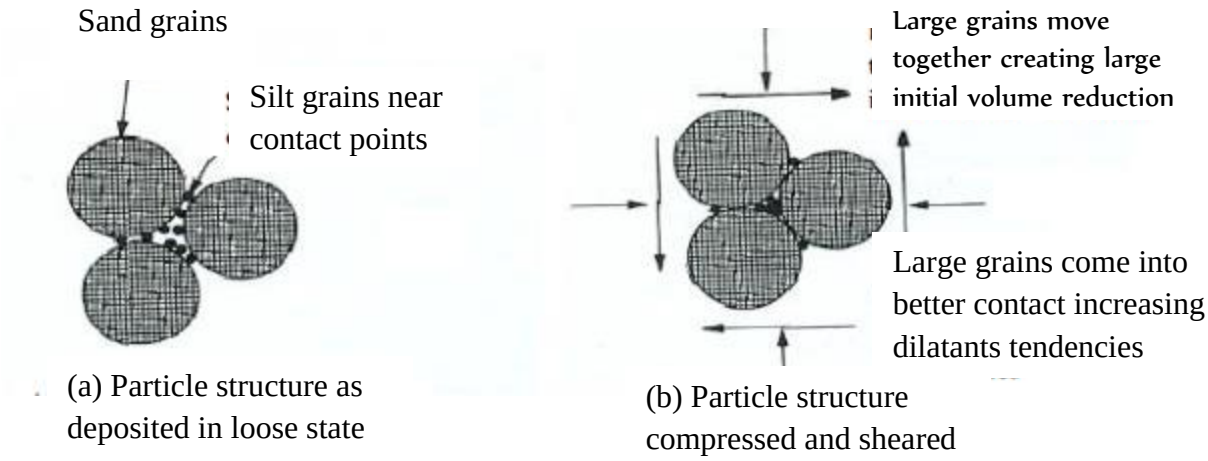

Figure 2. 2: Hypothetical Particle Structure of Loose Silty Sand with Low Silt Content (a) As Deposited and (b) After Densification due to Shearing. (Yamamuro & Lade, 1999)

2.4.2 Effect of Confining Pressure

Shear modulus and damping ratio are significantly affected by confining pressure (Shankar et al., 2013). The influence of confining pressure on the shear modulus is shown in Figure 2.3. It may be noticed from the figure that there is considerable influence of confining pressure on shear modulus. As the confining pressure increases the shear modulus increases significantly, however the shear modulus follows a converging trend towards larger shear strains irrespective of the confining pressure to which the samples are subjected (T. G. Sitharam, 2008).

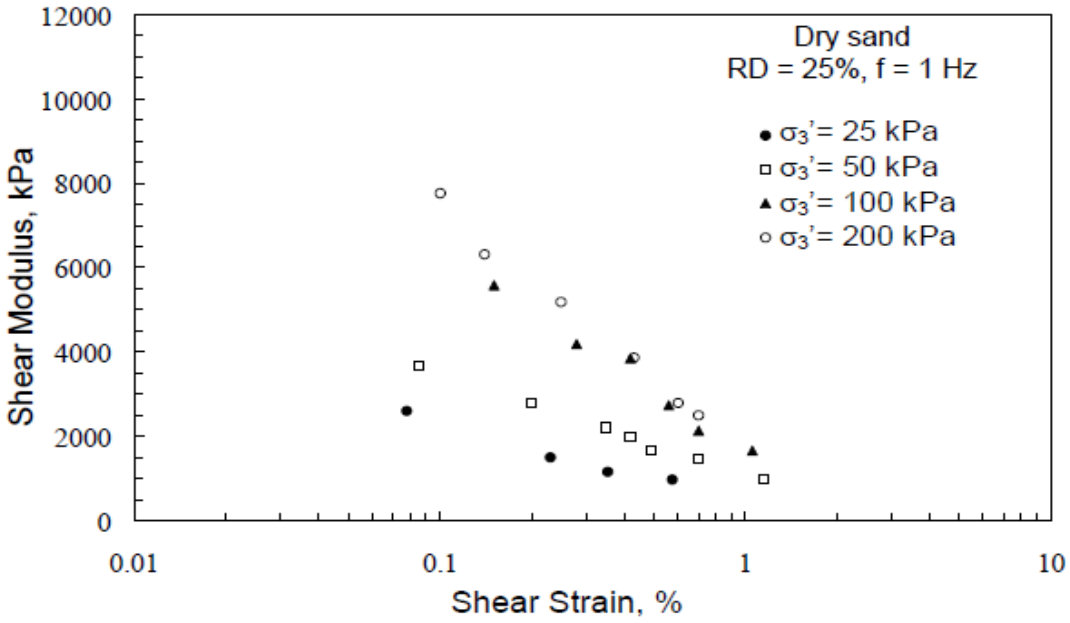

Figure 2. 3: Influence of Confining Pressure on Shear Modulus for Dry Sands (T. G. Sitharam, 2008)

Figure 2.4 below shows that the influence of confining pressure on the damping ratios. As seen in the figure, the damping ratio increases with increase in the shear strain at a given confining pressure but decreases with increase in the confining pressure. This clearly brings out the fact that the damping ratios in dry sands are influenced by the confining pressure.

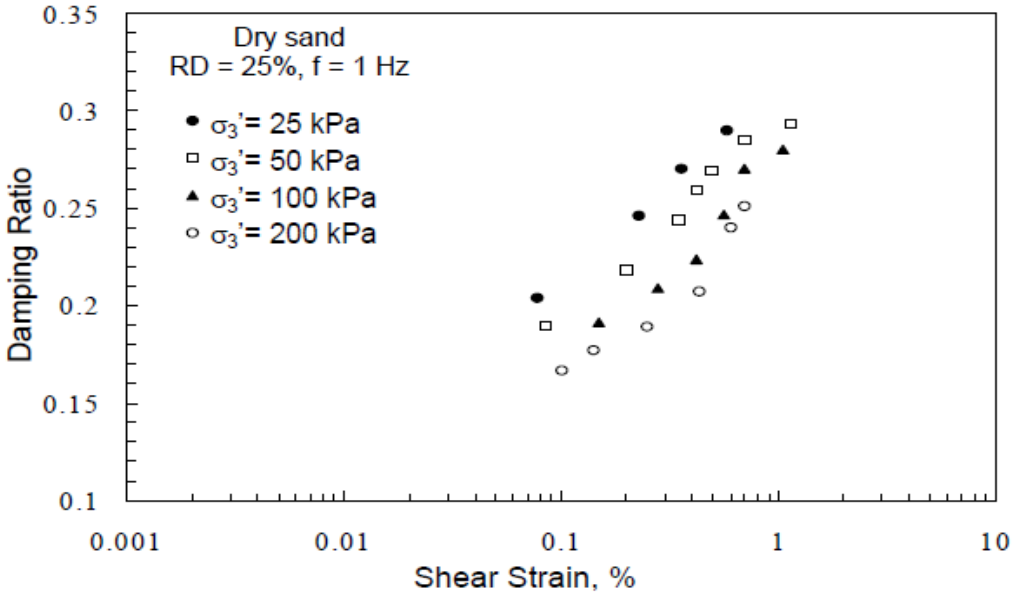

Figure 2. 4: Influence of Confining Pressure on Shear Modulus for Dry Sand (T. G. Sitharam, 2008)

2.4.3 Effects of Void Ratio

Void ratio is one of the mechanical properties of soil which is mainly influenced by the static/dynamic actions of loading. As the void ratio becomes lesser under the application of load, soil particles come closer to each other resulting in densification of soil sample. Densification or reduction in void ratio of soils due to confining pressure and method of sample preparation are the main causes increasing the cyclic strength. Kakusho(1982) performed a series of cyclic triaxial tests on isotropically consolidated saturated Toyoura sand subjected to specified effective confining stress and frequency and reported about the influence of void ratio on the strain dependent shear modulus and damping ratio (Shankar et al., 2013). It was observed that shear modulus decreases with increase of void ratio as show in figure 2.5 at different confining pressure. Void ratio increment causes damping characteristics of soil to decreases as studied by Dorby and Vucentic (1987).

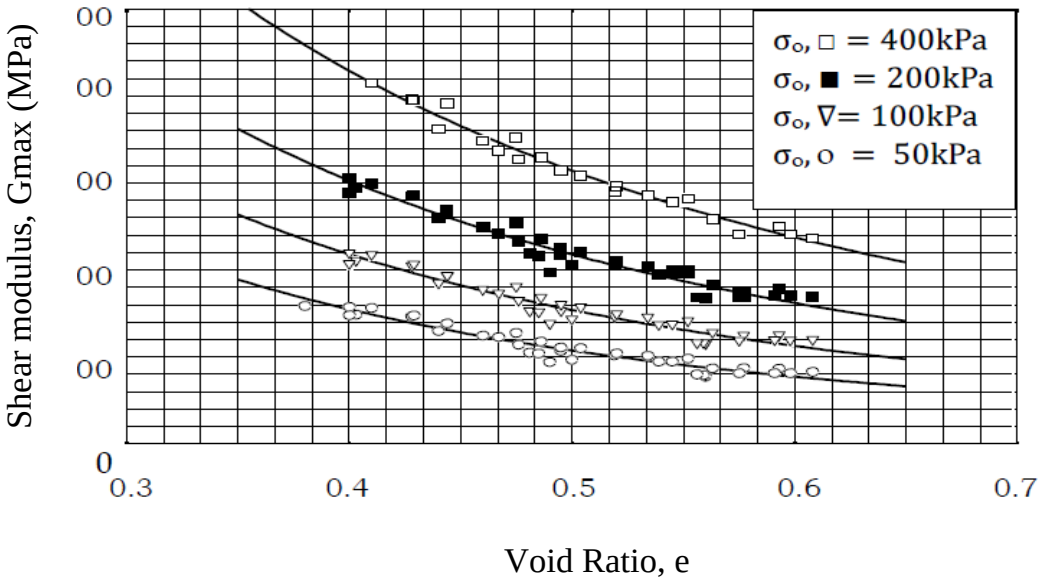

Figure 2. 5: Variation of small strains Shear modulus with void ratio under different confining pressure (Shankar et al., 2013).

2.4.4 Degree of saturation

Sharma (2016) found that the shear modulus of dry sand is greater than that of partially saturated sand and fully saturated sand. However, there is not much difference noticed in the shear modulus of partially saturated sand and that of fully saturated sand. When the shear strain is higher than 1%, the decrease in shear modulus almost reduces to a very low value for all the three states of soil. However, for dry sand, shear modulus is higher as compared to partially saturated and fully saturated sand. Similar trend for decrease in shear modulus for dry to fully saturated state was observed for Ahmedabad sands at high strain levels by Sharma (2016).

.

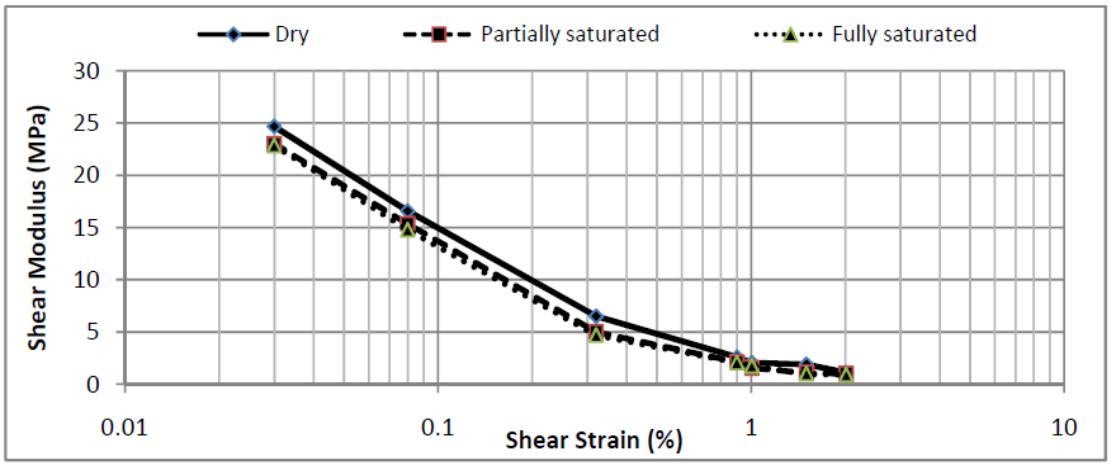

Figure 2. 6: Variation of shear modulus (G) with shear strain for different degrees of saturation (Sharma, 2016)

As degree of saturation increases, an increase in the damping ratio is observed with the increase in strain. It can be observed from Figure 2.7 that the damping ratio of saturated sands is greater than that of partially saturated and fully saturated sands at most of the strains. However, the difference in damping ratios of partially saturated and fully saturated sand is smaller. Sharma (2016) conducted series of resonant column tests to study the effect of saturation on damping ratio and concluded that minimum damping ratio is always associated with the dry state and reaches its maximum value for fully saturated sands.

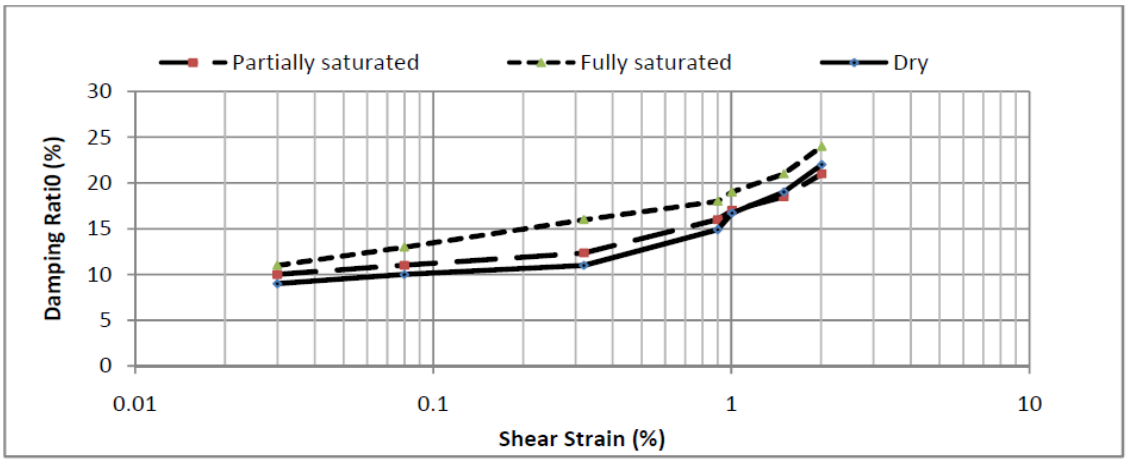

Figure 2. 7: Variation of damping ratio with shear strain for different degrees of saturation (Sharma, 2016)

In Figure 2.8, the variation of the normalized shear modulus ratio with the increase in shear strain is shown for different degrees of saturation. It can be observed that as the soil is in unsaturated condition, the normalized shear modulus ratio is relatively higher than that of the saturated sand sample. However, smaller difference is noticed for partially saturated and fully saturated samples of Solani Sand.

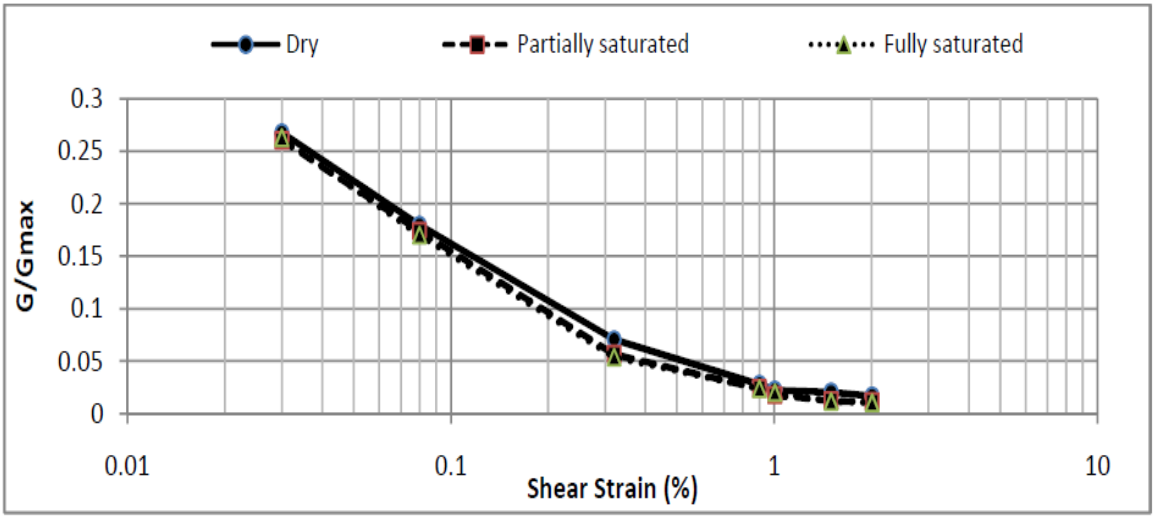

Figure 2. 8: Variation of normalized shear modulus (G/Gmax) with shear strain for different degrees of saturation (Sharma, 2016)

2.4.5 Number of Loading Cycles

T. G. Sitharam, (2008), reported that the shear modulus after first cycle of loading increases slightly with increase in the number of cycles up to 6 cycles of loading and thereafter the shear modulus remains constant with further increase in the number of cycles for shear strain levels of 0.15% and 0.28% which is shown in figure 2.9. Whereas for shear strain level of 0.42 % the shear modulus is almost constant after first cycle of loading, indicating that the soil densifies after first cycle of loading.

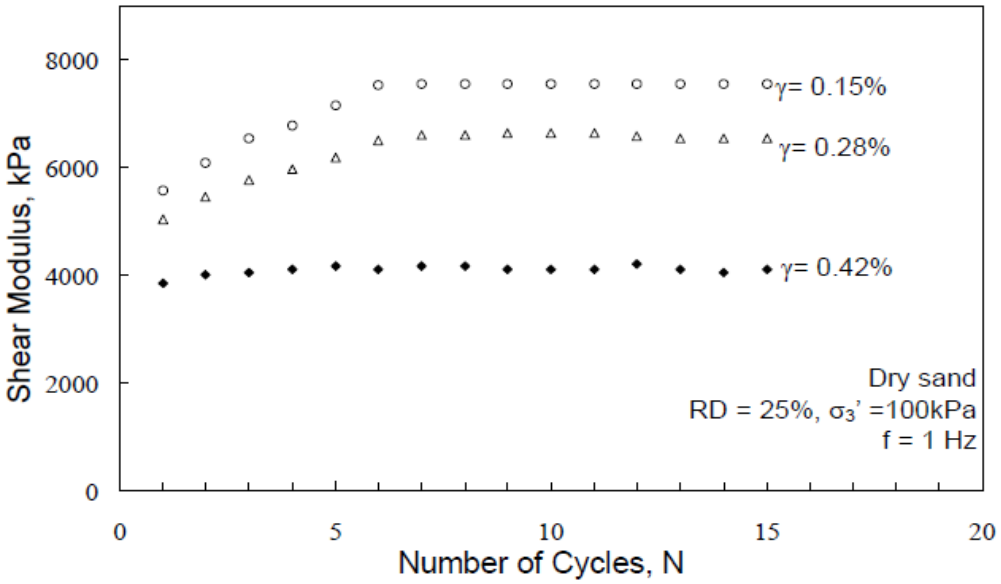

Figure 2. 9: Relationship between shear modulus and number of cycles at 25% RD for sand (T. G. Sitharam, 2008).

The relationship between the damping ratio and the number of cycles for reconstituted dry sand sample at 25% relative density is shown in Figure 2.10. It can be observed from the figure that except at first cycle of loading the damping ratio remains almost constant with increase in the number of cycles but decreases with increase in the cyclic strain amplitudes. This brings out the fact that the influence of number of loading cycles is not significant on damping ratios of the dry sand samples. But Hardin (1972) concluded that the shear modulus decreases for cohesive soils and increases slightly for cohessionless soils with the number of cycles of loading while the damping ratio decreases approximately with logarithm of number of cycles of loading in both cohesive and cohessionless soils, up to about 50,000 cycles.

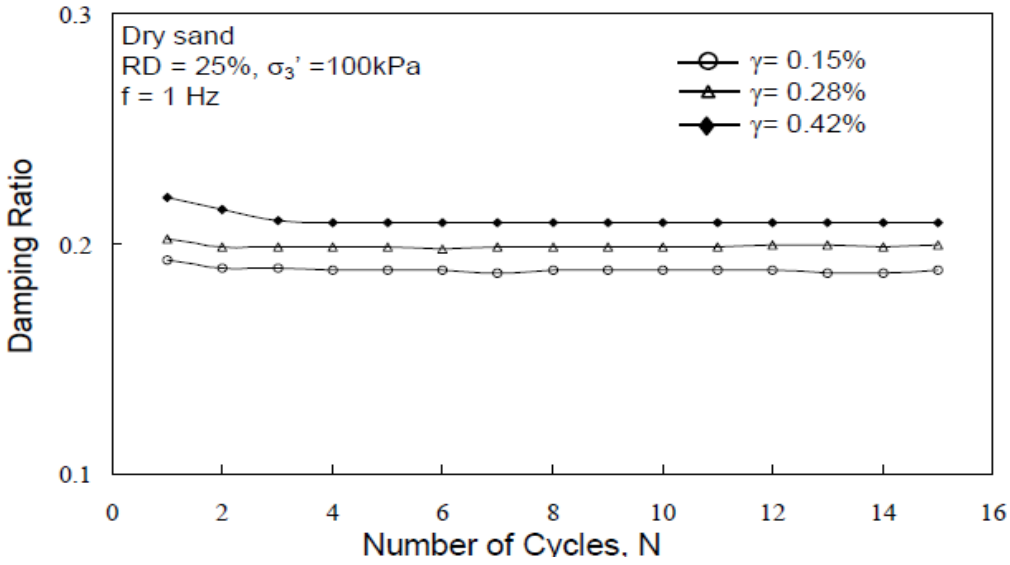

Figure 2. 10: Relationship between Damping ratio and number of cycles at 25% RD for sand (T. G. Sitharam, 2008).

2.4.6 Effects of Overconsolidation Ratio

The overconsolidation ratio (OCR) is a geotechnical parameter, which represents the historical changes in state of stress in the subsoil. The stress history, as indicated by the profile of OCR, of a soil deposit is one of the most dominant factors that influence the engineering behaviour of the soil (Shankar et al., 2013). It is recognized that small-strain shear moduli of soils increase with over consolidation ratio, especially for clayey soils. As Hardin (1972) studied that, the OCR had only small or no effect on the small-strain shear modulus for sand. As soil is loaded to higher stress, the relative movement between particles occurs resulting in soil having higher density, resulting in an increase in Gmax (Abraham, 2014).

2.4.7 Shearing Strain Amplitude

Strain has an extreme influence on dynamic properties of soil; therefore tests should be carried out at definite strain amplitude. In the geotechnical engineering and earthquake engineering fields, the small-strain range (i.e. the linear range) is defined as the range of

shear strain amplitudes over which the dynamic properties of soils (shear modulus, G, and material damping ratio, D) are constant. Because in that strain range the shear modulus is constant with the maximum value and the material damping ratio is constant with the minimum value. These dynamic properties are called Gmax and Dmin, respectively. In the technical literature, the small-strain range of sands is often described by strains less than 10^{-3} % (Shin, 2014). As strain increases beyond the small-strain range, the dynamic properties start to vary with the shear modulus decreasing and the material damping ratio increasing (Figure 2.11 and 2.12).

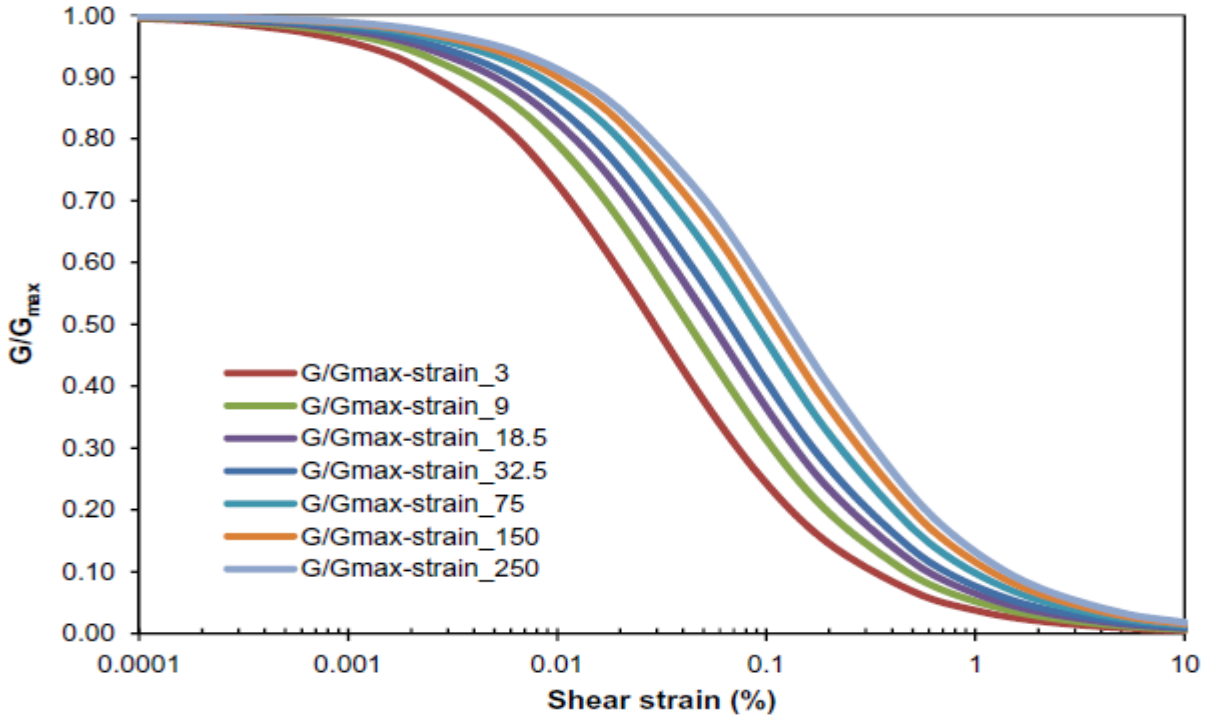

Figure 2. 11: Variation of Normalized shear modulus and shear strain (Muge, 2016)

Shin (2014) Discussed that variation of the dynamic soil properties with strain amplitude is termed the nonlinear behavior of soils and the strain boundary between linear (i.e. small-strain range) and nonlinear strain range is referred to elastic threshold shear strain, γ_t^e. The values of elastic threshold shear strain, γ_t^e, vary depending on the dynamic and engineering characteristics of the soils. Muge (2016), made an investigation from 104

boreholes in Erba, Tokat (Turkey) to show at different shear strain level the values of shear modulus and damping characteristics for sand and clay soils which obtained during drilling.

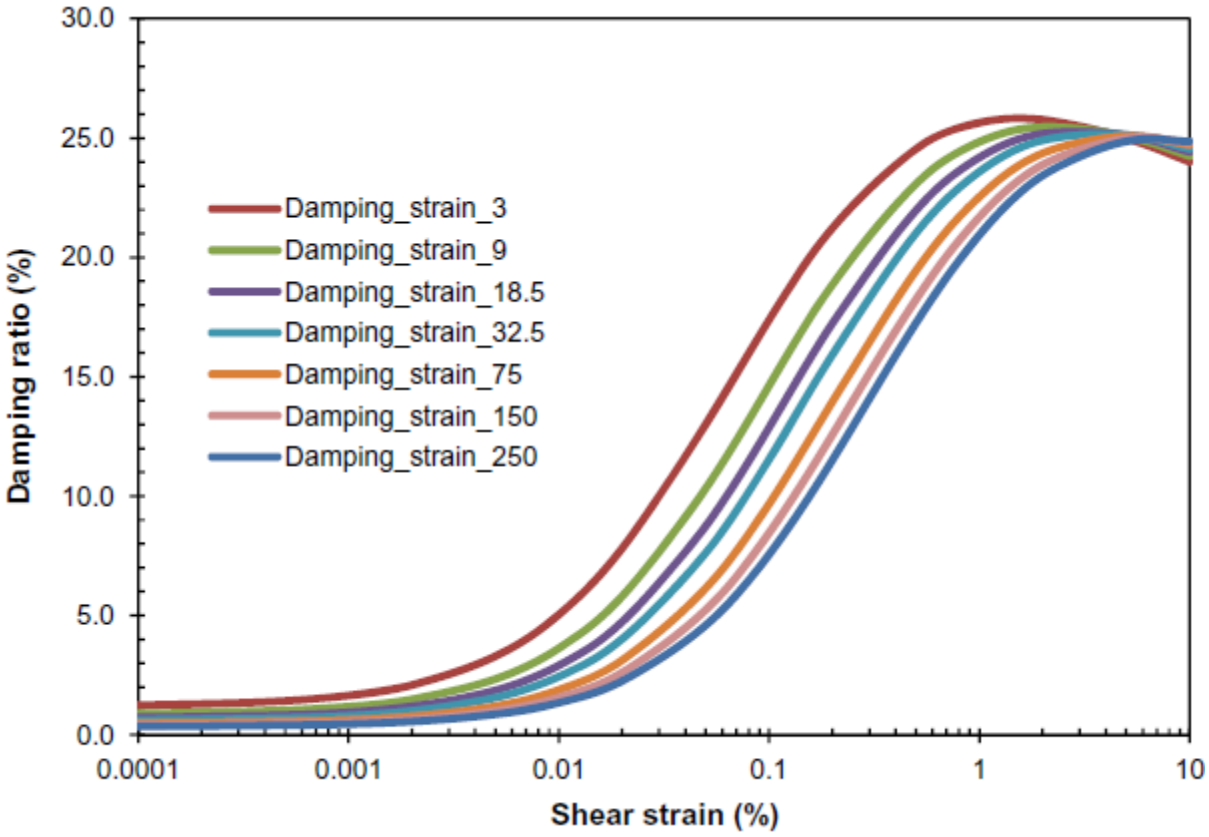

Figure 2. 12: Variation of damping ratio and shear strain (Muge, 2016)

2.4.8 Effect of soil plasticity

Vucentic and Dorby (1991) studied the influence of the plasticity index (PI) on the cyclic stress-strain parameters over normally consolidated and overconsolidated (OCR = 1–15) clay (Figure 13) and reported that PI is the main factor controlling modulus reduction curve G/G_{max} and damping ratio for a wide variety of soils; if for a given shear strain PI increases, G/G_{max} rises and damping ratio is reduced. It is concluded that soils with higher plasticity tend to have a more linear cyclic stress-strain response at small strains and to degrade less at larger shear strain than soils with a lower PI.

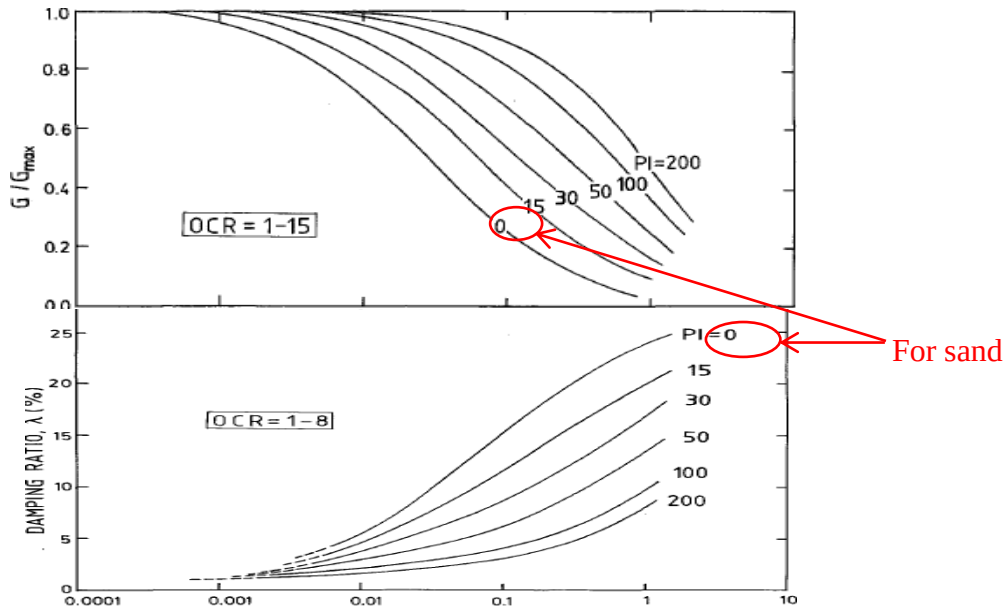

Figure 2. 13: Relations between G/Gmax versus γc and λ versus γc, Curves and Soil Plasticity (PI) for normally and overconsolidated soils (Vucetic & Dobry, 1991)

2.4.9 Effect of Frequency

Sitharam, (2008) Studied evaluation the strain dependent dynamic properties of the dry sand samples collected from the earthquake affected area of Ahmedabad. The effect of frequency on the dynamic properties of dry sand samples indicate that the frequency of loading has no significant influence on shear modulus but the damping ratios are influenced to some extent and there is an increasing trend with increase in the frequency for the range of frequencies and strain amplitudes adopted in their study. As Abraham (2014) reported that, the frequency of transient loadings from wave, seismic, traffic and machine loadings may range from 0.01 to 100 Hz which had only small or no influence on small-strain shear modulus for cohesionless soils. It is therefore common practice to carry out laboratory cyclic tests at a frequency range of 0.1 to 2 Hz. Mostly the frequency of 1 Hz preferred.

CHAPTER THREE

DESCRIPTION OF STUDY AREA

The town of Jimma is found in southwest part of Ethiopia at 354 km distance from the capital Addis Ababa. The major part of Jimma town, including the central, southern and western parts, is characterized by flat to gently sloping/undulating topography, while the northern and eastern parts of the town and its peripheries are characterized by hilly/ sloping landscape as ESIA reported in 2011.

Jimma characterized by temperate humid climate that has high precipitation, warm temperature and long wet period. The mean annual rainfall in the area is around 1500mm and annual potential evaporation is about 1465mm. The rainfall pattern shows major seasonal variation ranging from mean monthly rainfall of about 38mm in January to 229mm in August. The main rainy season extends from April to September. The mean temperature is between around 12^{o}C and 29^{o}C with the mean daily temperature of 19.5^{o}C.

As described in the Jimma City Profile of 2008/2009, temperature variation is observed among seasons with the warmest season extending from February to April and the coldest season from July to September.

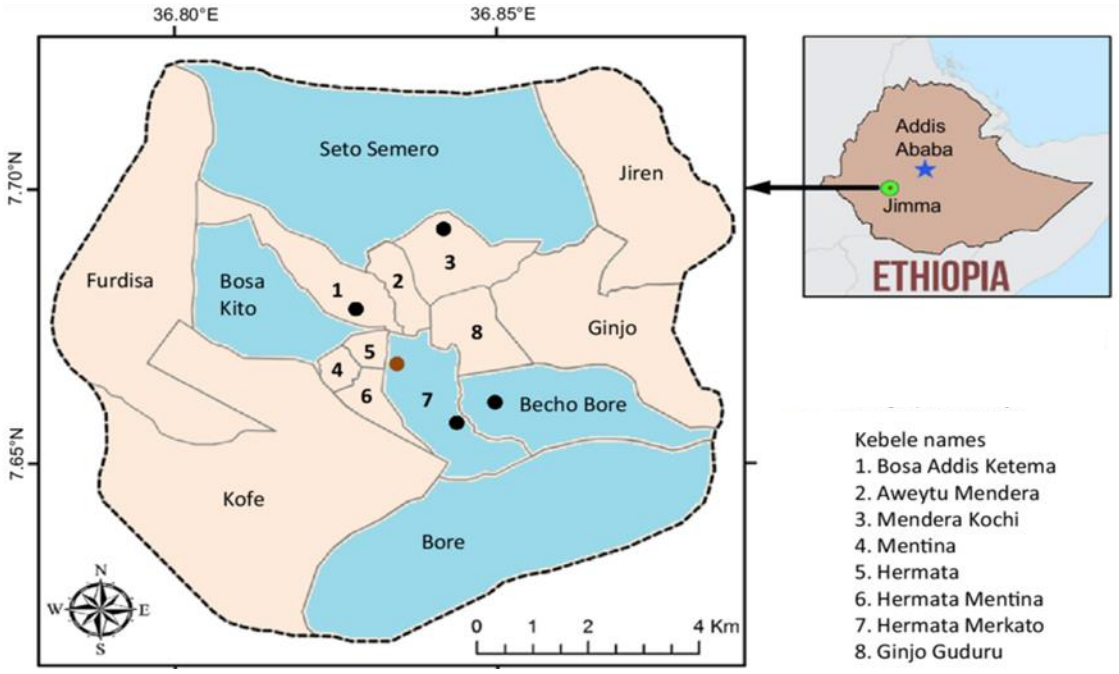

Figure 3. 1: Map of Jimma town with its administrative Kebeles

3.1 Geology

According to the geological map of Ethiopia 1:200,000 scale and the report compiled by Tefera (1996) the project area is generally made up of the following major geological formations.

Jimma Volcanics (Pjb and Pjr)

The name Jimma volcanics was given to trachybasalts and rhyolites which cover most parts of southwestern Ethiopia.The Jimma volcanics which are considered analogous to the Main Volcanic Sequence are a thick succession of basalts and salic rocks with basalts dominating the lower part of most sections. It was reported K/Ar age of 42.7-30.5 Ma for the Jimma volcanics. Two units (Jimma Basalts and Jimma Rhyolites) which show a conformable relation can be identified. The Jimma Rhyolites being the younger of the two units is equivalent to the Magadala Group of Kazmin of southwestern Ethiopia. The

Jimma volcanic almost always rests on the Precambrian basement, the unconformity being marked by basal residual sandstone. The basalt flows form an unbroken succession several hundred meters thick in some places. In others salic rocks are intercalated with basalt flows close to the base or form a thick succession just above the basal basalts.

Nazret Series

The name Nazret Series was given for a thick succession of Welded fiamme ignimbrites, pumice, ash and rhyolite flows and domes with rare intercalations of basalt flows which occur in the MER, rift margins and adjacent plateau. In the Nazret Series attains a thickness of up to 200 - 250 m. and tends to thin out on the escarpments. On the plateau margins a thickness of 1 - 30 m was reported at many localities. Ignimbrites of the Nazret Series are considered to be products of eruptions mainly from marginal centers in the rift .In composition the ignimbrites are alkaline rhyolites with transition to peralkaline rhyolites, pantellerites and trachytes.

Quaternary Sediments: Alluvial and lacustrine deposits consisting of sand, silt and clay.

3.1.1 Soil formation

The top most part of the pits is covered by silt, gravel and mixed crushed stone with grass root having an average 0.34m depth below NGL. Beneath the top soil layer, there is medium stiff to stiff, reddish and dark gray, high plastic, clayey silt/silty clay with little sand soil are the main soil layers through the test pits.

CHAPTER FOUR

EXPERIMENTAL PROGRAMME

4.1. Overview of testing equipment

To determine dynamic property of any type of soils various kind of machines are available. These include cyclic triaxial, resonant column, ultrasonic pulse, piezoelectric bender element, cyclic simple shear and cyclic torsional shear apparatuses (Kramer, 1996). Among these machines cyclic simple shear is used for this research.

4.1.1. Cyclic simple shear testing system

The system is designed to allow a sample to be consolidated and sheared under drained conditions. Cyclic simple shear tests can be conducted for a wider range of strain amplitude (that is, 10^{-2}% to about 5%). This range is the general range of strain encountered in the ground motion during seismic activities (Das, 1993).

The base machine consists of a simple shear load frame, an air receiver with axial (vertical) and lateral (horizontal) loading control valves and two 5 kN actuators, built into a specially designed floor-mounted cabinet, which also houses the Integrated Multi-Axis Control System (IMACS) and the PC. The axial and lateral actuators are fixed to the load frame, which supplies the reaction to the forces applied. Each actuator has an internal displacement transducer, which relays the actuator position back to the computer. This is very important when setting up a sample; it allows you to set enough travel for the test duration. The top half of the area where the sample is set up is rigidly fixed and houses a 50 (70) mm diameter vertical ram in a linear bearing to allow axial movement but prevent

lateral movement. The bottom half is mounted on roller bearings in the same way as in a standard shear box apparatus (UTS004, 2003).

While the specimen is being subjected to loading forces, the IMACS captures data from the transducers and transfers these, via the USB or RS232 link, to the PC for processing, display and storage.

The Integrated Multi-Axis Control System is a compact self- contained unit that provides all critical control, timing and data acquisition functions for the test and the transducers.

The standard sample is 70 mm diameter. The test can also be performed on 50 mm diameter samples using the other load arm which fits with the sample size. The sample is positioned on a pedestal with a top cap the same as a triaxial sample and covered by a rubber membrane placed and secured with O-rings. To maintain a constant diameter (K_0 conditions) the sample is laterally confined by a series of brass rings.

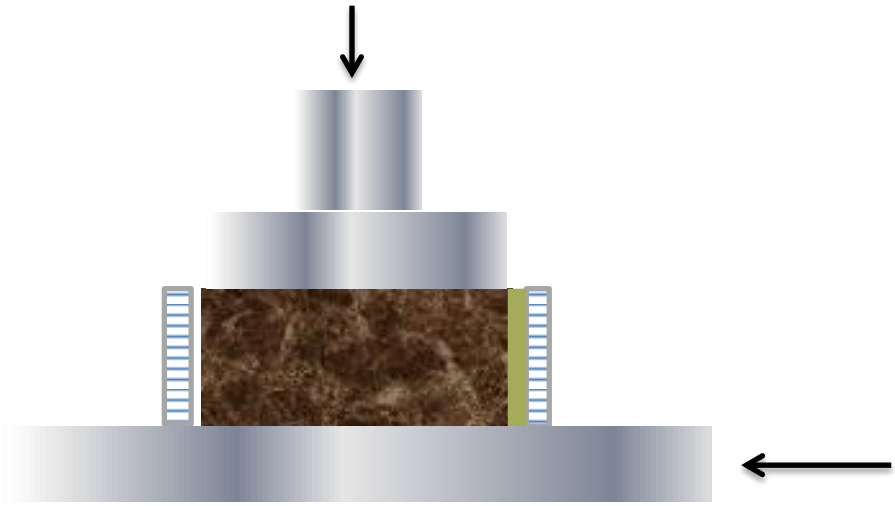

Figure 4. 1: Sample assembled on the cyclic simple shear equipment

4.2 Field and laboratory tests

To select sampling areas, visual site investigation which used for observation of soil stratification from deep cuts near buildings and open areas to locate the sampling points

in the town. Accordingly, four representative sampling areas were selected from different locations of the town. The selected points were Stadium (TP1), Ajip (TP2), around St. Gebriel church (TP3) and Kitto Furdissa (TP4). Pits were excavated to a depth of three meters below natural ground level where samples were taken starting from two and half meters. On the selected pointes both field and laboratory tests were performed. Tests like bulk density, index property test, one dimensional consolidation test and cyclic simple shear tests were used to clearly identify the material tested.

From the field test, bulk densities were determined for all samples which have 1.409 to 1.641 gm/cc values and specific gravity values of 2.527 to 2.653. Atterberg limits, particle size distribution and specific gravities tests were also conducted. Liquid limit and plastic limit values ranges from 71% to 84% and 31% to 46% respectively. Further, particle size distribution and Atterberg limit tests (Appendix A) were included with their respective soil classifications summarized in Table 4.1below.

Table 4. 1: Atterberg limits and soil classification

Sample from	liquid limit (%)	Plasticity index (%)	Specific gravity	Bulk density (gm/cc)	USCS classification symbols	Soil classification
TP1	67	31	2.620	1.641	MH	Clayey Silt
TP2	71	40	2.527	1.595	CH	Silty Clay
TP3	80	46	2.544	1.409	CH	Silty clay
TP4	84	39	2.653	1.510	MH	Clayey silt

4.2.1 One-dimensional Consolidation

The main aim of one dimensional consolidation test is to get better understanding on stress history of the soil under study. Additionally, the preconsolidation pressure which used to compute the maximum shear modulus of the soil in this paper was obtained from the test. Detailed calculation of test result is shown in Table B.1 to B.2 and graph of Figure B-1 to B-2 in the appendix B. The preconsolidation pressure is obtained from the graph and is found to be 65 to 85 kPa.

4.2.2 Simple cyclic shear test procedures

4.2.2.1 Preparation of specimens

The soil in the Shelby tube sample was extruded into a stainless steel ring with sharp cutting edge having the same diameter (70 mm) as the sampling tube. The stainless steel ring was positioned right above and in alignment with the axis of the tube during this process. Having the ring around the specimen, allowed careful confinement and securing of the soil specimen against disturbance after extrusion from the tube. The specimen secured in the steel ring as per above was trimmed at the top and bottom ends to obtain a specimen height of 20 mm. The prepared sample pushed slowly using wooden sample extruder from string holding by hand and then specimen of 20 mm height and 70 mm diameter sample were obtained.

4.2.2.2 Setup of cyclic simple shear testing

The machine uses highly filtered compressed air from huge compressor where it's required to connect everything, to fill the air chamber before beginning any type of tests. Then, sample preparation, consolidation and cyclic shearing are common procedure in the laboratory to carry out cyclic simple shear test. The sample is set up in the cyclic

simple shear equipment, which has a rigidly fixed top half and a moving bottom half. The top half houses the vertical ram. This is housed in a linear bearing to allow vertical movement and prevent horizontal movement. The bottom half is mounted on roller bearings as in a standard shear box (Abraham, 2014). The sample is supported by a rubber membrane placed and secured with O-rings.

To maintain a constant diameter throughout the test, the sample is supported by a series of slip rings. During shear the rings slide across each other as shown Figure 4.2. The rings maintain a constant sample diameter.

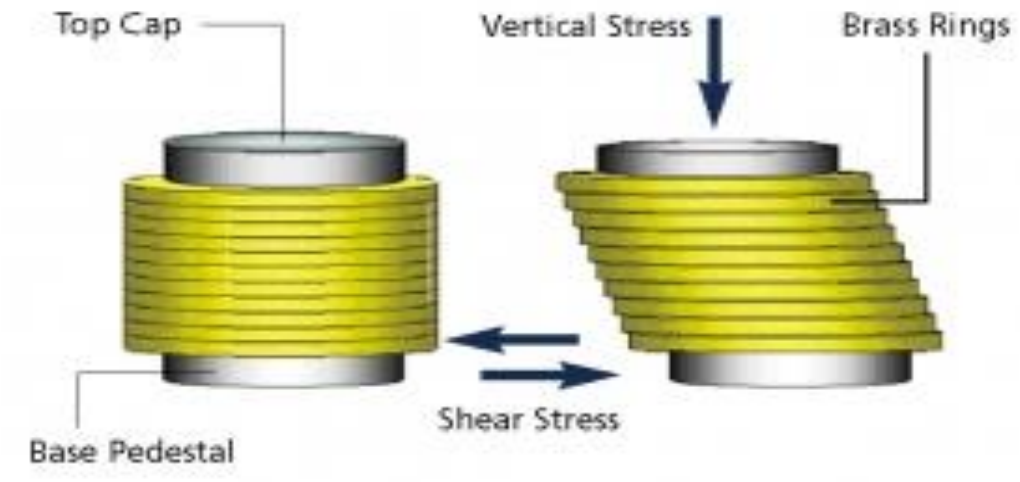

Figure 4. 2: Brass ring

4.2.2.3 The compression stage

After the sample was prepared and mounted properly on the machine, set the required loading, number of cycles, shear strain amplitude, frequency and the other parameters on the system.

The consolidation stage is the application of a static axial loading stress to the specimen while the lateral loading (shear) axis is held stationary. Axial stress and specimen

displacements (axial and lateral) data are measured over time and logged by the system shown in Figure 4.3. Logged data is also displayed to the operator in the form of charts and tables as the test stage proceeds. The consolidation stage was continued until the rate of vertical strain becomes less than 0.05% per hour (Abraham, 2014). When it reaches this level axial strain against time curve is closing to be horizontal, then manually terminated by the operator.

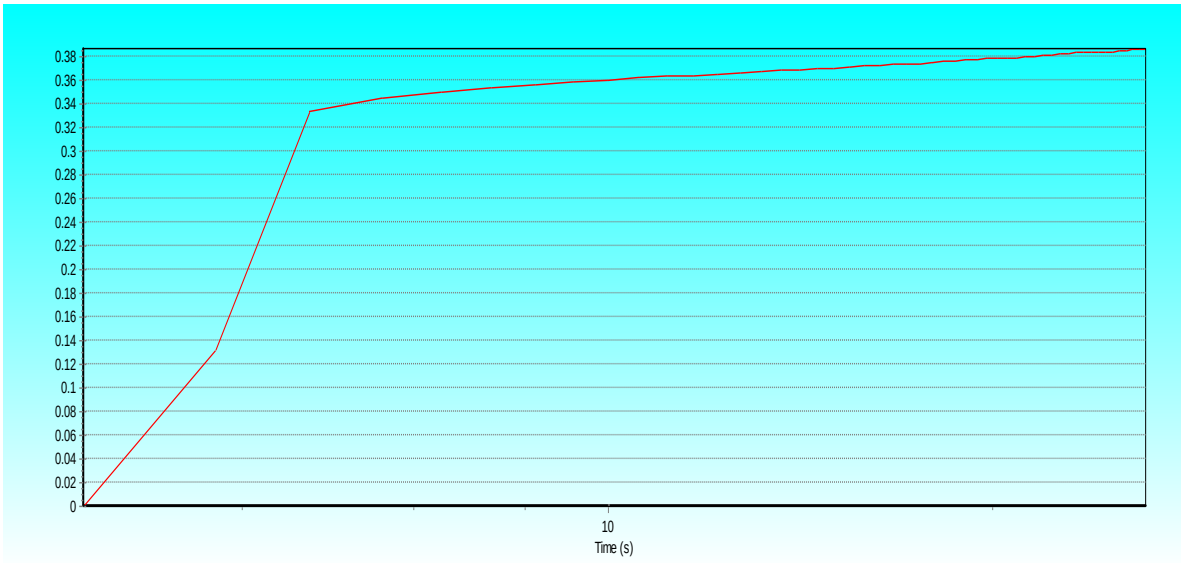

Figure 4. 3: Compression stage of soil specimen of TP1 at 5% using 100 kPa axial load

4.2.2.4 Cyclic Simple Shear Stage

Following the consolidation phase, the specimen was constrained against vertical deformations by clamping the vertical loading ram; this allowed maintaining constant volume conditions throughout monotonic or/and cyclic loading. Depending on whether the test was stress or strain controlled, the horizontal shear loading was applied either by means of double acting piston or a constant speed motor respectively. Cyclic tests were conducted under strain controlled conditions; the shear load was applied in the form of sinusoidal wave with a frequency of 0.1 Hz. Every specimen was tested with different

cyclic shear stress amplitude, so preparations of specimens and testing have been done for each strain level and axial load for all representative test pits (Abraham, 2014). Both lateral force and specimen displacements are measured for each loading cycle. Measured data is obtained from 50 points on the sample captured over a single cycle period (UTS004 2003).

4.2.3 Presentation of Cyclic Shear Test results

4.2.3.1 Axial loads and Shear Strain Levels used

Applied shearing strain values on the cyclic simple shear machine in all series of tests varied from 0.01% up to 5% with their respective different axial loads. In this study, axial loads of 100 kPa, 250 kPa and 400 kPa were used (see Table 4.2).

Table 4. 2: Axial stress and shear strain values used for the study

Soil type	Sample type	Axial stress (kPa)	Shear strain (%)				
Silty Clay soil	Undisturbed	100	0.01	0.1	1	2.5	5
		250	0.01	0.1	1	2.5	5
		400	0.01	0.1	1	2.5	5
Clayey Silt soil	Undisturbed	100	0.01	0.1	1	2.5	5
		250	0.01	0.1	1	2.5	5
		400	0.01	0.1	1	2.5	5

4.2.3.2 Shear stress and strain parameters

For single cyclic loading, the cyclic simple shear test gives series of raw data at 50 data points. Measured data can be displayed to the operator on Microsoft Excel spreadsheet.

Out of these data, Lateral Lvdt (specimen displacements) and Lateral force were used to calculate the shear stress (τ) and shear strain (γ) values. Using the specimen height after consolidation (< 20 mm) and its diameter, 70 mm, the shear stress and shear strain of the specimen can be calculated based on the following equation.

$$\text{shear stress}(\tau) = \frac{\text{Force}}{\text{Area}} = \frac{\text{Shear Force}}{\pi * 35^2} * 10^3 \text{ (Mpa)} \qquad 4.1$$

$$\text{shear strain } (\gamma) = \frac{\Delta L}{L} = \frac{\text{displacement}}{\text{height after cosolidation}} * 10^3 \text{ (Mpa)} \qquad 4.2$$

In most seismic events, the number of significant cycles is likely to be less than 20, so the specimen were cyclically loaded through 40 cycles (Das, 1993) using a uniform sinusoidal load at a frequency of 1.0 Hz, which is commonly used in laboratory tests. For all practical purposes the values determined at fifth cycles is likely to provide reasonable values (Ayalew, 2013). Sinusoidal loading cycle shape has been selected as it is the most common type of seismic wave shape for analysis (Das, 1993). Sinusoidal wave shapes for 2.5% strain and 1Hz and for three cycles is shown in Figure: 4.4.

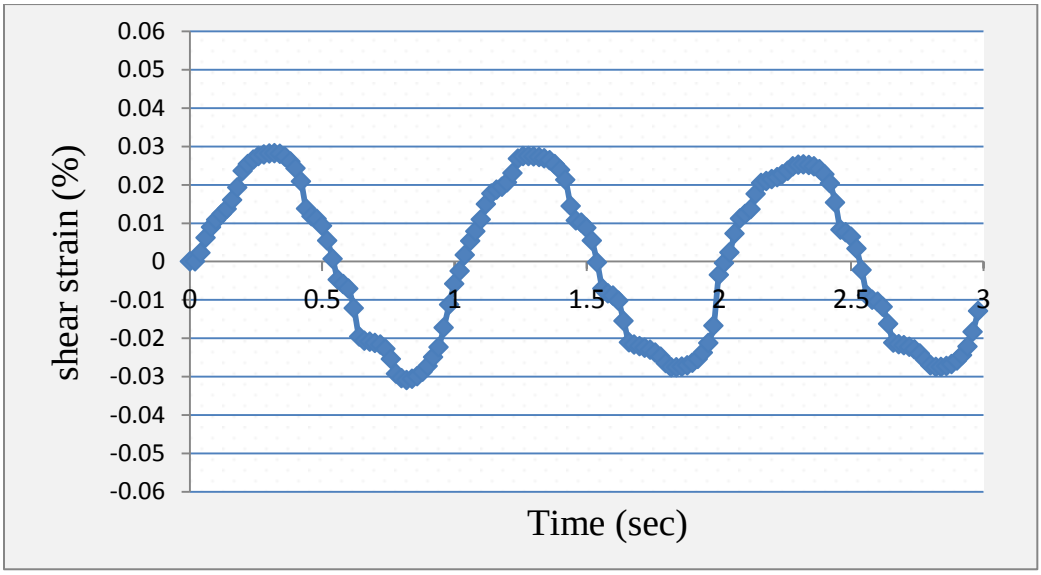

Figure 4. 4: Sinusoidal wave shapes for 2.5% strain and 1Hz and for three cycles

Table 4.3 below shows sample tabulation of shear strain and shear stress from the lateral force and specimen displacement taken from the 5th cycle test result of silt soil with peak-to-peak cyclic strain amplitude of 2.5%. The loading frequency used in this study is 1 Hz, which is commonly used in laboratory tests.

Using the lateral force and specimen displacement record of 50 points at 5th cycle was used for sample calculation (Table 4.3). The given result was obtained from the TP2 soil loaded 250 kPa at 5% cyclic strain amplitude.

Table 4. 3: Shear stress and shear strain values for single cycle.

No. cycle	Time (sec)	Lateral Lvdt	Lateral Force	Area of sample (mm^2)	Shear stress=(F/A)*10^3 Mpa	Shear strain=(disp./19.103)
5	0	-0.247100	0.005125	3848.45	0.0013317	-0.0129351
	0.019	-0.188140	0.027790	3848.45	0.0072211	-0.0098487
	0.038	-0.109310	0.042815	3848.45	0.0111253	-0.0057221
	0.057	-0.049230	0.059600	3848.45	0.0154868	-0.0025771
	0.076	0.013440	0.073925	3848.45	0.0192090	0.0007036
	0.095	0.092720	0.081255	3848.45	0.0211137	0.0048537
	0.114	0.134230	0.086050	3848.45	0.0223597	0.0070266
	0.133	0.178780	0.095040	3848.45	0.0246957	0.0093587
	0.152	0.227220	0.101910	3848.45	0.0264808	0.0118945
	0.171	0.258830	0.107775	3848.45	0.0280048	0.0135492
	0.190	0.291730	0.113670	3848.45	0.0295366	0.0152714
	0.209	0.319110	0.120585	3848.45	0.0313334	0.0167047
	0.228	0.340600	0.126130	3848.45	0.0327742	0.0178297
	0.247	0.354190	0.130605	3848.45	0.0339370	0.0185411
	0.266	0.364150	0.133930	3848.45	0.0348010	0.0190625
	0.285	0.371380	0.136215	3848.45	0.0353948	0.0194409
	0.304	0.376760	0.137350	3848.45	0.0356897	0.0197226
	0.323	0.386810	0.136560	3848.45	0.0354844	0.0202487
	0.342	0.378080	0.133700	3848.45	0.0347413	0.0197917
	0.361	0.373990	0.128090	3848.45	0.0332835	0.0195776
	0.380	0.364320	0.116565	3848.45	0.0302888	0.0190714
	0.399	0.344750	0.096705	3848.45	0.0251283	0.0180469
	0.418	0.304490	0.062405	3848.45	0.0162156	0.0159394

No. cycle	Time (sec)	Lateral Lvdt	Lateral Force	Area of sample (mm2)	Shear stress=(F/A)*103 Mpa	Shear strain=(disp./19.103)
5	0.437	0.237400	0.022025	3848.45	0.0057231	0.0124274
	0.456	0.152950	-0.010105	3848.45	-0.0026257	0.0080066
	0.475	0.050690	-0.026370	3848.45	-0.0068521	0.0026535
	0.494	0.011320	-0.030045	3848.45	-0.0078070	0.0005926
	0.513	-0.041390	-0.041490	3848.45	-0.0107810	-0.0021667
	0.532	-0.108370	-0.057340	3848.45	-0.0148995	-0.0056729
	0.551	-0.181930	-0.076320	3848.45	-0.0198314	-0.0095236
	0.570	-0.239920	-0.095840	3848.45	-0.0249035	-0.0125593
	0.589	-0.292110	-0.106730	3848.45	-0.0277332	-0.0152913
	0.608	-0.335420	-0.109745	3848.45	-0.0285167	-0.0175585
	0.627	-0.415790	-0.113860	3848.45	-0.0295859	-0.0217657
	0.646	-0.479560	-0.121460	3848.45	-0.0315608	-0.0251039
	0.665	-0.489740	-0.124290	3848.45	-0.0322961	-0.0256368
	0.684	-0.500270	-0.129840	3848.45	-0.0337383	-0.0261880
	0.703	-0.518410	-0.138730	3848.45	-0.0360483	-0.0271376
	0.722	-0.547080	-0.149045	3848.45	-0.0387286	-0.0286384
	0.741	-0.573140	-0.161965	3848.45	-0.0420858	-0.0300026
	0.76	-0.590820	-0.168410	3848.45	-0.0437605	-0.0309281
	0.779	-0.597720	-0.170155	3848.45	-0.0442139	-0.0312893
	0.798	-0.600720	-0.170430	3848.45	-0.0442854	-0.0314464
	0.817	-0.600750	-0.169290	3848.45	-0.0439891	-0.0314479
	0.836	-0.599440	-0.166915	3848.45	-0.0433720	-0.0313794
	0.855	-0.594340	-0.161445	3848.45	-0.0419507	-0.0311124
	0.874	-0.584420	-0.151365	3848.45	-0.0393314	-0.0305931
	0.893	-0.565930	-0.132880	3848.45	-0.0345282	-0.0296252
	0.912	-0.527020	-0.100595	3848.45	-0.0261391	-0.0275883
	0.931	-0.474720	-0.063105	3848.45	-0.0163975	-0.0248505

4.2.4 Computation of shear modulus and damping ratio values

The measured values of shear force and lateral displacement have been translated to shear stress and shear strain. Once shear stress and shear strain were computed, hysteretic loops of each cycle can be plotted using the shear stress and strain values obtained from 50 sample points in a cycle. The cyclic shear stress and shear strain graph with their

respective hysteresis loop were illustrated in Figure 4.5 to 4.7 which is used for the calculation of shear modulus and damping ratio for each cycle. Additional cyclic shear test results are shown in appendix C.

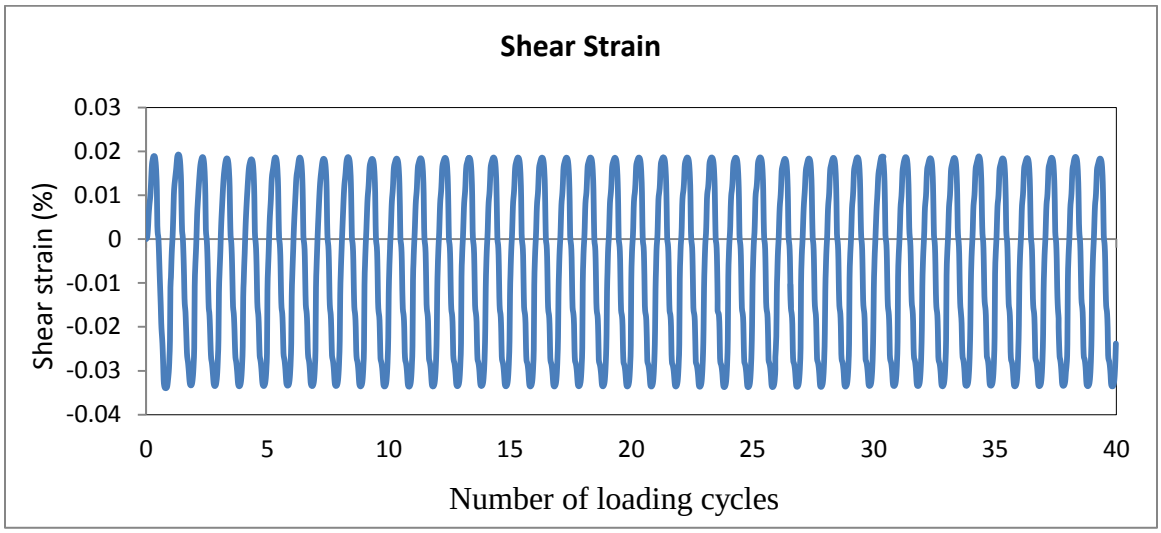

Figure 4. 5: Shear strain versus Number of cycles

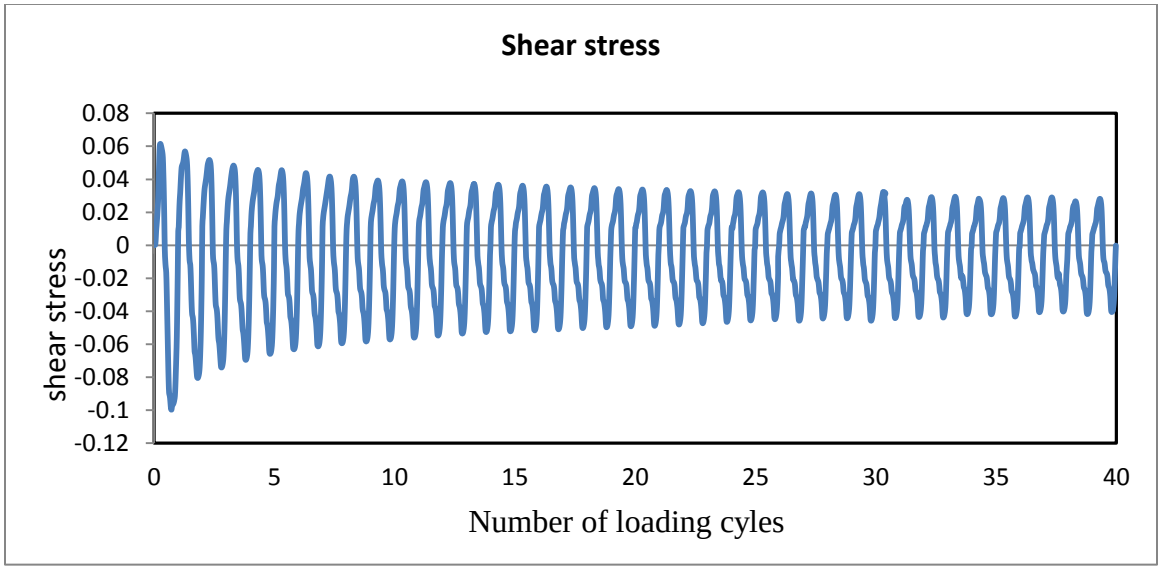

Figure 4. 6: Shear stress versus Number of cycles

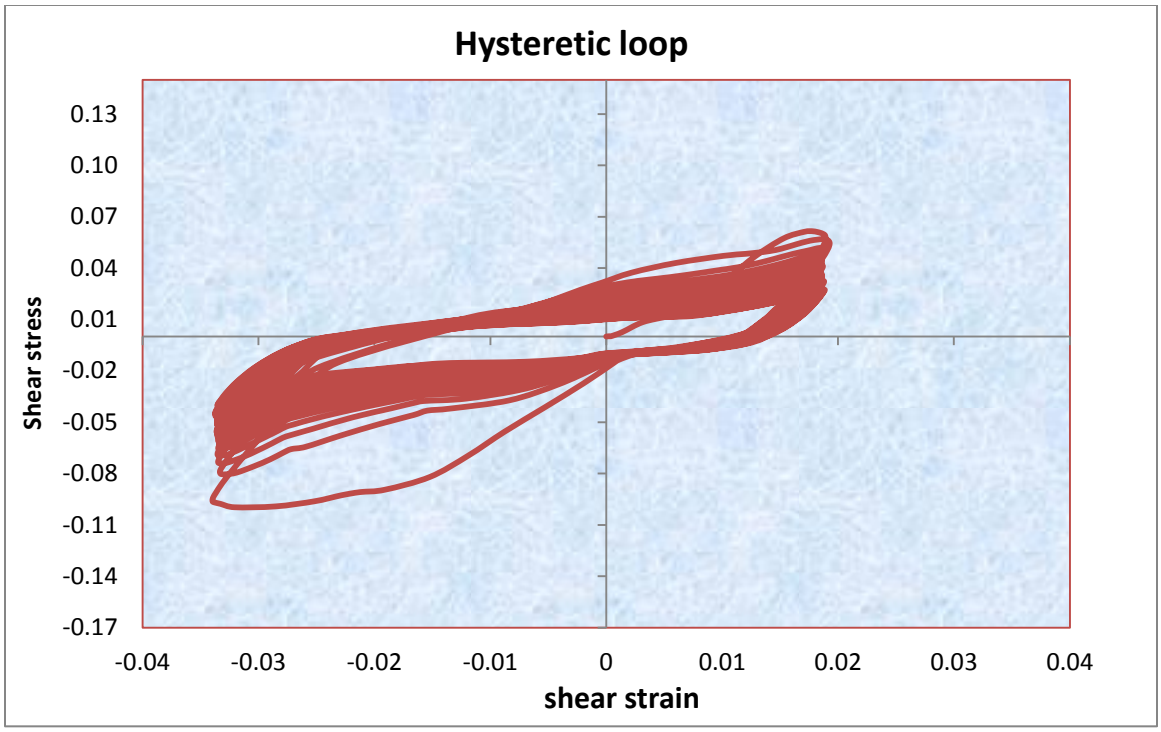

Figure 4. 7: Shear stress vs. shear strain (hysteretic loop) @ 250 kPa

Table 4. 4: Typical tabulation for shear stress and shear strain values

Cycle No.	Time (sec)	Lateral Lvdt	Lateral Force	shear stress=(F/A)*10^3 Mpa	shear strain=(disp. /19.95)	(τi-τi+1)*(γi+γi+1)
5	0	-0.1259	0.0520	0.013517	-0.006374	1.4650251E-05
	0.019	0.0019	0.0610	0.015851	0.000095	-1.4627485E-05
	0.038	0.1198	0.0701	0.018226	0.006064	-5.0697135E-05
	0.057	0.2277	0.0812	0.021107	0.011529	-9.5514265E-05
	0.076	0.3485	0.0938	0.024381	0.017644	-1.3303489E-04
	0.095	0.4471	0.1065	0.027684	0.022637	-1.9277961E-04
	0.114	0.5450	0.1213	0.031522	0.027593	-2.2304575E-04
	0.133	0.6340	0.1357	0.035258	0.032100	-2.8719384E-04
	0.152	0.7127	0.1519	0.039470	0.036084	-2.9291853E-04
	0.171	0.7826	0.1668	0.043340	0.039624	-2.9407050E-04
	0.190	0.8383	0.1806	0.046923	0.042444	-2.6748642E-04
	0.209	0.8847	0.1924	0.049989	0.044794	-2.1296863E-04
	0.228	0.9199	0.2014	0.052320	0.046577	-1.3118419E-04
	0.247	0.9438	0.2067	0.053710	0.047788	-6.4620428E-05

	0.266	0.9599	0.2093	0.054380	0.048603	-2.5423623E-04
	0.285	0.9705	0.2193	0.056981	0.049141	3.0758793E-04
Cycle No.	Time (sec)	Lateral Lvdt	Lateral Force	shear stress=(F/A)*10^3 Mpa	shear strain=(disp. /19.95)	(τi-τi+1)*(γi+γi+1)
5	0.304	1.0057	0.2075	0.053907	0.050921	2.0816535E-04
	0.323	0.9721	0.1995	0.051829	0.049218	5.2811411E-04
	0.342	0.9606	0.1787	0.046432	0.048635	1.1280467E-03
	0.361	0.9292	0.1333	0.034643	0.047050	1.7800494E-03
	0.380	0.8428	0.0570	0.014803	0.042674	1.1766045E-03
	0.399	0.7036	-0.0009	-0.000223	0.035626	2.6346431E-04
	0.418	0.5503	-0.0168	-0.004373	0.027864	9.8279153E-05
	0.437	0.4800	-0.0241	-0.006257	0.024305	1.5485084E-04
	0.456	0.3698	-0.0379	-0.009856	0.018723	6.7206751E-05
	0.475	0.1807	-0.0472	-0.012267	0.009148	1.8400525E-05
	0.494	0.1065	-0.0521	-0.013533	0.005393	1.7369650E-05
	0.513	0.0336	-0.0615	-0.015980	0.001703	-2.0329273E-05
	0.532	-0.1655	-0.0732	-0.019026	-0.008379	-2.7805375E-05
	0.551	-0.2572	-0.0782	-0.020325	-0.013023	-7.7198888E-05
	0.570	-0.3027	-0.0887	-0.023048	-0.015326	-2.2570596E-04
	0.589	-0.4993	-0.1101	-0.028606	-0.025283	-1.1634676E-04
	0.608	-0.5844	-0.1183	-0.030727	-0.029589	-1.3482580E-04
	0.627	-0.6128	-0.1268	-0.032951	-0.031026	-4.8468959E-04
	0.646	-0.7352	-0.1541	-0.040052	-0.037225	-3.8509203E-04
	0.665	-0.8351	-0.1728	-0.044896	-0.042282	-8.9921035E-05
	0.684	-0.8525	-0.1768	-0.045948	-0.043164	-2.9760566E-04
	0.703	-0.8835	-0.1899	-0.049334	-0.044735	-6.2318699E-04
	0.722	-0.9610	-0.2155	-0.056007	-0.048657	-9.6839919E-05
	0.741	-0.9966	-0.2193	-0.056984	-0.050461	7.8924821E-07
	0.76	-1.0030	-0.2193	-0.056976	-0.050785	4.8098959E-05
	0.779	-1.0057	-0.2175	-0.056503	-0.050922	1.0952140E-04
	0.798	-1.0050	-0.2133	-0.055428	-0.050887	2.2041343E-04
	0.817	-1.0013	-0.2050	-0.053258	-0.050700	4.9845151E-04
	0.836	-0.9906	-0.1859	-0.048316	-0.050155	1.1696748E-03
	0.855	-0.9582	-0.1403	-0.036461	-0.048517	1.6039157E-03
	0.874	-0.8780	-0.0739	-0.019210	-0.044458	1.0703316E-03
	0.893	-0.7684	-0.0245	-0.006371	-0.038908	5.0661607E-04
	0.912	-0.6343	0.0029	0.000761	-0.032118	2.2889655E-04
	0.931	-0.5110	0.0181	0.004708	-0.025873	-1.2182212E-04

Using shear stress and shear strain values of table 4.3, the hysteresis loop is plotted. The triangle with A and B side dimensions were presented in Figure 4.8.

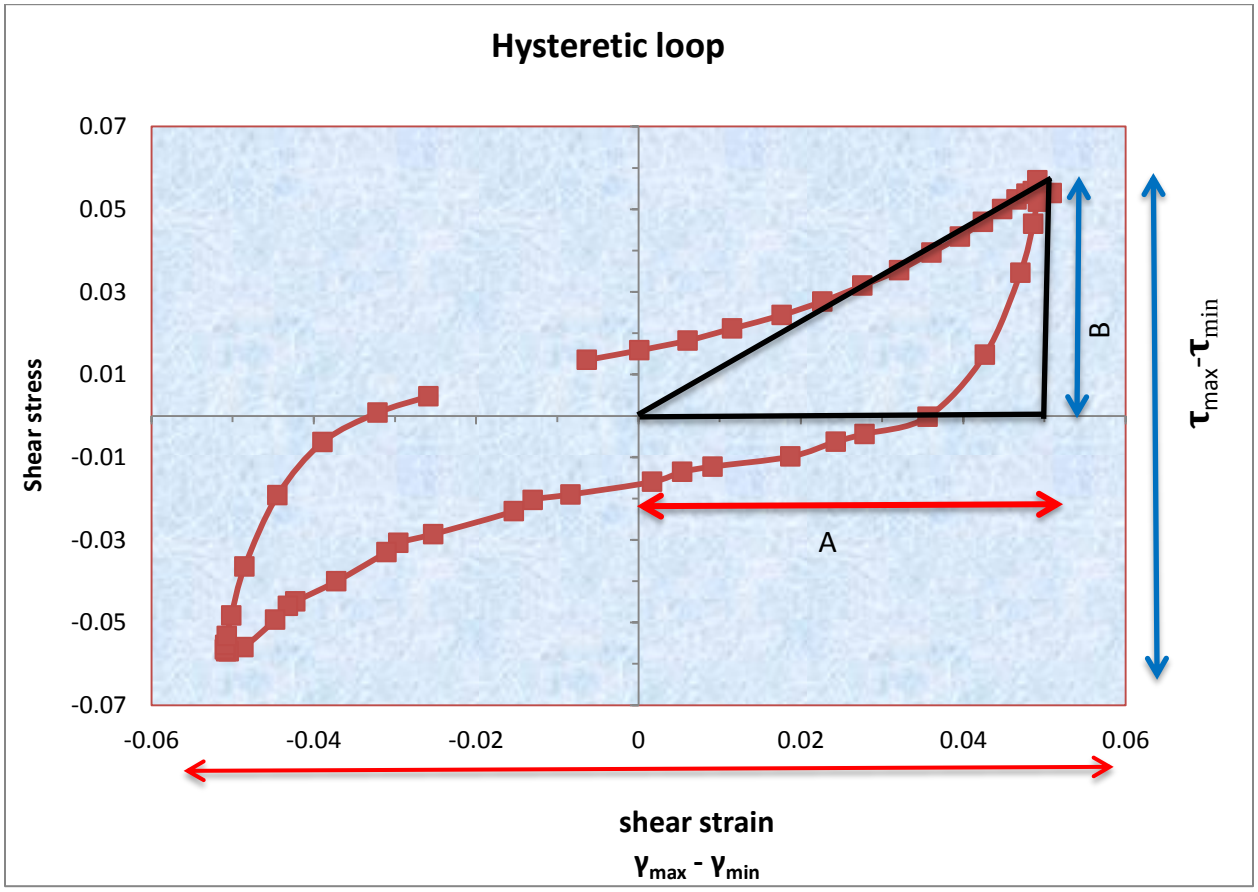

Figure 4. 8: The hysteretic loop and triangle plotted using table 4.4 stress and strain

Shear modulus and damping ratio of hysteresis loop are calculated using the following equations:

The equivalent shear modulus of the hysteresis loop was calculated by using Equation 4.3 to 4.6.

$$G = \frac{(\tau_{max} - \tau_{min})}{(\gamma_{max} - \gamma_{\min})} \qquad 4.3$$

$$D = \frac{A_{loop}}{4\Pi * A_{\Delta}} \qquad 4.4$$

$$A_{loop} = 0.5 * (\tau_i - \tau_{i+1}) * \gamma_i + \gamma_{i+1} \quad 4.5$$

$$A_{\Delta} = 0.5 * A * B \quad 4.6$$

2A – The difference between the maximum and the minimum values of shear strain

2B - The difference between the maximum and the minimum values of shear stress

Table 4. 5: Typical calculation for shear modulus and damping ratio using table 4.3 and figure 4.8

Calculation of Shear Modulus		Calculation of Damping Ratio	
$\boldsymbol{\tau}_{max}$	0.0570	Area of hystress loop $= 0.5 * (\tau_i - \tau_{i+1}) * \gamma_i + \gamma_{i+1}$	0.0030
$\boldsymbol{\tau}_{min}$	-0.0570	Area of a triangle $= 0.5 * A * B$	0.0058
$\boldsymbol{\tau}_{max} - \boldsymbol{\tau}_{min} = 2B$	0.1140		
$\boldsymbol{\gamma}_{max}$	0.0509	$D = \frac{A_{loop}}{4\Pi * A_{\Delta}} * 100\%$	16.474
$\boldsymbol{\gamma}_{min}$	-0.0509		
$\boldsymbol{\gamma}_{max} - \boldsymbol{\gamma}_{min} = 2A$	0.1018		
$G = \frac{(\tau_{max} - \tau_{min})}{(\gamma_{max} - \gamma_{min})}$ in MPa	1.1190		

Based on Table 4.3 and Table 4.4, the value of shear modulus and damping ratio of each cycle in a test can be determined. In this study, a single specimen was tested up to 40 cycles and Table 4.5 shows shear modulus and damping ratio values of each cycle for TP2 under an axial stress of 200 kPa.

Table 4. 6: Shear modulus and damping ratio values for TP2 under an axial stress of 250 kPa

Strain level	0.01%	0.1%	1%	2.5%	5%	0.01 %	0.1%	1%	2.5%	5%
Cycle No.	G (MPa)					D (%)				
1	5.294	3.465	2.310	1.864	1.663	4.396	5.655	11.304	17.991	21.405
2	5.191	3.322	2.301	1.850	1.651	4.546	5.649	10.645	17.792	21.393
3	4.763	3.315	2.277	1.831	1.651	4.173	5.589	9.861	16.500	21.388
4	4.648	3.098	2.003	1.794	1.600	4.252	5.162	9.956	15.205	20.719
5	4.621	3.086	1.994	1.762	1.549	4.001	5.574	10.112	15.161	20.659
6	4.528	2.980	1.976	1.711	1.535	4.231	5.162	9.137	14.656	20.250
7	4.356	2.969	1.971	1.684	1.527	4.010	5.068	9.439	13.956	20.006
8	4.321	2.964	1.864	1.652	1.526	4.260	5.122	8.984	14.306	19.188
9	4.300	2.961	1.862	1.634	1.516	4.100	4.987	9.156	13.365	18.684
10	4.255	2.960	1.877	1.613	1.515	3.969	5.077	9.439	14.031	18.612
11	4.255	2.948	1.851	1.592	1.481	3.848	4.923	8.783	13.165	18.311
12	4.183	2.948	1.844	1.581	1.455	3.727	5.006	8.681	13.790	18.304
13	4.127	2.945	1.838	1.559	1.431	3.946	4.936	8.677	13.389	18.047
14	4.089	2.944	1.833	1.546	1.409	3.625	4.875	8.485	13.974	17.949
15	4.109	2.938	1.830	1.537	1.389	3.932	4.936	8.433	13.374	17.730
16	4.070	2.721	1.751	1.530	1.368	3.653	5.090	8.803	12.599	17.682
17	4.077	2.721	1.748	1.524	1.357	3.880	4.964	8.388	13.339	17.630
18	4.049	2.721	1.747	1.508	1.343	3.603	4.958	8.568	12.718	17.591
19	4.051	2.719	1.741	1.505	1.326	3.854	4.923	8.308	13.277	17.540
20	4.040	2.715	1.751	1.500	1.312	3.580	4.895	8.971	12.728	17.426
21	4.029	2.719	1.737	1.498	1.302	3.836	4.940	8.296	13.181	17.344

22	4.022	2.714	1.735	1.486	1.290	3.556	4.852	8.396	12.733	17.184
Strain level	0.01%	0.1%	1%	2.5%	5%	0.1%	0.1%	1%	2.5%	5%
Cycle No	G (MPa)					D (%)				
23	4.017	2.717	1.731	1.480	1.278	3.317	4.808	8.230	13.319	17.122
24	4.001	2.707	1.731	1.476	1.267	3.558	4.846	8.319	12.580	17.068
25	4.010	2.710	1.656	1.470	1.257	3.270	4.721	8.287	13.311	16.793
26	3.964	2.684	1.653	1.465	1.250	3.503	4.873	8.133	12.516	16.428
27	3.949	2.685	1.650	1.455	1.245	3.250	4.987	8.451	12.180	16.426
28	3.949	2.682	1.650	1.449	1.229	3.528	4.870	8.164	12.807	16.368
29	3.939	2.674	1.647	1.441	1.217	3.220	5.041	8.480	12.362	16.302
30	3.922	2.658	1.647	1.436	1.216	3.228	4.721	8.480	12.992	16.199
31	3.922	2.651	1.645	1.431	1.204	3.207	4.813	8.258	12.412	16.179
32	3.916	2.654	1.642	1.425	1.195	3.505	4.810	8.131	13.222	16.145
33	3.915	2.646	1.643	1.419	1.193	3.206	4.897	8.281	12.512	16.138
34	3.909	2.645	1.638	1.414	1.184	2.986	4.816	8.098	13.370	16.116
35	3.822	2.593	1.585	1.408	1.181	3.148	4.806	8.062	12.682	16.095
36	3.858	2.597	1.584	1.403	1.166	2.997	4.627	8.228	13.534	16.055
37	3.890	2.593	1.583	1.397	1.166	2.919	4.839	8.109	12.726	16.049
38	3.795	2.590	1.580	1.393	1.150	2.836	5.092	8.374	12.276	16.006
39	3.806	2.593	1.580	1.388	1.159	2.847	4.788	7.929	12.932	15.911
40	3.806	2.590	1.585	1.384	1.152	2.829	4.619	8.062	12.445	15.851

CHAPTER FIVE

RESULT AND DISCUSSIONS

5.1 Dependency of shear modulus and damping ratio on shear strain amplitude

According to test results obtained, the shear modulus decreases and damping ratio increase as the cyclic shear strain increases. Shear modulus versus cyclic strain amplitude and damping ratio versus cyclic strain amplitude were plotted in Figure 5.1 and Figure 5.2.

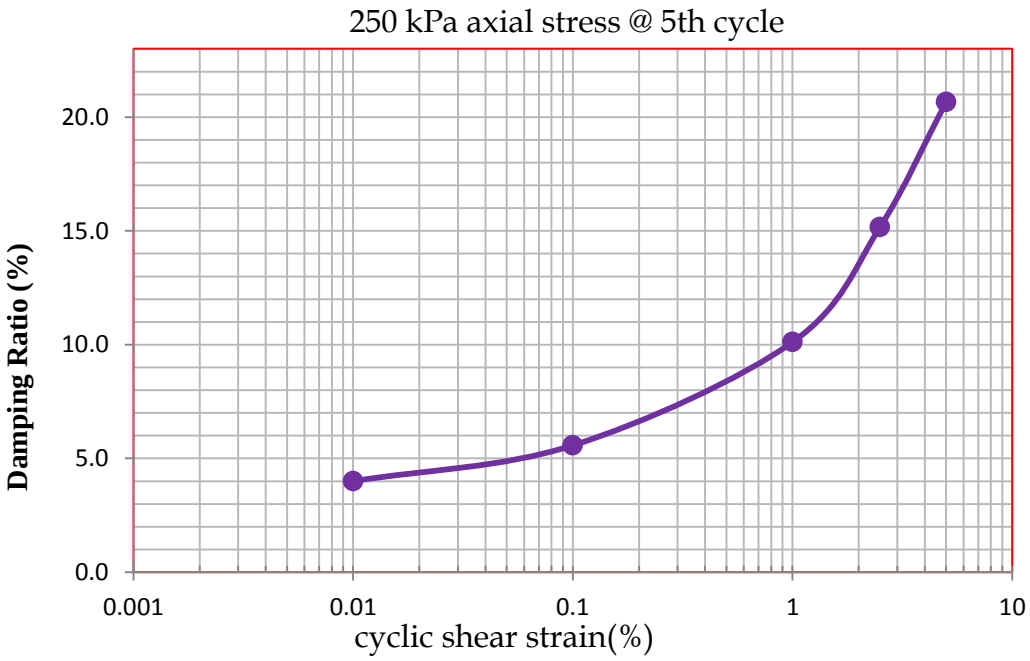

Figure 5. 1: Effect of cyclic shear strain on the values of damping ratio

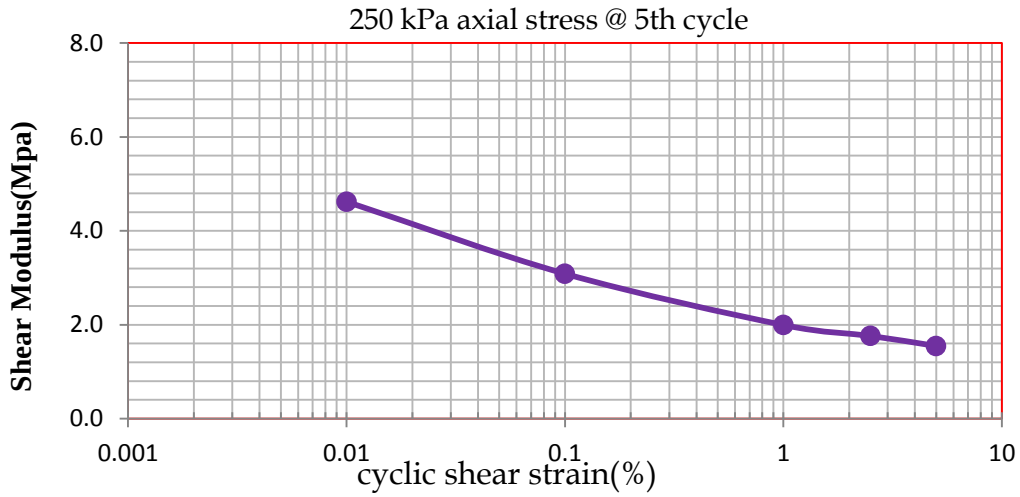

Figure 5. 2: Effect of cyclic shear strain on the values of shear modulus (MPa)

5.2 Influence of effective vertical stress on Shear Modulus and damping ratio

The vertical stress has a major influence on shear modulus and damping characteristics. Samples were consolidated under different axial stress in order to evaluate the influence of vertical stress. The result showed that soil samples confined to a higher stress have higher shear modulus and lower damping ratio values as shown in figure 5.3 and 5.4.

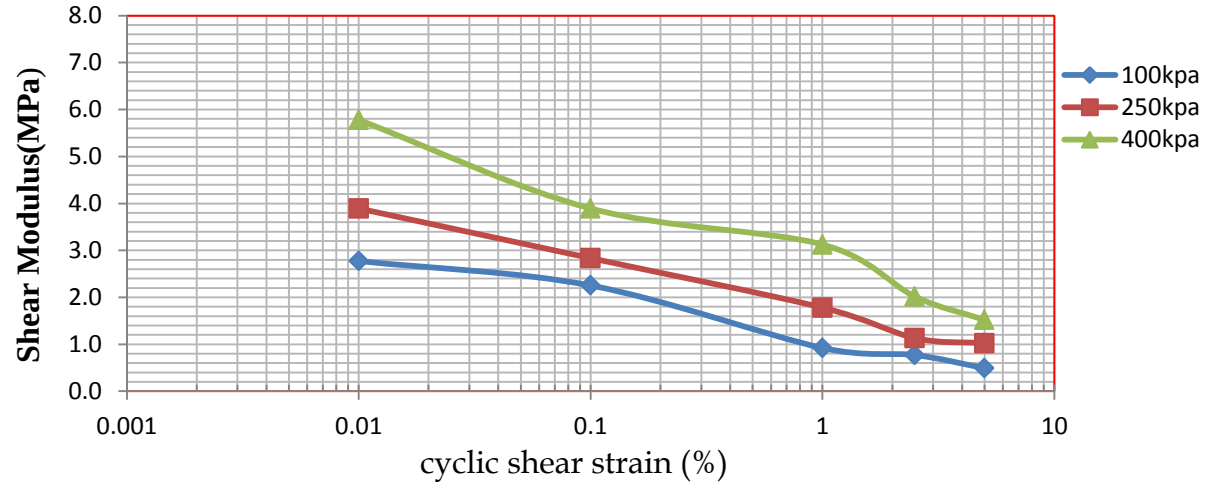

Figure 5. 3: Effect of vertical stress on shear modulus (MPa)

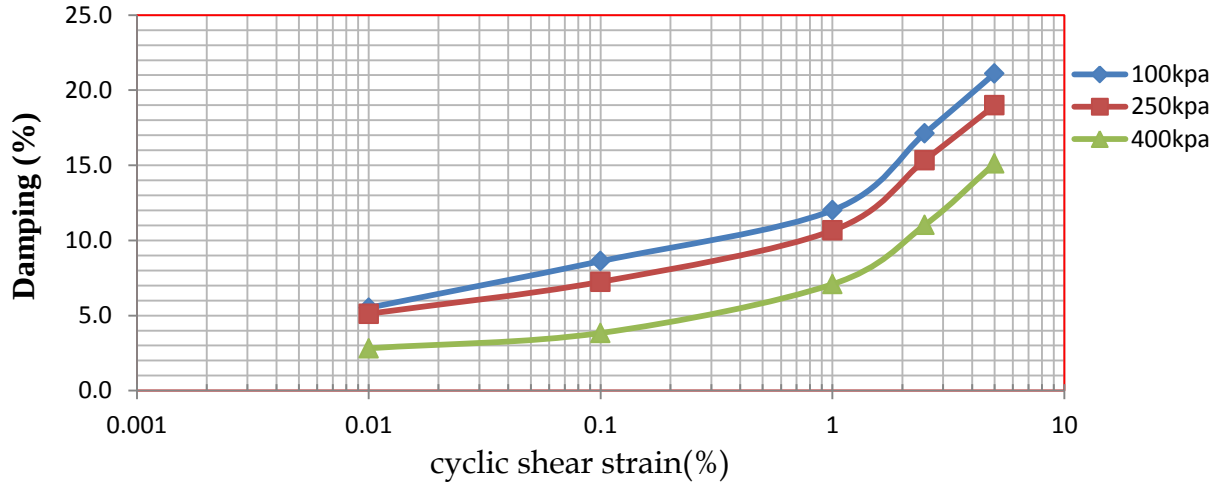

Figure 5. 4: Effect of vertical stress on damping ratio (%)

5.3 Influence of number of loading cycles on shear modulus and damping ratio

From the test result, it can be observed that the shear modulus and damping ratio decreases with increasing number of loading cycle shown in Figure 5.5 and 5.6. During cyclic shearing process soil specimen grains comes closer to each other resulting increases the cyclic shear modulus.

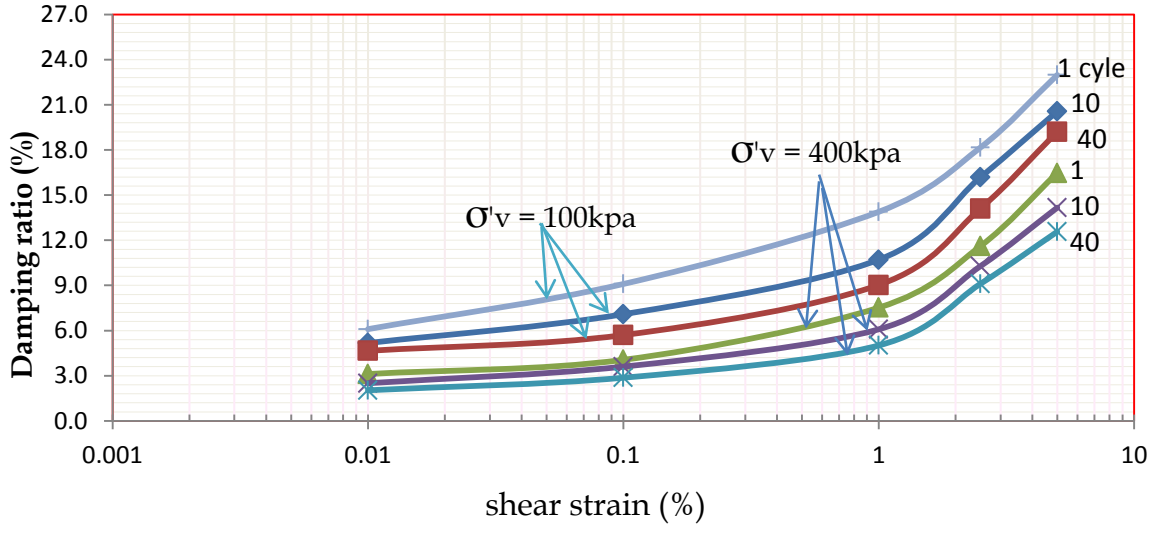

Figure 5. 5: Effects of number of loading cycles on the value of damping ratio (%)

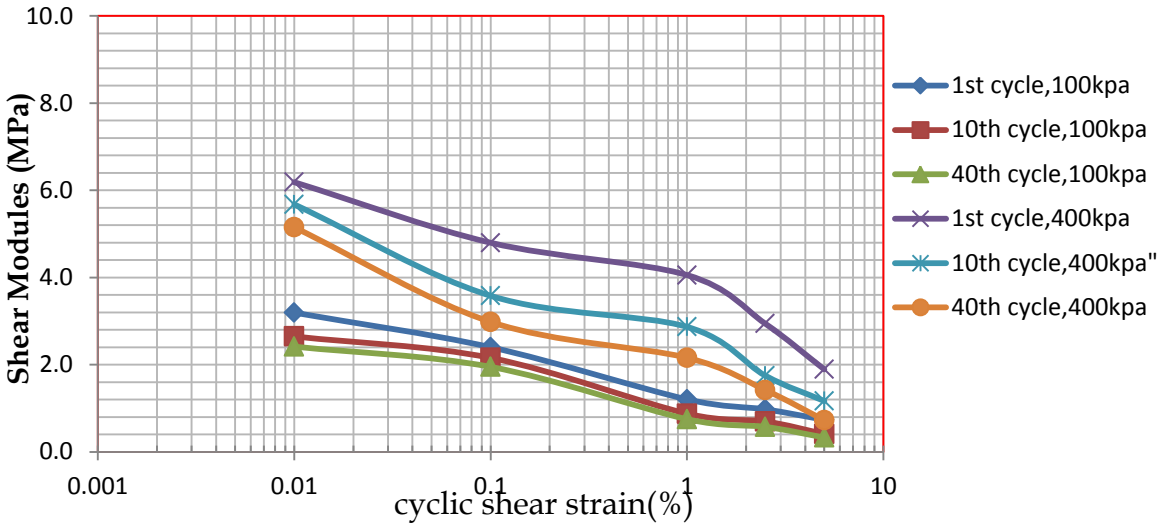

Figure 5. 6: Effects of number of loading cycles on the value of shear modulus (MPa)

5.4 Effect of void ratio on damping ratio

When void ratio decreases, the area of contact between soil particles becomes closer which has its impact on the dynamic behavior of soils. The influence of void ratio on the damping characteristics was presented in Figure 5.7. It could be observed from the test result that the specimens having higher initial void ratio have lower damping ratio.

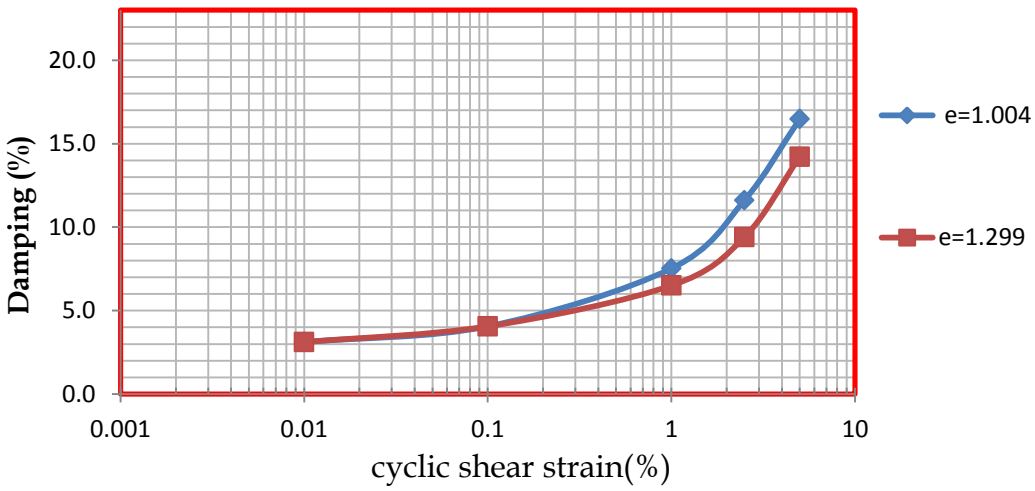

Figure 5. 7: Effects of void ratio on the values of damping ratio (%)

5.5 Effect of soil plasticity on damping ratio and shear modulus

The values of shear modulus and damping ratio are influenced by the physical properties of soils mainly plasticity index. The dependency of shear modulus and damping ratio value on plasticity index were drawn in Figure 5.8 and 5.9 below. From these figures it was observed that when the plasticity of the soil increases the damping ratio decreases and shear modulus value increases.

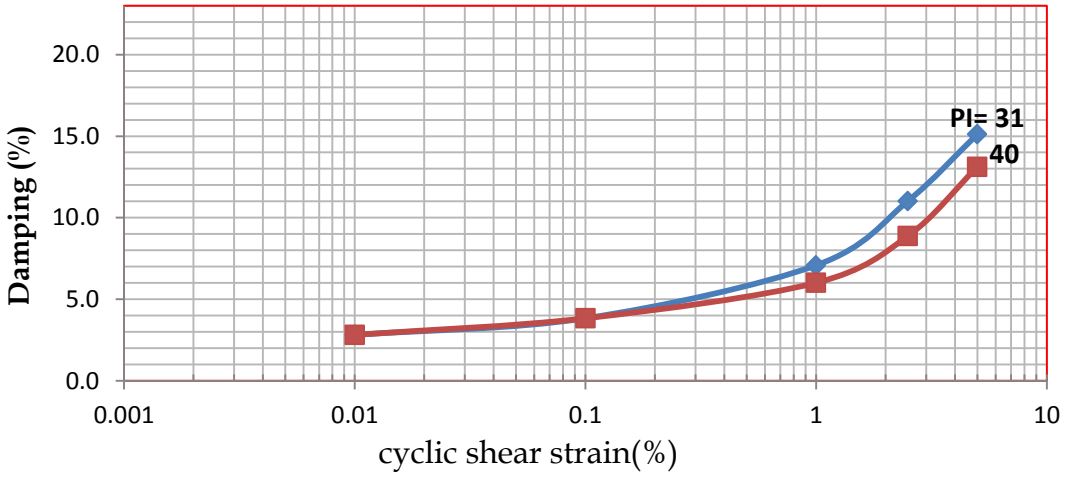

Figure 5. 8: Effects of plasticity index on the values of damping ratio (%)

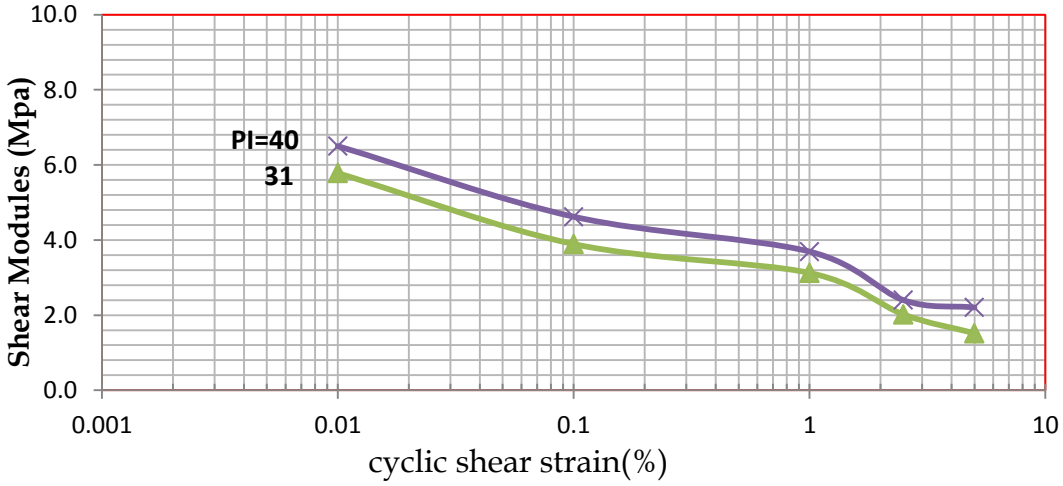

Figure 5. 9: Effects of plasticity index on the values of shear modulus (MPa)

5.6 Determination of maximum shear modulus

Maximum shear modulus ($Gmax$) is the peak value of secant shear modulus at very low strain amplitude (in the elastic range; typically lower than $\boldsymbol{\gamma}$ of 10^{-4} %) which is not possible directly measure using cyclic simple shear test. $Gmax$ is soil stiffness parameter and noted that it plays a vital part in determination of normalized shear modulus (G/Gmax). The maximum shear modulus could be estimated using the following equation for sands and undisturbed cohesive soils (Hardin 1972).

$$G_{max} = 1230 * \frac{(2.973-e)^2 * (OCR)^a * (\sigma'_m)^{0.5}}{1+e} \quad \text{.....5.1}$$

Where: OCR = over consolidation ratio, $\frac{P_r}{P_o}$

P_r = Pre consolidation pressure of a specimen

P_o = Present effective vertical pressure

e = void ratio of the soil

σ'_m = mean effective confining stress

K = 0.5, is the coefficient of lateral pressure at rest

a = parameter that depends on the plasticity index of the soil

$$\sigma'_m = \frac{\sigma_1 + \sigma_2 + \sigma_3}{3} \text{..... ....5.2}$$

$$\sigma_3 = \sigma_2 = K * \sigma_1 \text{..... ..... 5.3}$$

Depending on plasticity index linear interpolation was used for the determination of a using Table 2.1 Based on equation 5.1 to 5.3, the values of G_{max} can be calculated and presented in Table 5.1 and summary of the values of G_{max} is presented in Table 5.2.

Table 5. 1: maximum shear modulus determination at different axial stress

Test pit	Parameter	Axial stress		
		100 kPa	250 kPa	400 kPa
TP1	Void ratio (e)	1.004	1.004	1.004
	a	0.246	0.246	0.246
	Over consolidation ratio (OCR)	0.850	0.340	0.213
	Maximum shear modulus (Gmax in kPa)	85312.58	107668.62	121320.86
TP2	Void ratio (e)	1.299	1.299	1.299
	a	0.30	0.30	0.30
	Over consolidation ratio (OCR)	0.650	0.260	0.1625
	Maximum shear modulus (Gmax in kPa)	49162.96	59049.41	64929.14

From the Table 5.1, the normalized shear modulus (G/Gmax) curves were determined and presented at fifth cycle for different axial stress. The result was summarized in Table 5.2.

Table 5. 2: Normalized shear modulus (G/Gmax) versus shearing strain amplitude

Test pit	Axial pressure	Shear strain (%)				
		0.01	0.1	1	2.5	5
		G/G_{max}				
TP1	100 kPa	0.033	0.026	0.011	0.009	0.006
	250 kPa	0.036	0.026	0.017	0.011	0.010
	400 kPa	0.048	0.032	0.026	0.017	0.013
TP2	100 kPa	0.087	0.058	0.028	0.022	0.015
	250 kPa	0.078	0.052	0.034	0.030	0.026
	400 kPa	0.100	0.071	0.057	0.033	0.034

From the table 5.2 the curve normalized shear modulus (G/Gmax) versus shear strain amplitude drawn to indicate the influence of plasticity index in figure 5.10. Curves of effect of axial stress on G/Gmax shown in appendix D.

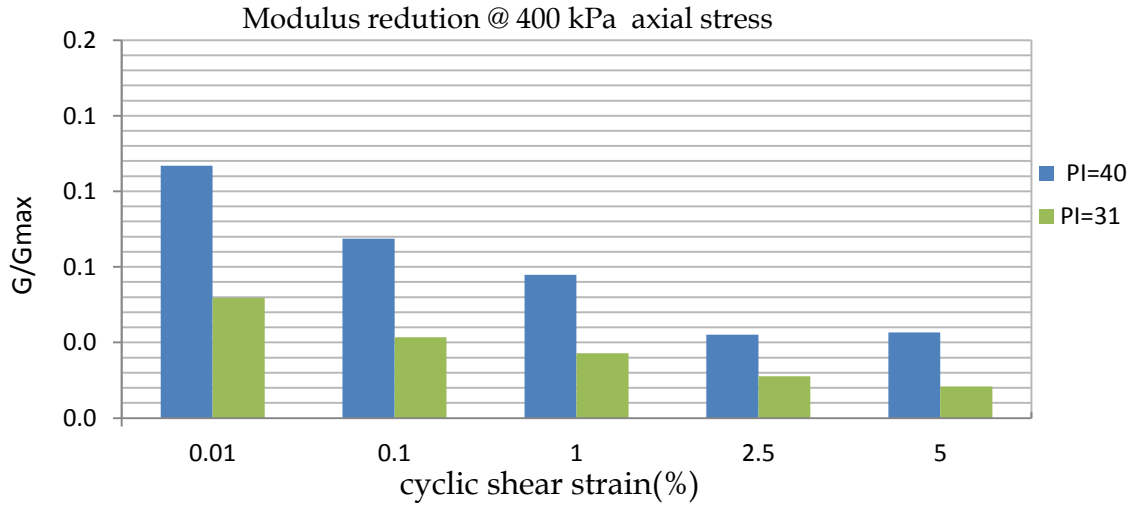

Figure 5. 10: Effect of plasticity index on normalized shear modulus (G/Gmax)

5.7 Comparison of test result with previous studies

For different soil types, previously some researchers developed different modulus reduction and damping ratio curves. Abenezer (2017) perfomed a simple shear test on silt soils of Addis Ababa, while Mengesha's (2013) work were done on silt and clay soils of Arba Minch. Tesfaye (2012) determined the clay soils of Dessie and Abraham (2014) investigated the silty sand and sandy silt soils of Ziway. Ayalew (2013) also tasted the silt soils of Hawassa.

5.7.1 Shear modulus reduction

The computed normalized shear modulus (G/Gmax) values from Table 5.9 are plotted against shear strain on the curves developed by Tesfaye (2012), Mengesha (2013), Ayalew (2013), Abraham (2014) and Abenezer (2017) as shown in Figure 5.11 to 5.15.

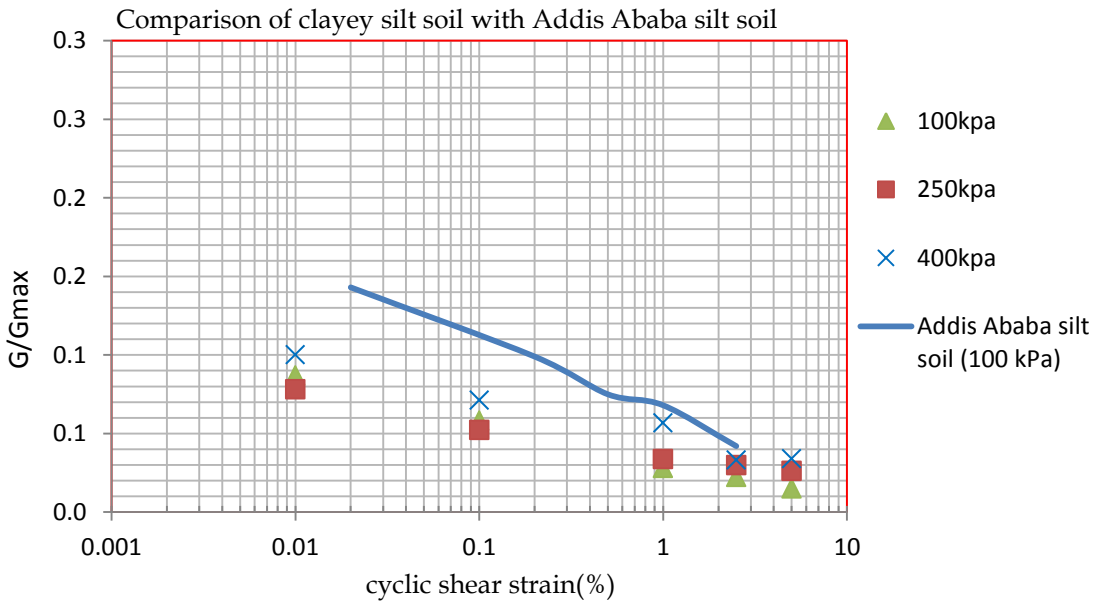

Figure 5. 11: (G/Gmax) of clayey silt soil with curve drawn by Abenezer (2017)

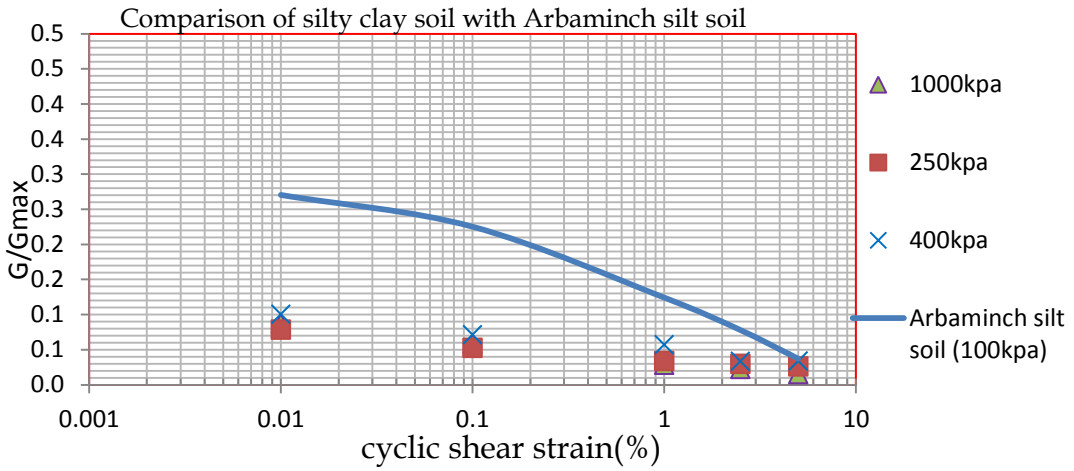

Figure 5. 12 (G/Gmax) of silty clay soil with curve drawn by Mengesha (2013)

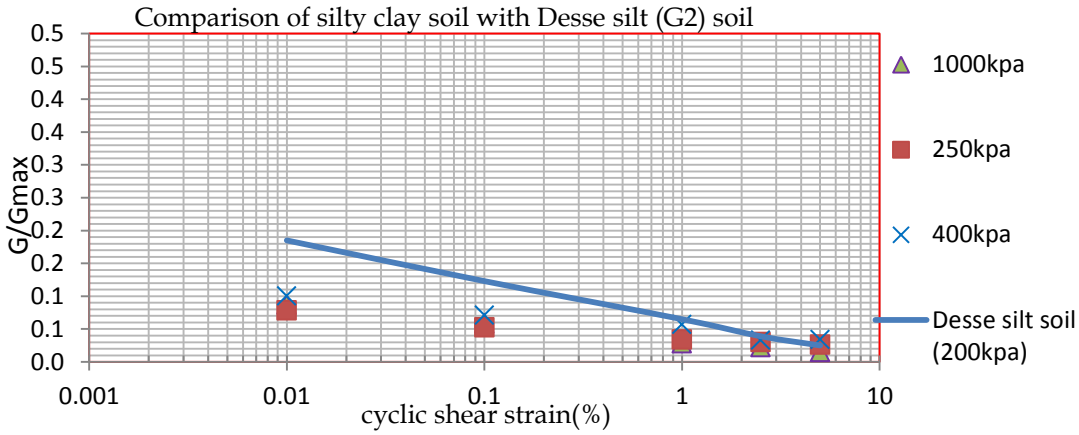

Figure 5. 13: (G/Gmax) of silty clay soil with curve drawn by Tesfaye (2012)

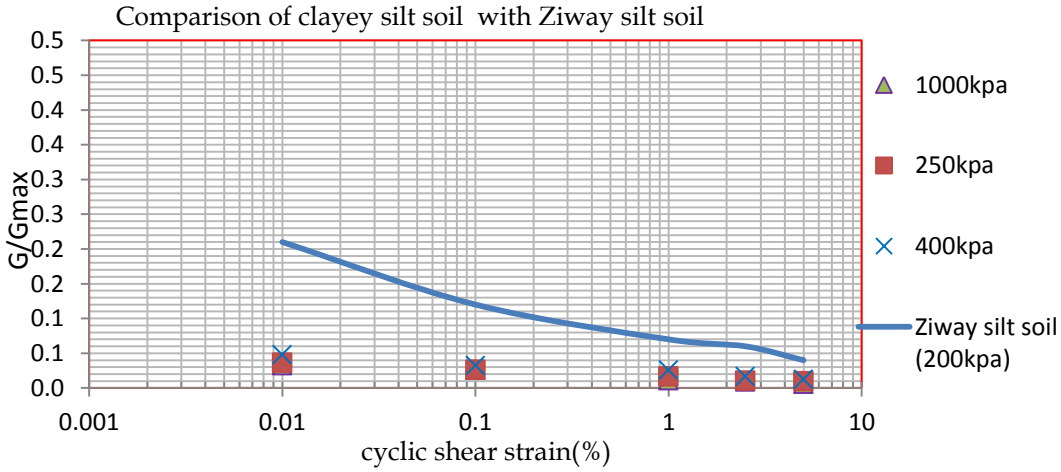

Figure 5. 14: (G/Gmax) of clayey silt soil with curve drawn by Abraham (2014)

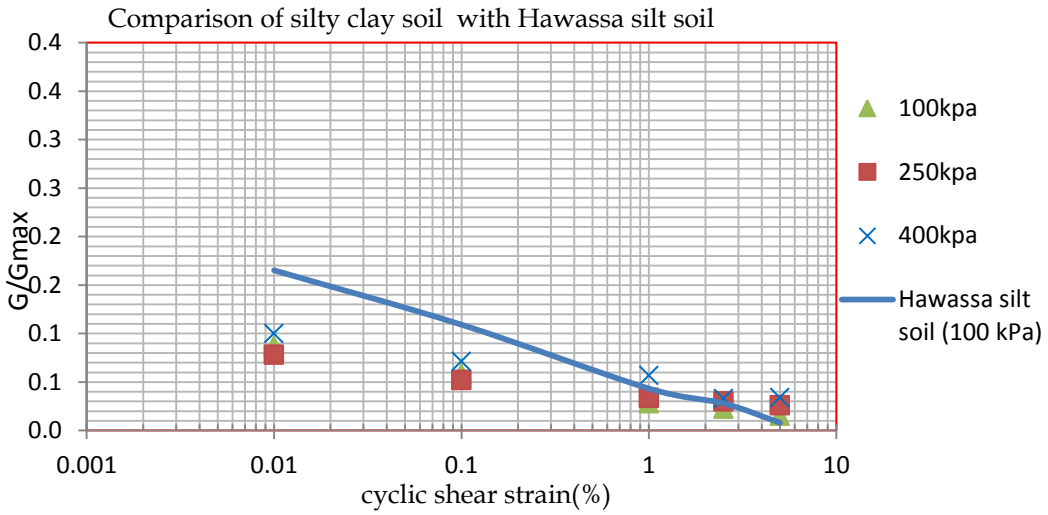

Figure 5. 15: (G/Gmax) of silty clay soil with curve drawn by Ayalew (2013)

It was illustrated in the above figures that the normalized shear modulus values have good agreement with curve developed by Abenezer (2017) and Ayalew (2013) and with other curves at higher strain values. However, the values at lower strain amplitude is lower than the curves developed by Tesfaye (2012), Mengesha (2013), Abraham (2014), the variation may come from different reasons like over consolidation ratio and sampling technique.

5.7.2 Damping ratio Comparison

The damping ratio test result obtained in the laboratory were drawn in the figure 5.16 to 5.18 with different axial loads to compare the damping value of this study and the previously published work by Ayalew (2013), Mengesha (2013) and Abraham (2014) and was plotted in figure below. It's shown that the damping ratio value of silt soils developed by Abraham (2014) were larger than clayey silt soil of Jimma, at higher strain. However the clay silt soil has a good agreement with clay soil which is studied by Mengesha (2013), and silt soil reported by Ayalew (2013).

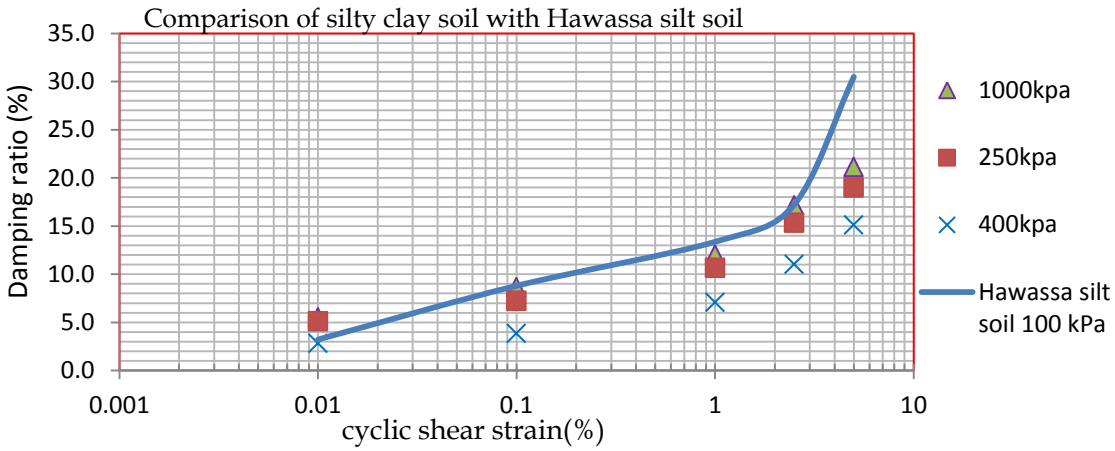

Figure 5. 16: Damping ratio of silty clay soil with curve drawn by Ayalew (2013)

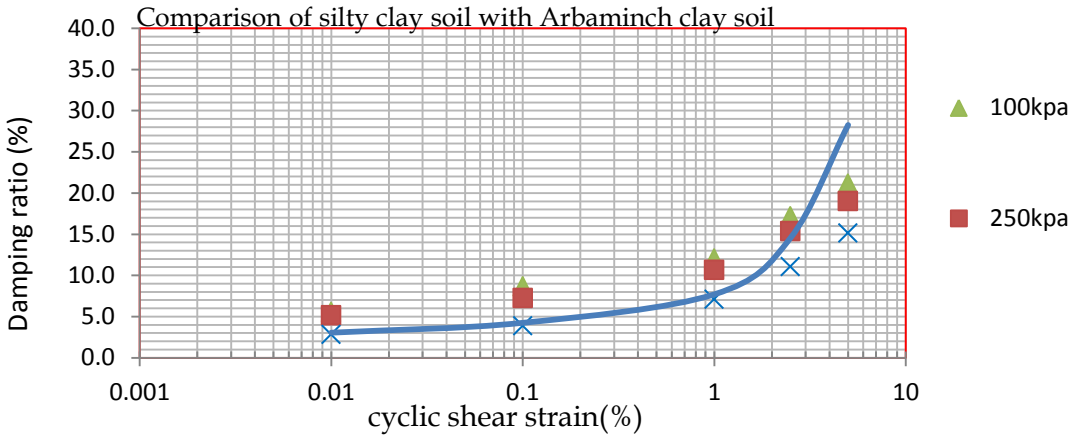

Figure 5. 17: Damping ratio of silty clay soil with curve drawn by Mengesha (2013)

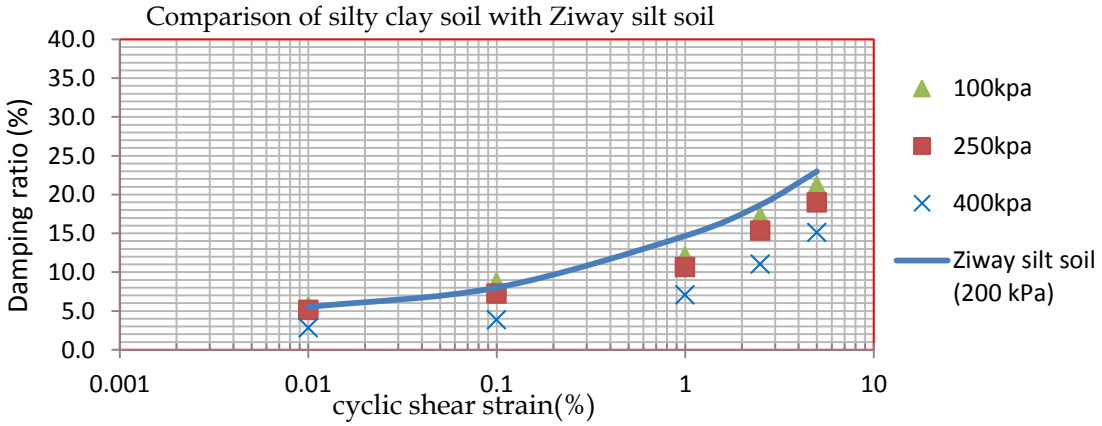

Figure 5. 18: Damping ratio of silty clay soil with curves drawn by Abraham (2014)

CHAPTER SIX

CONCLUSIONS AND RECOMMENDATIONS

6.1 Conclusions

The experimental investigation of dynamic soil property using cyclic simple shear machine was taken from four different points in Jimma town. Using undisturbed samples the shear modulus and damping characteristics of silty clay and clayey silt soil were determined. From a series of cyclic shear test for shearing strain range of 0.01% to 5%, the following conclusion was drawn.

- Generally with increasing the number of loading cycles both shear modulus and damping ratio decreases, but the rate of decrement is not uniform throughout the loading cycles for silty clay and clayey silt soils.
- Shear modulus reduction (G/Gmax) values at higher strain level agree with previous studies, but at lower strain level it is lower.
- The maximum shear modulus value increases as the pre consolidation pressure increases and vice versa.
- The normalized shear modulus values decreases as the rate of strain increases and damping ratio increases as the shear strain increases.
- Damping ratio values obtained in the lab ranges from 2.03% to 22.98% and shear modulus value ranges from 0.33MPa to 6.98MPa.
- As strain increases, the normalized shear modulus decreases and damping ratio values increases.

6.2 Recommendations for Future work

- The results obtained from this research study provide some basic insights about normalized shear modulus and damping characteristics of soil in Jimma town.
- More data on modulus and damping on the soil from various locations using different testing equipment would help to construct more accurate specific modulus reduction and damping curves for silty clay and clayey silt soil of Jimma town.
- Tests using cyclic triaxial and resonant column devices would provide additional information regarding the influence of loading mode, anisotropy and principal stress rotation on monotonic and cyclic strength of soil.
- Investigation to a very deep sub surface profile using some drilling equipment can also give the depth effect of dynamic soil parameters.

REFERENCES

Abenezer T.,"Investigation of the Damping Ratio and Shear Modulus of Soil along Light Rail Transit Route in Megenagna-Hayat Road," International Journal of Scientific & Engineering Research, 2017, v 8, pp.111-122.

Aberham Mengistu, "Investigation in to some dynamic properties of soils around ziway", Addis Ababa University,2014.

Abu Gemechu," Shear modulus and Damping ratio values of soils found in Adama", Addis Ababa University, 2011.

ASTM, "American society for testing and materials", Annual Book of ASTM Standards,1998

Ayalew Gashaw, "Shear modulus and Damping ratio values of soils found in Adama ", Addis Ababa University, 2013.

Boonam Shin," Effects of Oversized Particles on the Dynamic Properties of Sand Specimens Evaluated by Resonant Column Testing, Austin" University of Texas, 2014.

Das, B.M., "Principles of Soil Dynamics", California State University, Scramento:, 1993.

David Umberg," Dynamic Properties of Soils with Non-Plastic Fines," Austin: University of Texas, 2012

Girmachew Yimer," shear modulus and Damping Ratio of Dry Koka Sand Cyclic Simple Shear Test", Addis Ababa University, 2010

Hardin, B. O. and V. P. Drnevich, "Shear Modulus and Damping in Soils: Design Equations and Curves." Journal of the Soil Mechanics and Foundations Division, ASCE, 1972 Vol. 98, No.SM7, pp. 667-692.

H. Bolton Seed, Robert T. Wong, I.M Idriss and K. Tokimatsu, University of California. Moduli and Factors for Dynamic Analyses of Cohesionless Soils, 1984.

Kakusho, T.,"Cyclic triaxial test of Dynamic soil properties for wide strain ranges," Central Research Institute of Electric Power Industry, 1979, pp.305-312.

Kramer S.I., "Geotechnical Earthquake Engineering," University of Washington, Prentice-Hall Inc., United States of America,1996

Luna, R., and Jadi, H.,"Determination of dynamic soil properties using Geophsical methods," Department of Civil Engineering, University of Missouri-Rolla, 2000.

MengeshaTefera, Tadiwos Chernet and Workineh Haro,"Geological Survey of Ethiopia," Regional Geology Department EIGS, 1996.

Muge K.," Dynamic soil characterization and site response estimation for Erbaa, Tokat (Turkey," Ankara: Middle East Technical University, 2016.

Priyanka Sharma," Effect of saturation on dynamic properties of Solani sanD," Indian Geotechnical Conference, 2016, pp.01- 05.

Seed, H.B. and Idriss, I.M., "Soil Moduli and Damping factors for dynamic response analyses", EERC/70-10, College of Engineering university of California, Berkeley, 1970

Sentheepan Thirugnanasampanther,"Cyclic behaviour and dynamic properties of soils under simple shear loading," University of East London, 2012.

Shankar S.," Parameters Influencing dynamic Soil Properties," nternational Journal of Innovative Research in Science, Engineering and Technology.,2013, v 03, pp.47-60.

Soheil Moayerian," Effect of Loading Frequency on Dynamic Properties of Soils Using Resonant Column," Canada: university of waterloo, 2012.

Tesfaye, Alemnew, "Index Properties, Shear Strength and Dynamic Properties of Soils Found in Dessie," Addis Ababa University, 2012.

T. G. Sitharam," Dynamic Properties of Dry Sands," Indian Geotechnical Journal, 2008, v 38, pp.334-344.

UTS004, "Simple shear test software reference", Universal testing system, IPC Global limited, 2003

Vucetic and Dobry, "Soil Dynamics and Earth Quake Engineering", 199.

Yamamuro, J. A. and Lade, P. V, "Steady-State Concepts and Static Liquefaction of Silty Sands," Journal of Geotechnical and Geo-environmental Engineering,1998 Vol. 124, pp. 868-87.

APPENDIX A

Atterberg limit test results

Table A- 1: Determination of Liquid Limit, Plastic Limit and Plastic Index (for TP1)

	LIQUID LIMIT			PLASTIC LIMIT	
No. Blows	30	24	17		
Wt.of cont. + wet soil (g.)	31.27	31.90	30.94	15.47	15.17
Wt.of cont. + dry soil (g.)	24.38	24.06	23.86	14.89	14.57
Wt. of water (g.)	6.89	7.84	7.08	0.58	0.60
Wt. container (g.)	13.40	12.30	13.25	13.27	12.88
Wt. dry soil (g.)	10.98	11.76	10.61	1.62	1.69
Water (%)	62.75	66.67	66.73	35.80	35.50
LL = 67		PI = 31		AV. PL (%)	35.70

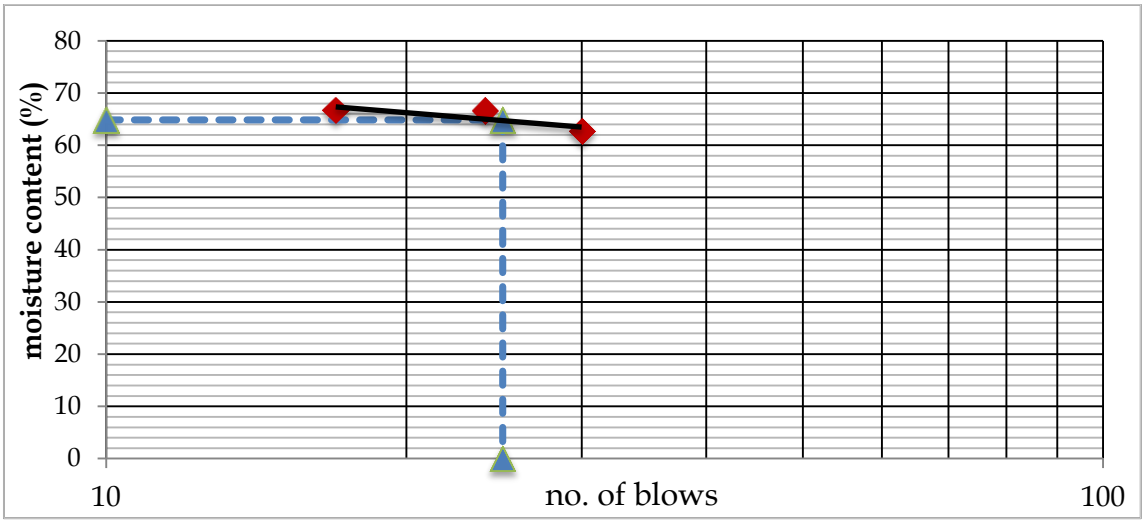

Figure A- 1: Water content versus No. blows

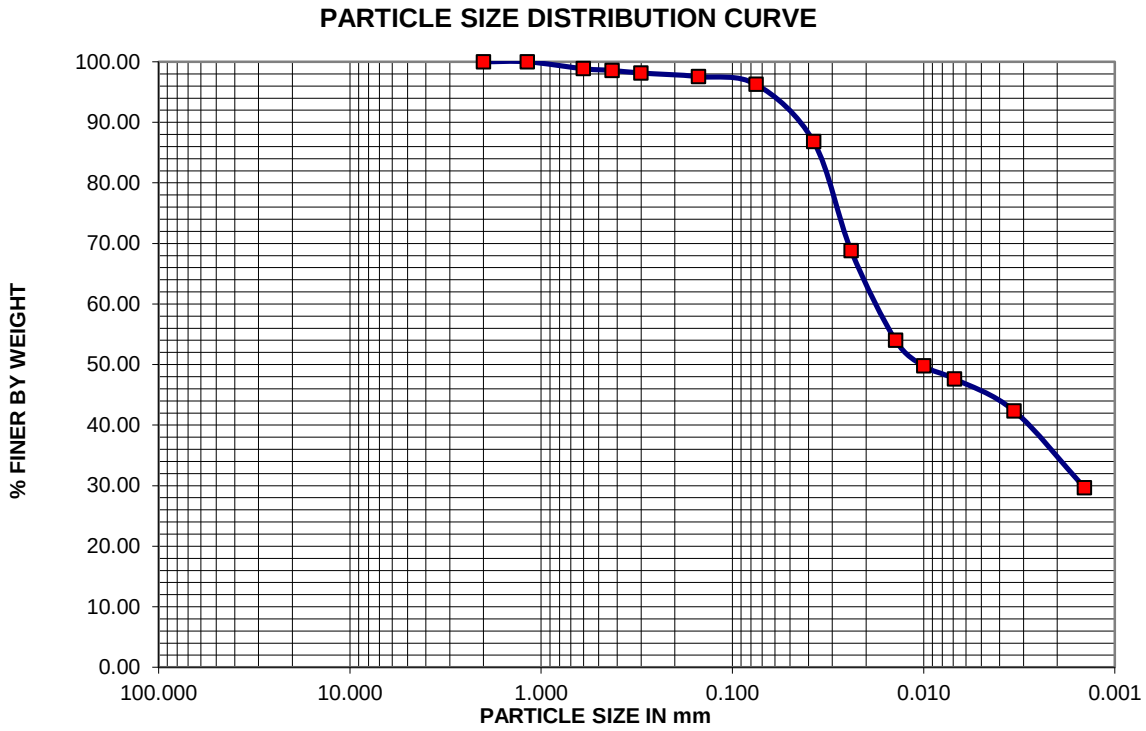

Figure A- 2: Particle size distribution curve for TP1

Table A- 2: Determination of Liquid Limit, Plastic Limit and Plastic Index (for TP2)

	LIQUID LIMIT			PLASTIC LIMIT	
No. Blows	30	25	20		
Wt.of cont. + wet soil (g.)	31.30	31.35	31.20	16.49	16.31
Wt.of cont. + dry soil (g.)	24.22	24.06	23.71	15.82	15.60
Wt. of water (g.)	7.08	7.29	7.49	0.67	0.71
Wt. container (g.)	13.99	13.80	13.35	13.62	13.33
Wt. dry soil (g.)	10.23	10.26	10.36	2.20	2.27
Water (%)	69.21	71.05	72.30	30.45	31.28
LL = 71		PI = 40		**AV. PL (%)**	30.90

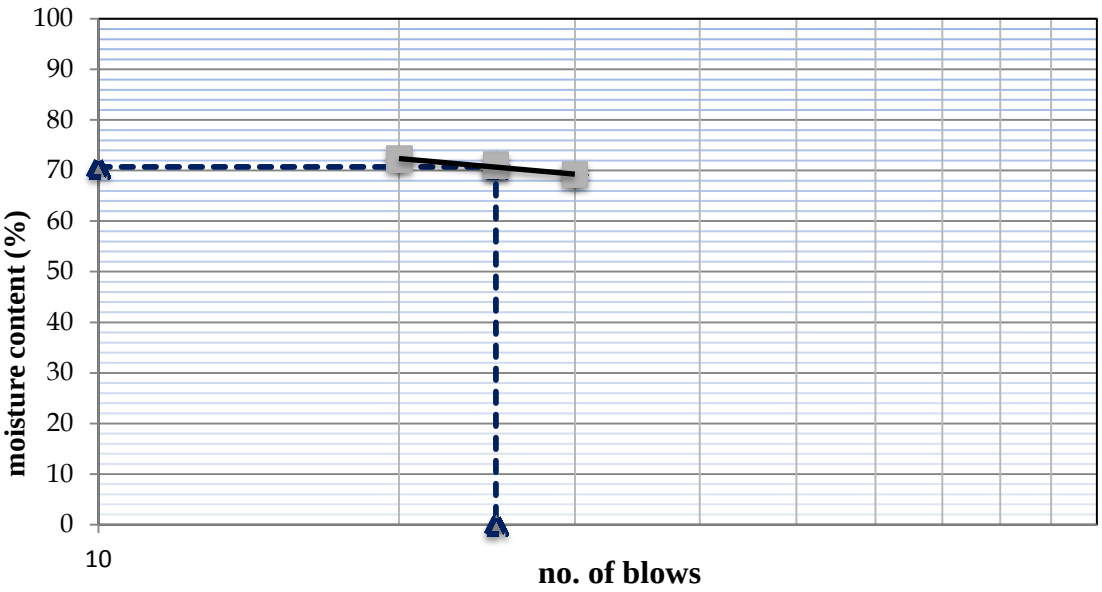

Figure A- 3: Water content versus No. blows

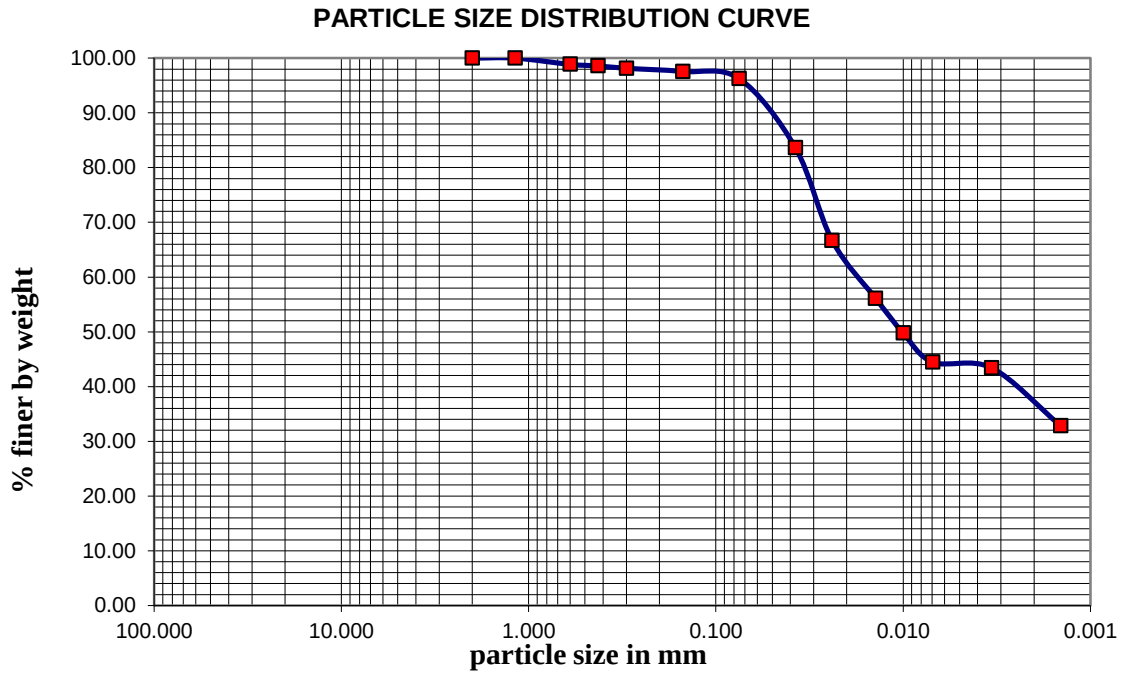

Figure A- 4: Particle size distribution curve for TP2

Table A- 3: Determination of Liquid Limit, Plastic Limit and Plastic Index (for TP3)

	LIQUID LIMIT			PLASTIC LIMIT	
No. Blows	34	28	22		
Wt.of cont. + wet soil (g.)	29.41	29.50	29.36	15.92	15.40
Wt.of cont. + dry soil (g.)	22.20	22.29	22.26	15.13	14.74
Wt. of water (g.)	7.21	7.21	7.10	0.79	0.66
Wt. container (g.)	13.04	13.29	13.51	12.81	12.80
Wt. dry soil (g.)	9.16	9.00	8.75	2.32	1.94
Water (%)	78.71	80.11	81.14	34.05	33.92
LL = 80		PI = 46		AV. PL (%)	34.0

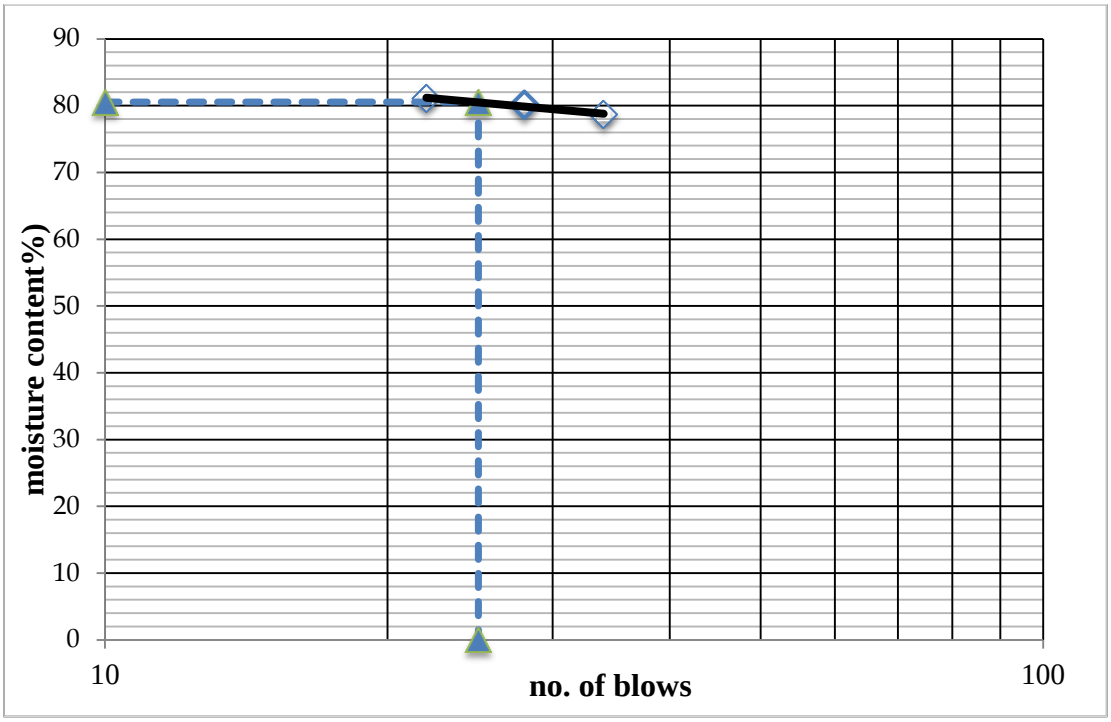

Figure A- 5: Water content versus No. blow

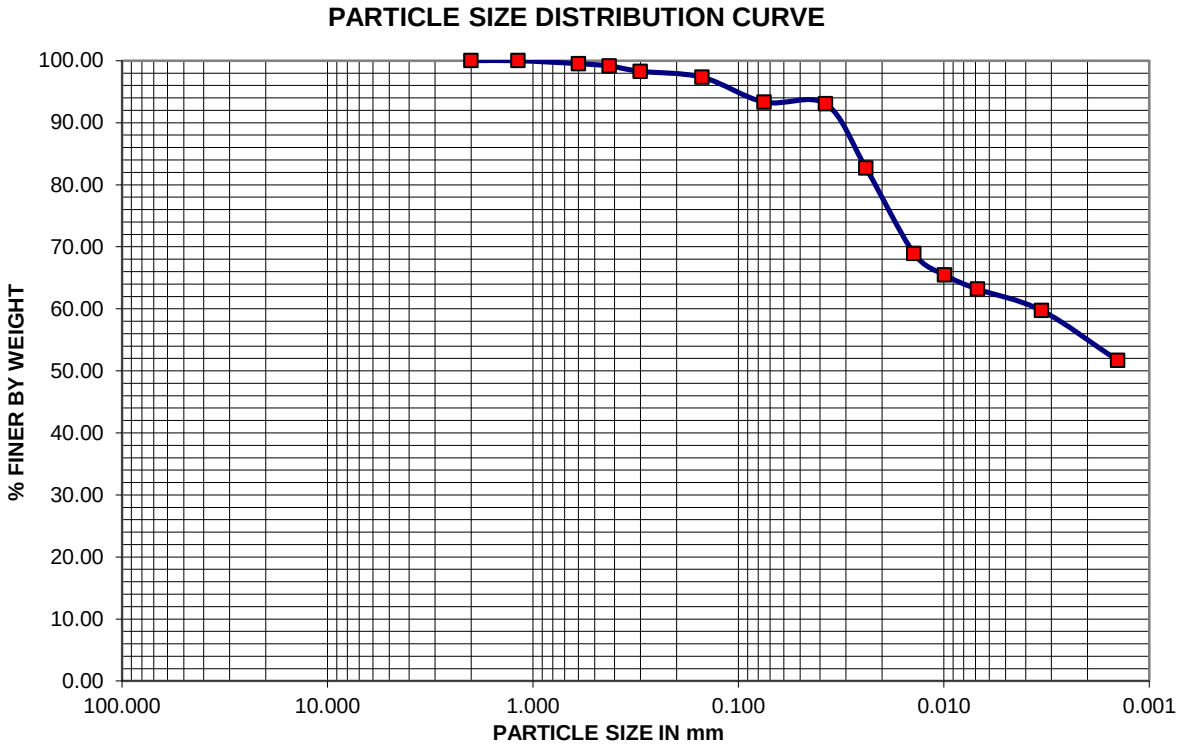

Figure A- 6: Particle size distribution curve for TP3

Table A- 4: Determination of Liquid Limit, Plastic Limit and Plastic Index (for TP4)

	LIQUID LIMIT			PLASTIC LIMIT	
No. Blows	34	28	22		
Wt.of cont. + wet soil (g.)	30.24	30.20	30.16	15.94	15.56
Wt.of cont. + dry soil (g.)	22.34	22.36	22.28	15.07	14.74
Wt. of water (g.)	7.90	7.84	7.88	0.87	0.82
Wt. container (g.)	12.78	12.99	13.06	13.18	12.89
Wt. dry soil (g.)	9.56	9.37	9.22	1.89	1.85
Water (%)	82.64	83.67	85.47	46.03	44.32
LL = 84		PI = 38		AV. PL (%)	45.2

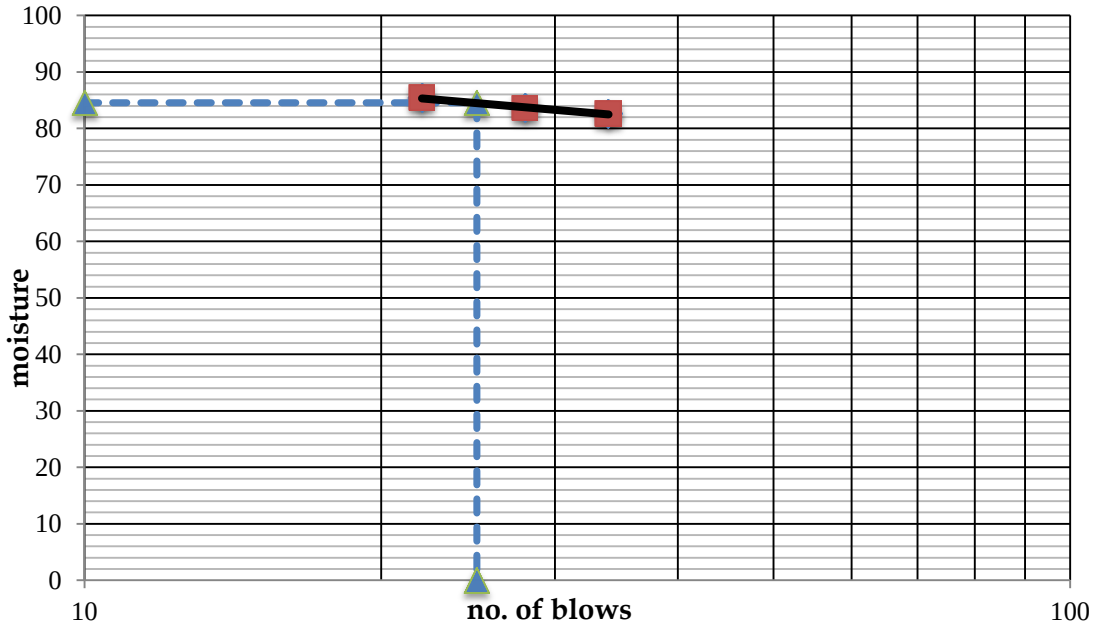

Figure A- 7: Water content versus No. blow

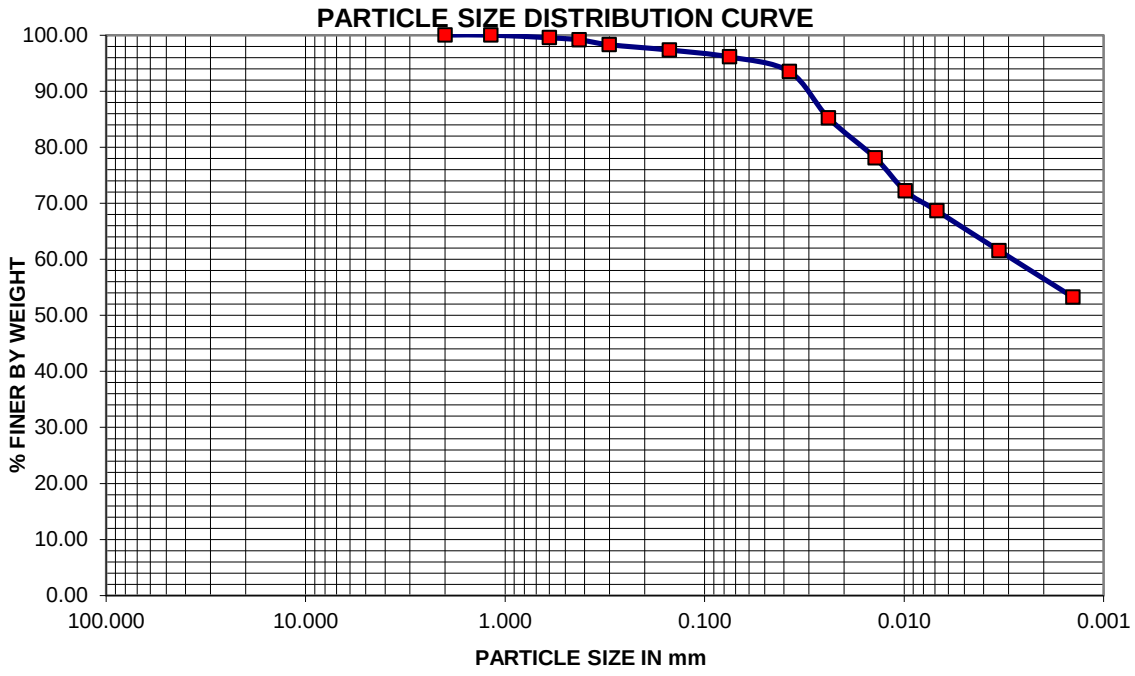

Figure A- 8: Particle size distribution curve for TP4

Preparation and assembling of test specimens

Figure A- 7: Sample preparation and positioning it on the testing equipment

APPENDIX: B

Consolidation test results

Table B- 1: Determination of Pre-consolidation pressure for TP1

Before test		After the test	
Ring No	1	Ring No	1
Ring Diameter (sample), cm	5	Ring Diameter (sample), cm	5
Ring Height (sample), mm	20	Ring Height (sample), mm	18.19
Moisture content (%)	30	Moisture content (%)	27.2
Volume of sample (cc)	60.351	Volume of sample (cc)	52.390
Bulk density (g/cc)	1.641	Bulk density (g/cc)	1.790
Dry density (g/cc)	1.262	Dry density (g/cc)	1.473
Initial Void Ratio $\mathbf{e_o} = \frac{G_S}{\delta_{dry}} - 1$	1.004	Final Void Ratio e_f	0.798

ODEMETR TEST

Increment No.	Pressure (KN/m2)	Change in Height(mm) ΔH	$\Delta e = [\frac{1+e_o}{H_o}] * \Delta H$	Void ratio $e = e_o - \Delta e$	Mean specimen Height, Havg(mm)
	0	0			
1	12.5	0.03990	0.004	1.00100	19.96010

2	25	0.18953	0.019	0.98600	19.81047
3	50	0.39900	0.040	0.96500	19.60100
4	100	0.61845	0.062	0.94300	19.38155
5	200	0.94763	0.095	0.91000	19.05237
6	400	1.30673	0.131	0.87400	18.69327
7	800	1.68579	0.169	0.83600	18.31421
8	1600	2.06484	0.207	0.79800	17.93516

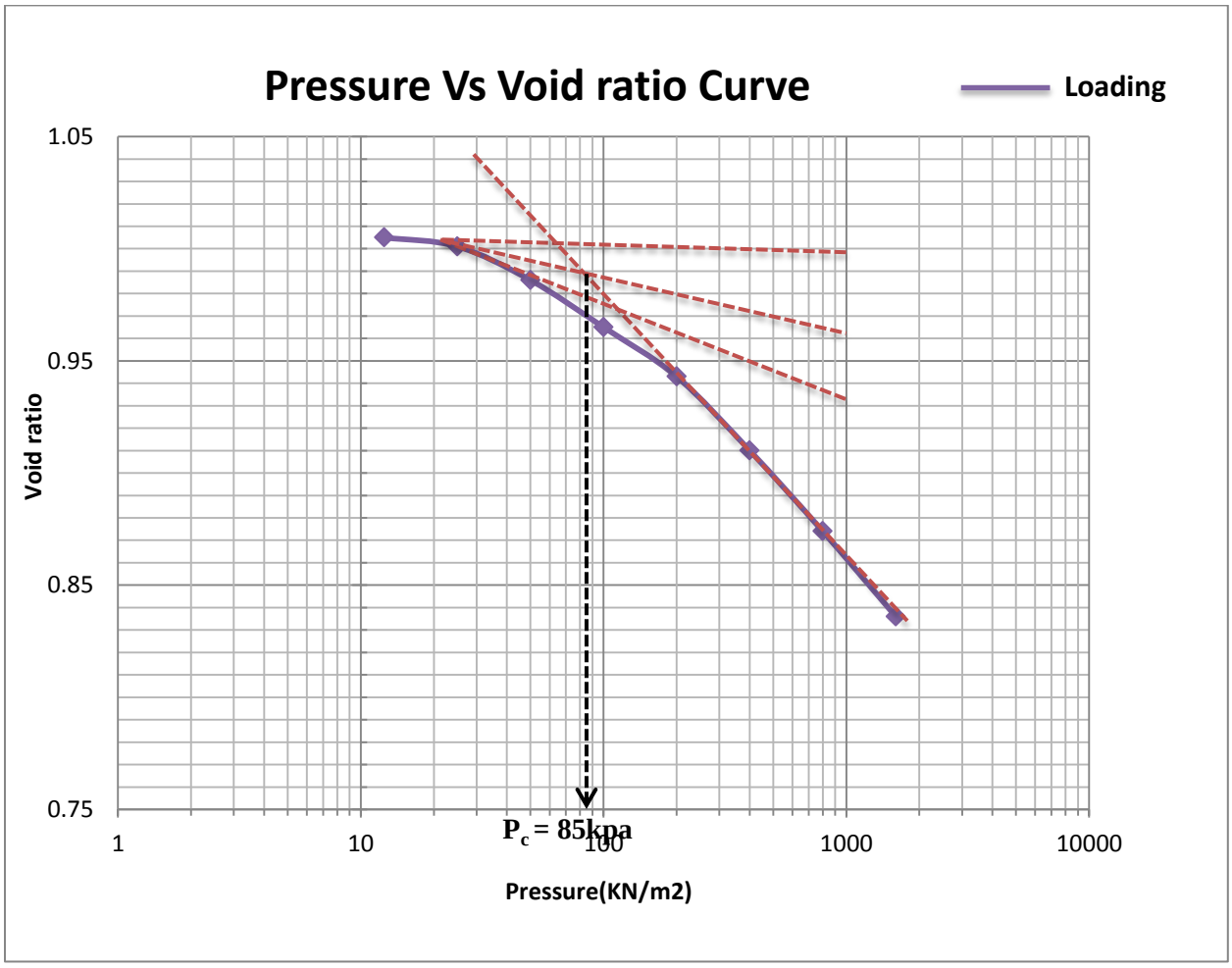

Figure B- 1: Consolidation pressure versus void ratio for TP1

Table B- 2: Determination of Pre-consolidation pressure for TP2

Before test		After the test	
Ring No	1	Ring No	1
Ring Diameter (sample), cm	5	Ring Diameter (sample), cm	5
Ring Height (sample), mm	20	Ring Height (sample), mm	18.19
Moisture content (%)	37.4	Moisture content (%)	36.2
Volume of sample (cc)	40.02	Volume of sample (cc)	35.69
Bulk density (g/cc)	1.595	Bulk density (g/cc)	1.931
Dry density (g/cc)	1.139	Dry density (g/cc)	1.419
Initial Void Ratio $\mathbf{e_o} = \frac{G_S}{\delta_{dry}} - 1$	1.299	Final Void Ratio e_f	0.8420

ODEMETR TEST

Increment No.	Pressure (KN/m2)	Change in Height(mm) ΔH	$\Delta e = [\frac{1+e_o}{H_o}] * \Delta H$	Void ratio $e = e_o - \Delta e$	Mean specimen Height, Havg(mm)
	0	0			
1	12.5	0.04739	0.0048	1.021	19.953
2	25	0.10662	0.0108	1.015	19.893
3	50	0.24484	0.0248	1.001	19.755
4	100	0.50153	0.0508	0.975	19.498

5	200	0.75822	0.0768	0.949	19.242
6	400	1.06427	0.1078	0.918	18.936
7	800	1.39994	0.1418	0.884	18.600
8	1600	1.81459	0.1838	0.842	18.185

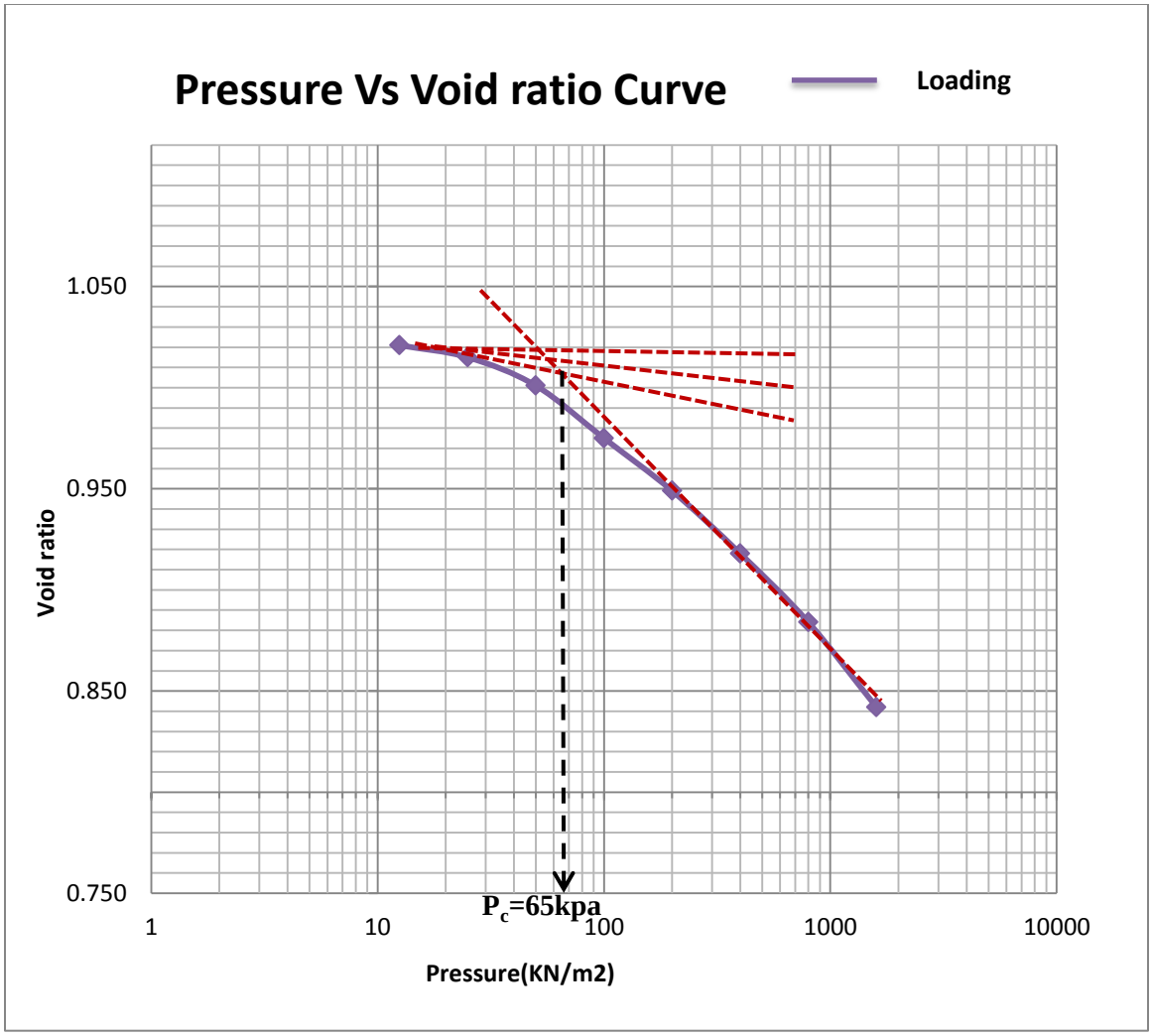

Figure B- 2: Consolidation pressure versus void ratio for TP2

APPENDIX C

Cyclic shear test result

C.1 Shear stress versus number of cycles, shear strain versus number of cycles and shear strain versus stress curve for selected point

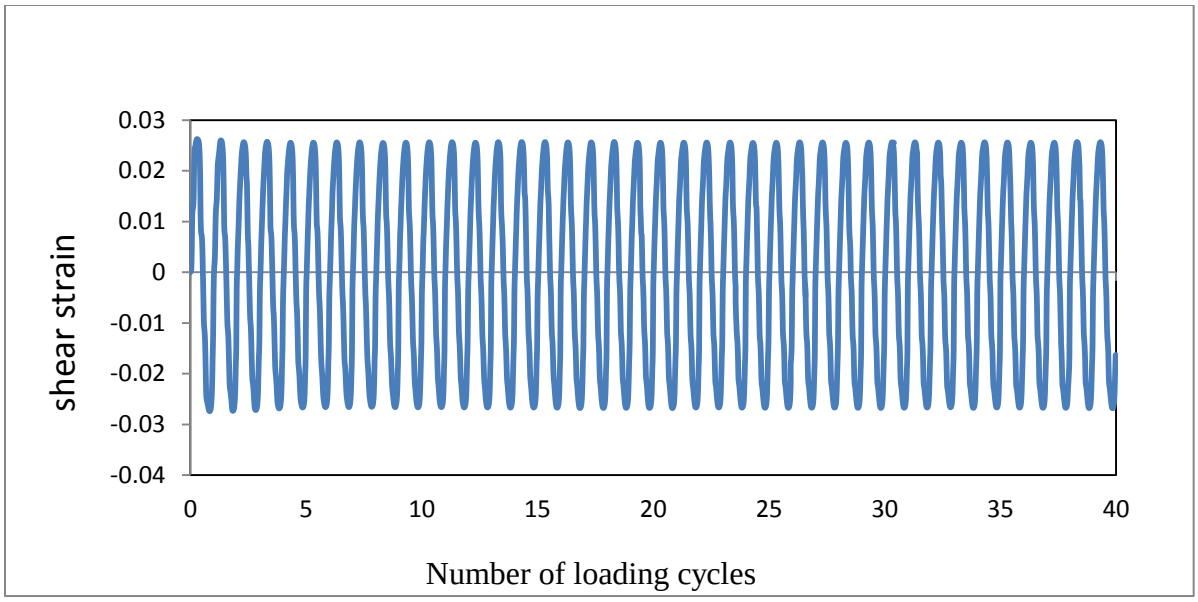

Figure C- 1: Shear strain vs number of loading cycles (γ =2.5%, σ'_v =100 kPa) of TP1

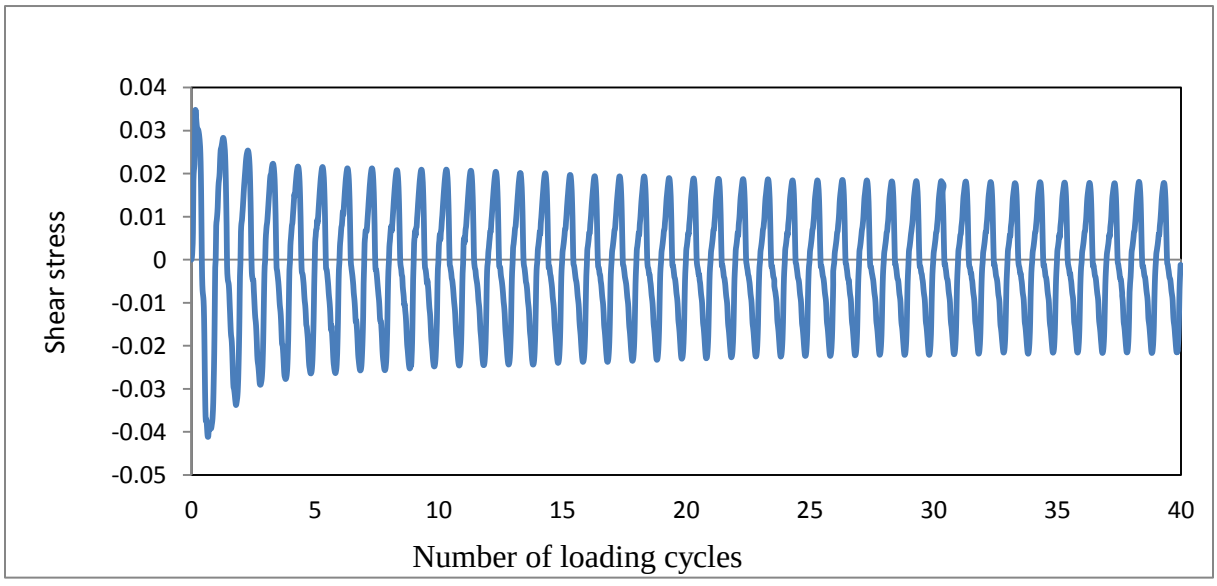

Figure C- 2: Shear stress vs number of loading cycles (γ =2.5%, σ'_v =100 kPa) of TP1

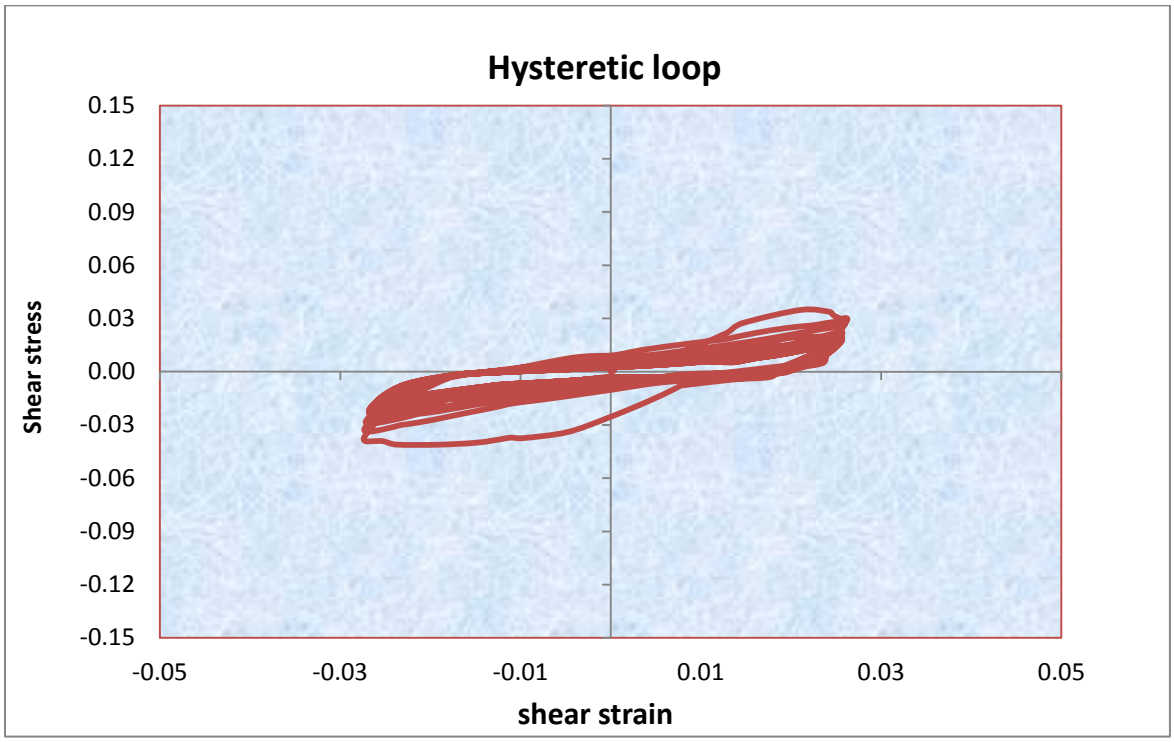

Figure C- 3: Shear stress vs shear strain (γ =2.5%, σ'_v =100 kPa) of TP1

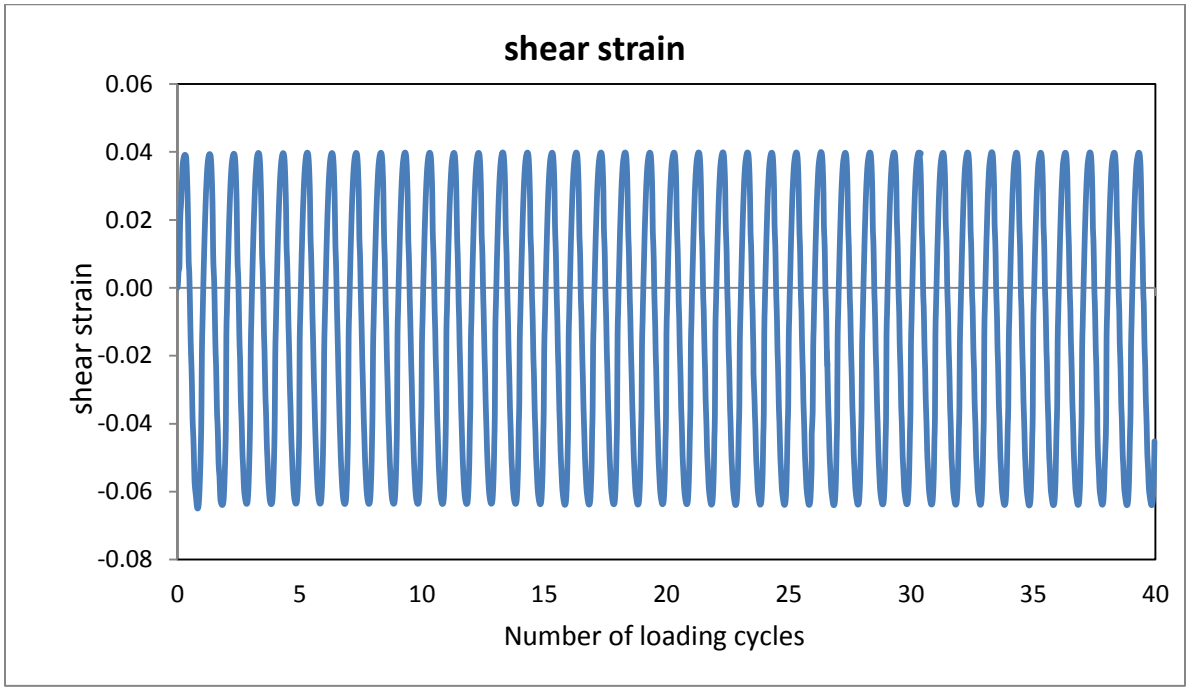

Figure C- 4: Shear strain vs number of loading cycles (γ = 5%, σ'_v =400 kPa) of TP2

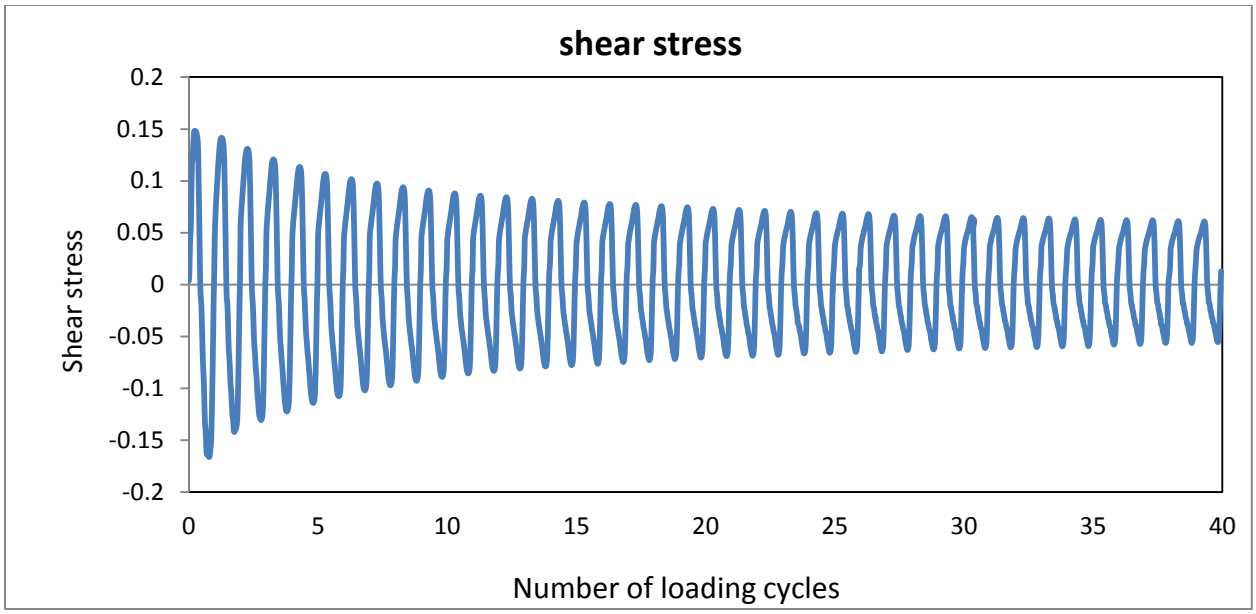

Figure C- 5: Shear stress vs number of loading cycles (γ =5%, σ'_v =400 kPa) of TP2

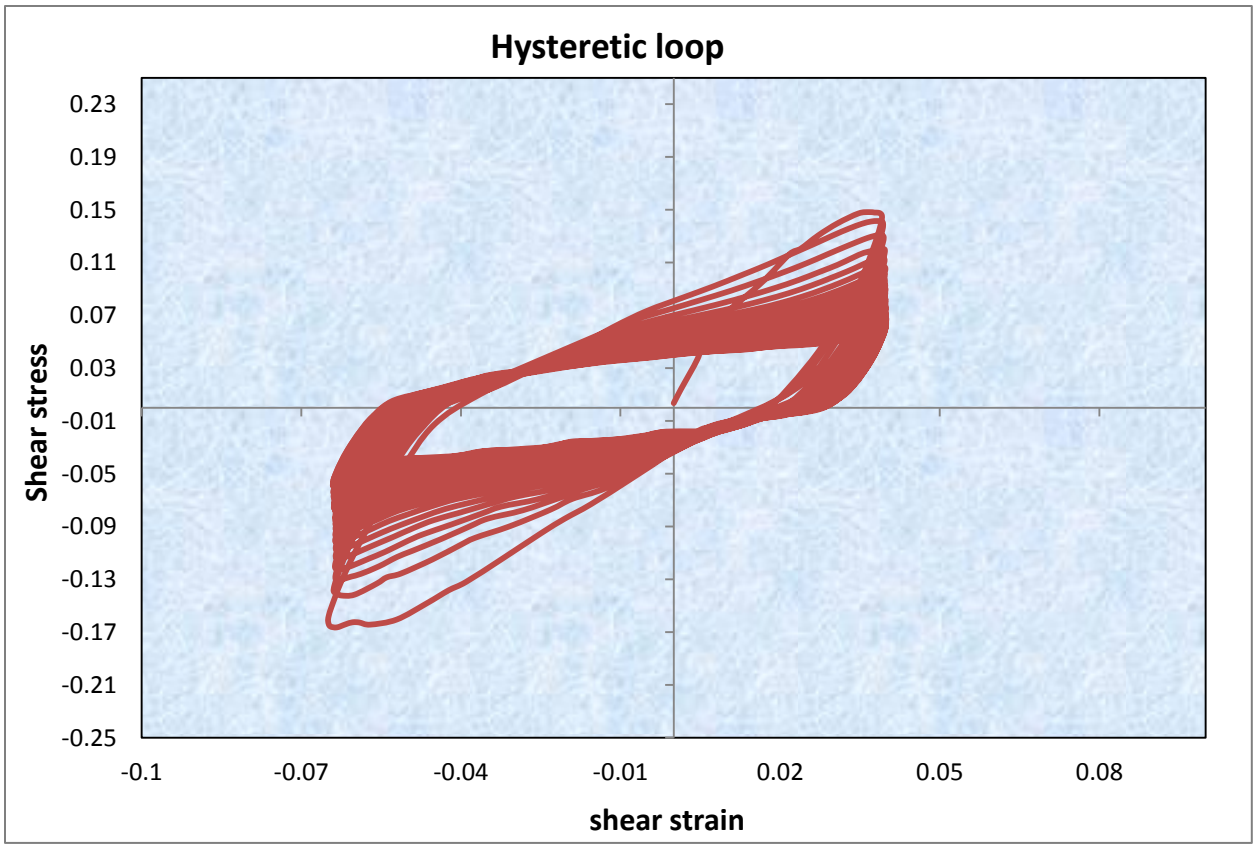

Figure C- 6: Shear stress vs shear strain (γ =5%, σ'_v =400 kPa) of TP2

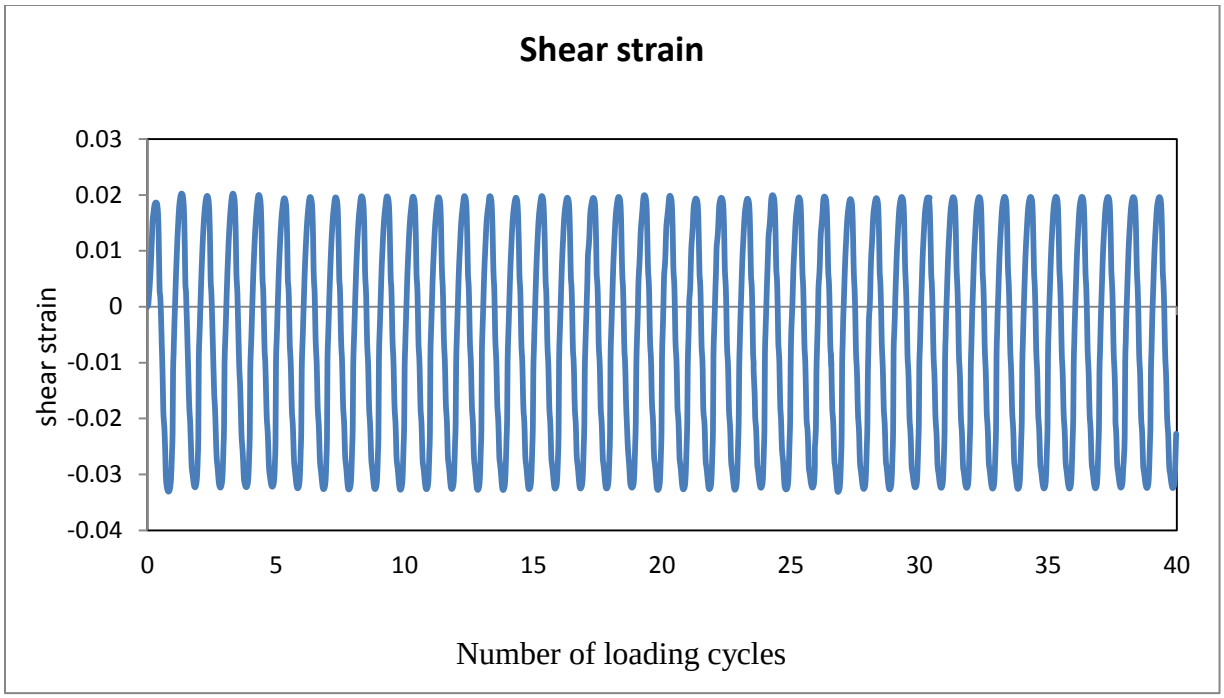

Figure C- 7: Shear strain vs number of loading cycles (γ= 2.5%, σ'_v =400 kPa) of TP2

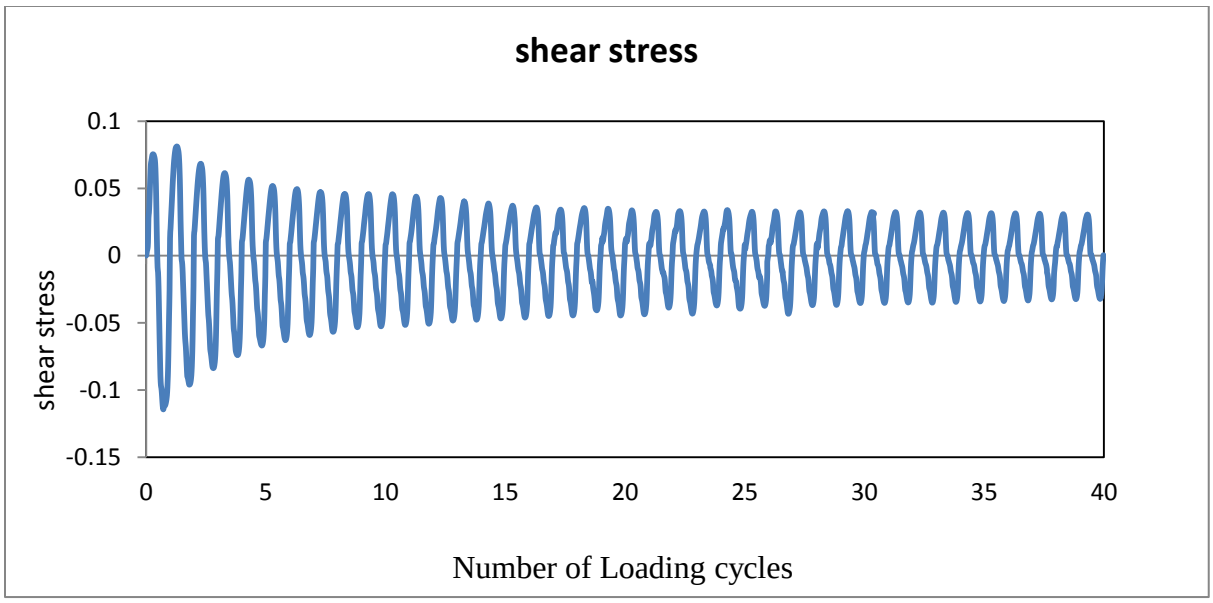

Figure C- 8: Shear stress vs. number of loading cycles (γ=2.5%, σ'_v =400 kPa) of TP2

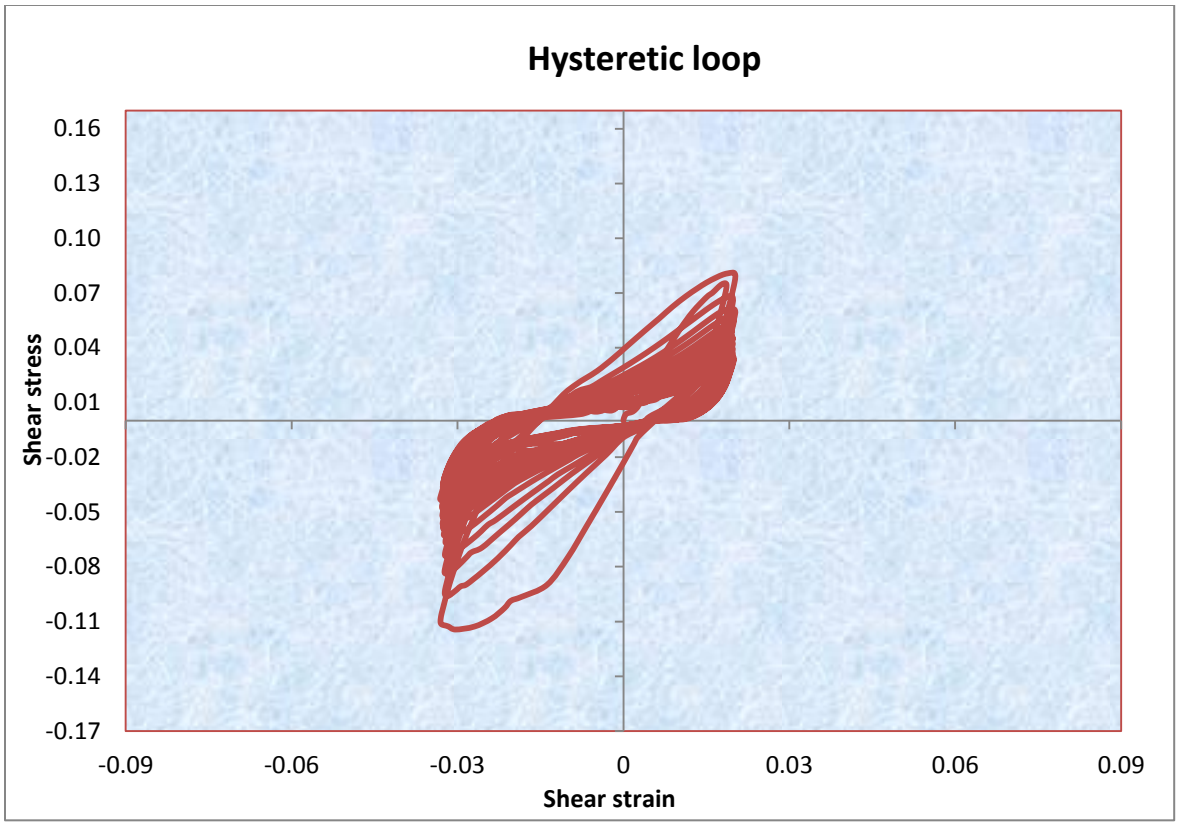

Figure C- 9: Shear stress vs shear strain (γ =2.5%, σ'_v =400 kPa) of TP2

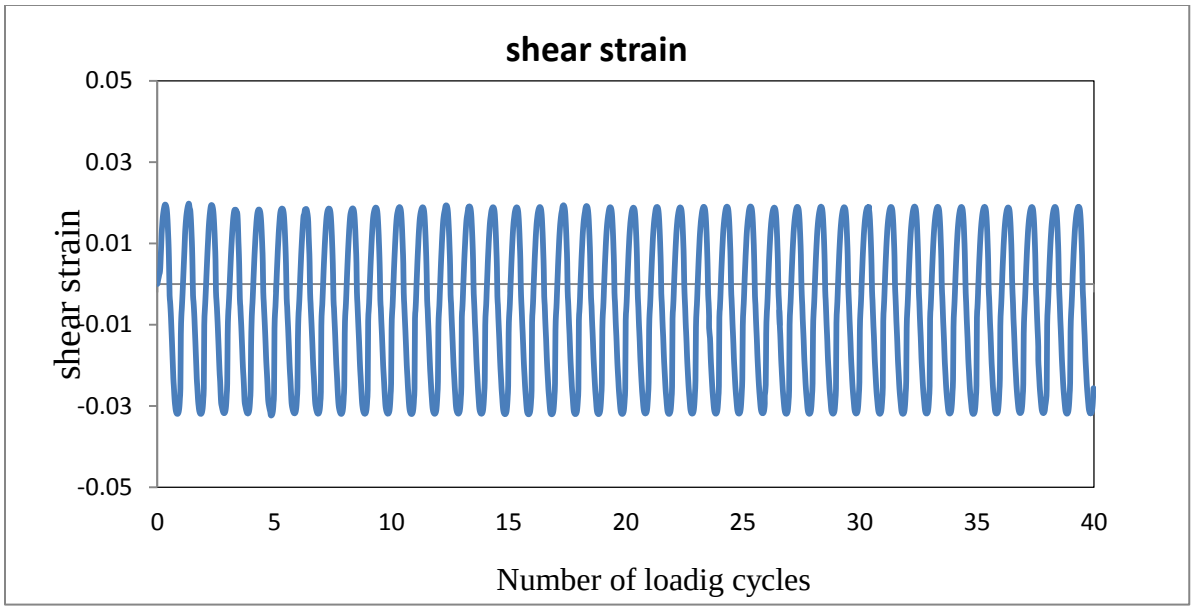

Figure C- 10: Shear strain vs number of loading cycles (γ= 2.5%, σ'_v =250 kPa) of TP2

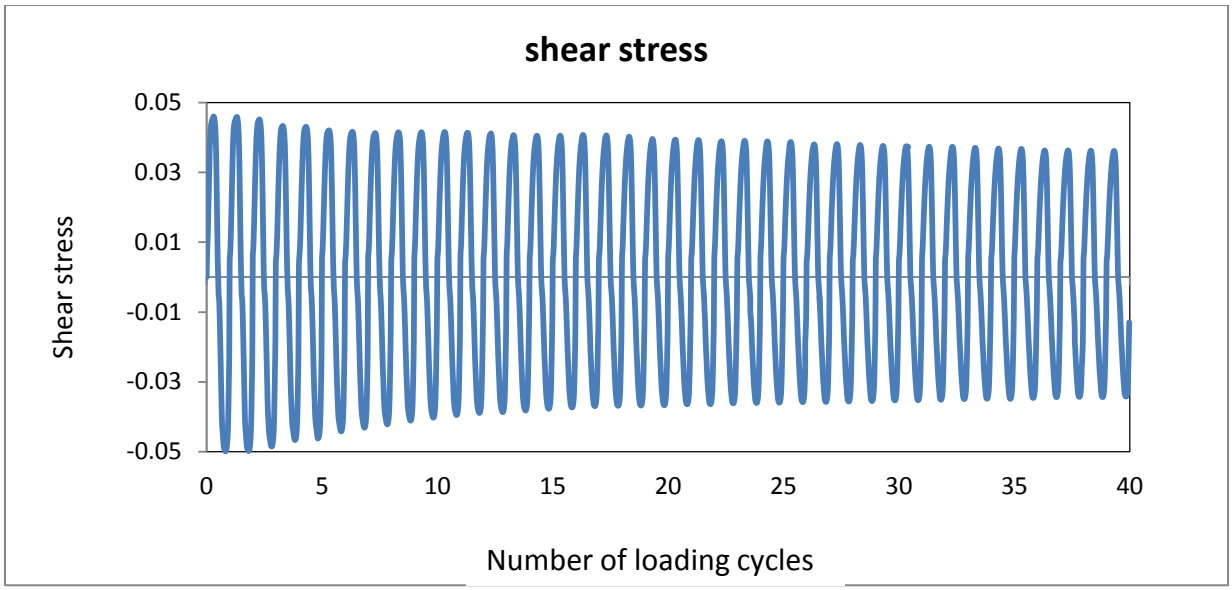

Figure C- 11: Shear stress vs number of loading cycles (γ =2.5%, σ'_v =250 kPa) of TP2

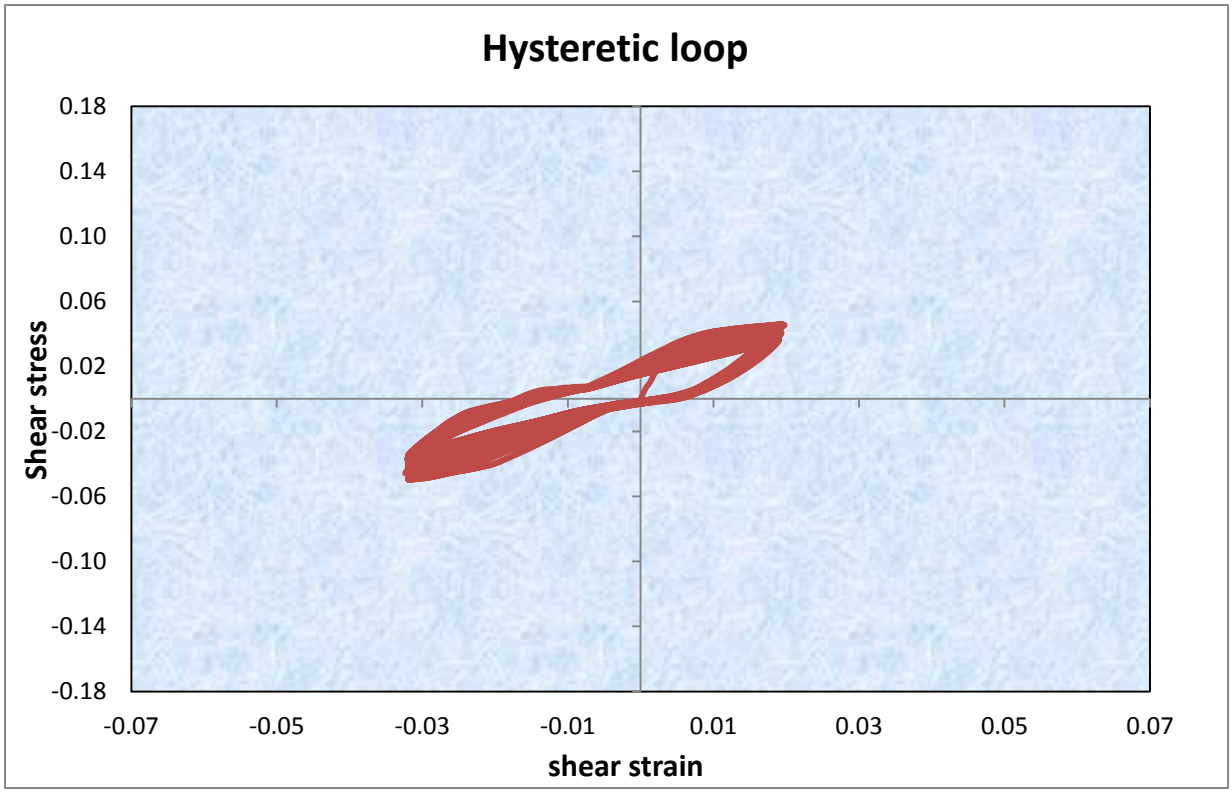

Figure C- 12: Shear stress vs shear strain (γ =2.5%, σ'_v =250 kPa) of TP2

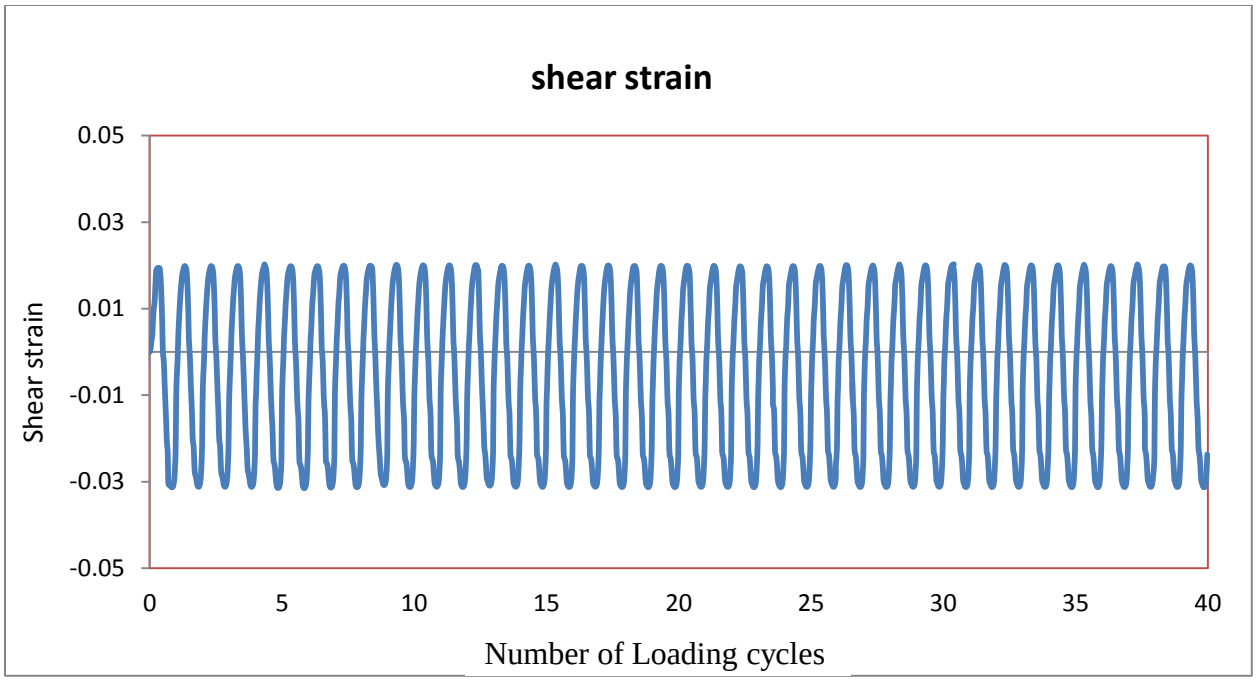

Figure C- 13: Shear strain vs number of loading cycles (γ = 5%, σ'_v =250 kPa) of TP2

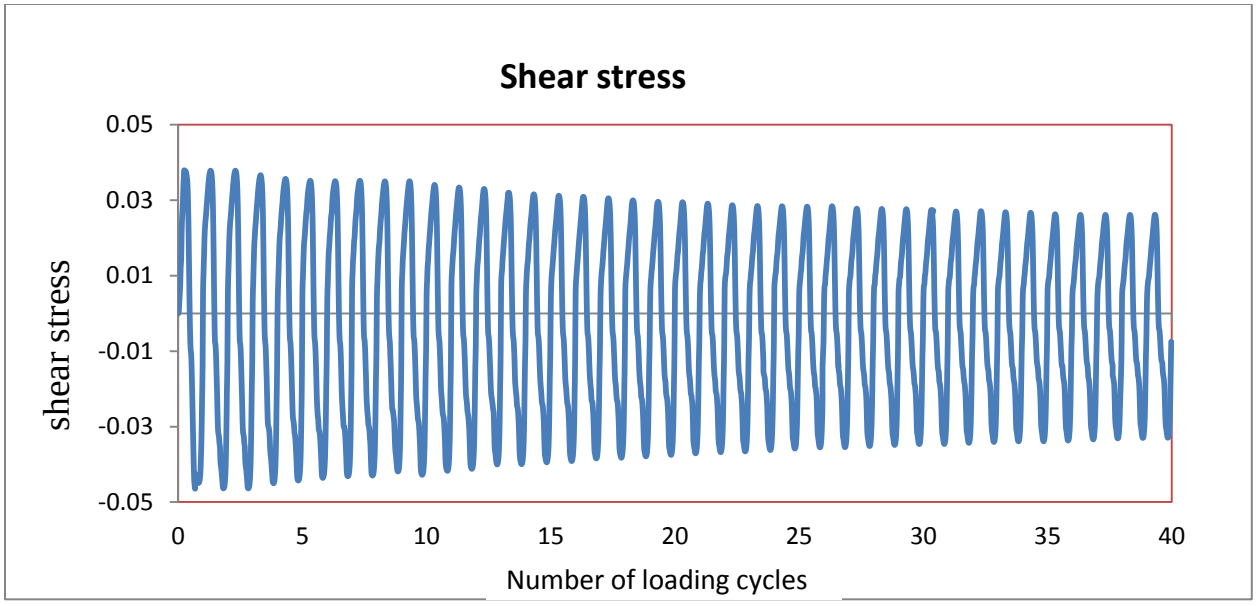

Figure C- 14: Shear stress vs number of loading cycles (γ =5%, $\sigma'v$ =250 kPa) of TP2

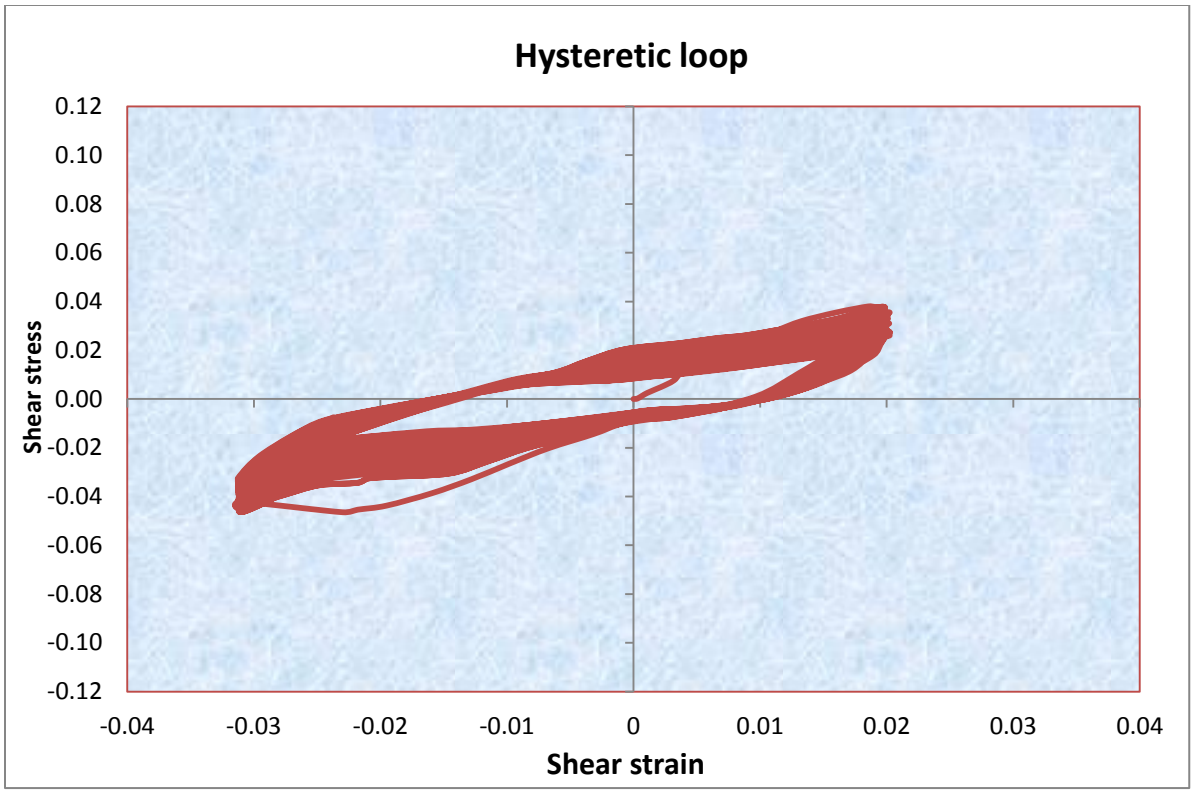

Figure C- 15: Shear stress vs shear strain (γ =5%, σ'v =250 kPa) of TP2

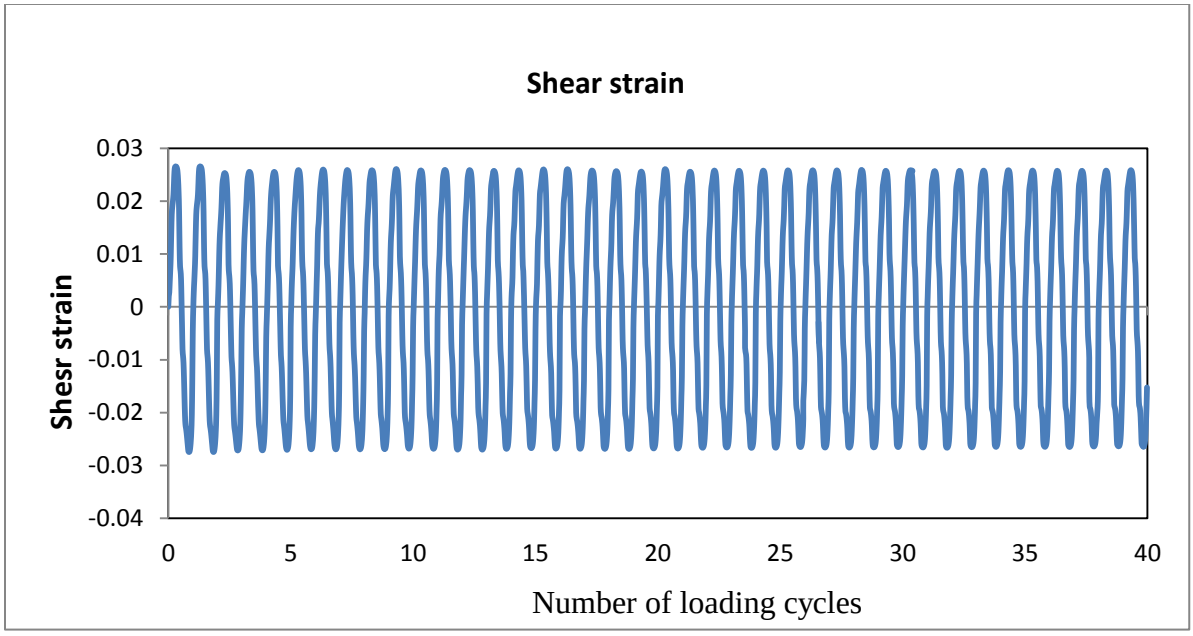

Figure C- 16: Shear strain vs number of loading cycles (γ= 2.5%, σ'_v =100 kPa),TP2

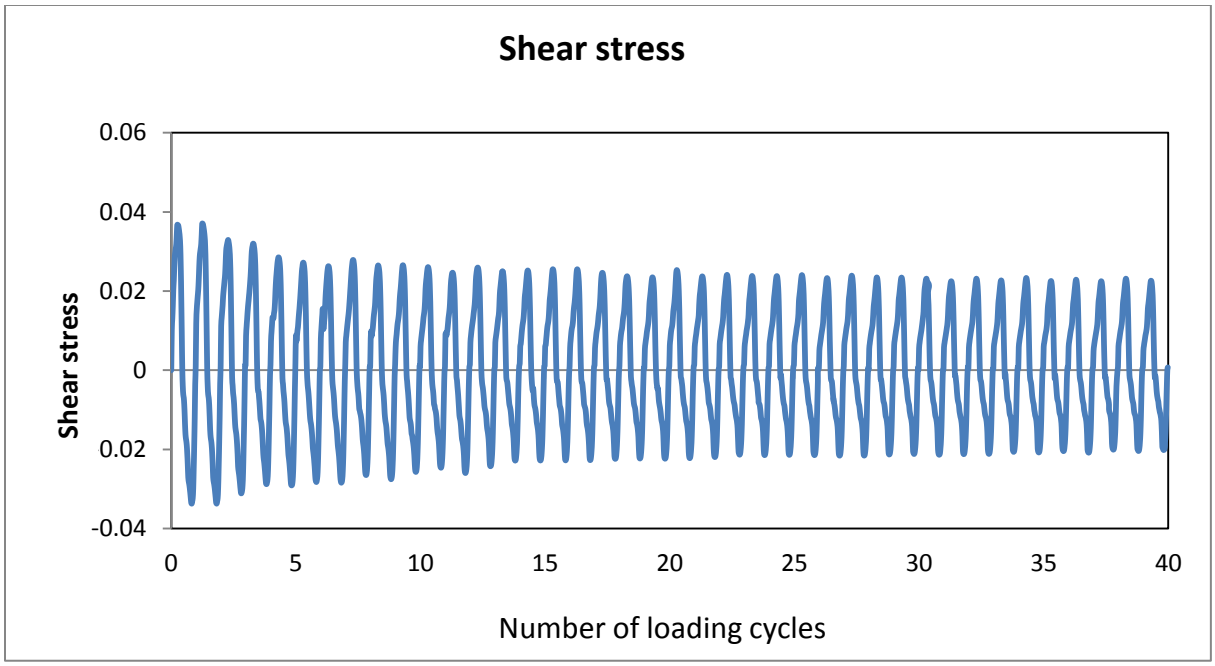

Figure C- 17: Shear stress vs number of loading cycles (γ =2.5%, σ'_v =100 kPa) of TP2

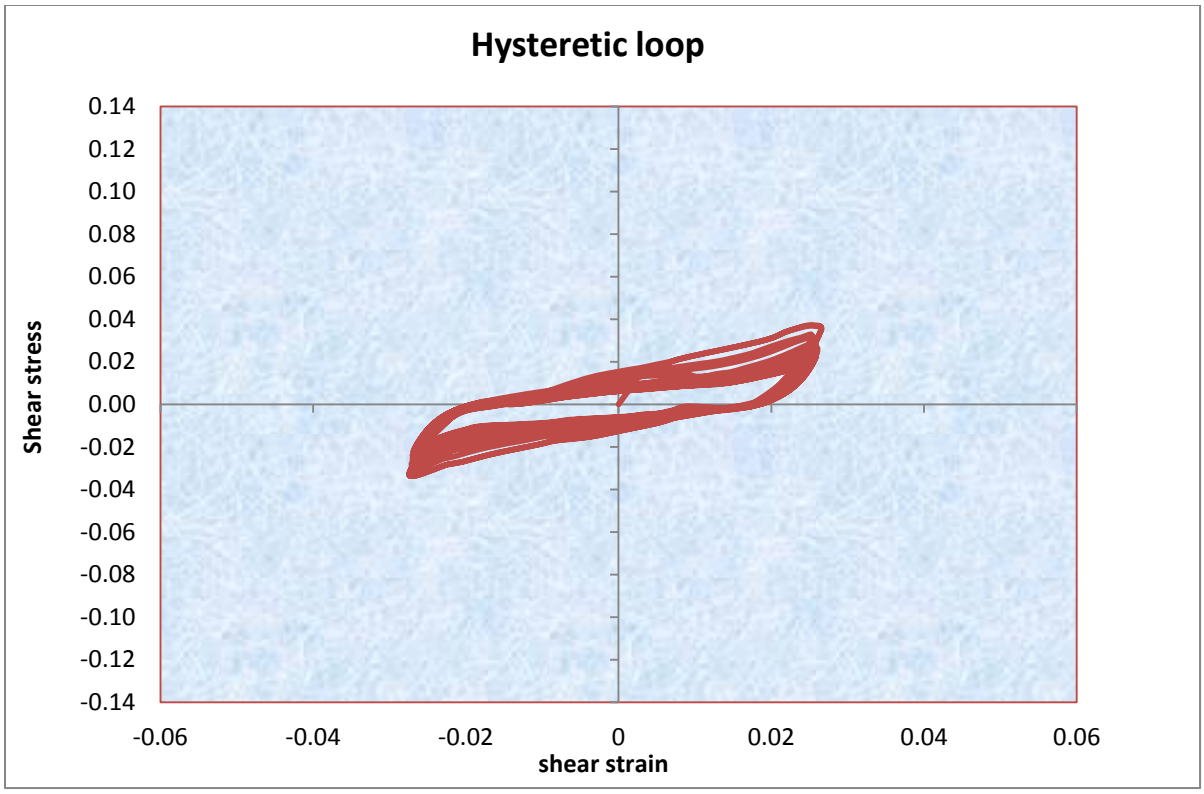

Figure C- 18: Shear stress vs shear strain (γ =2.5%, σ'_v =100 kPa) of TP2

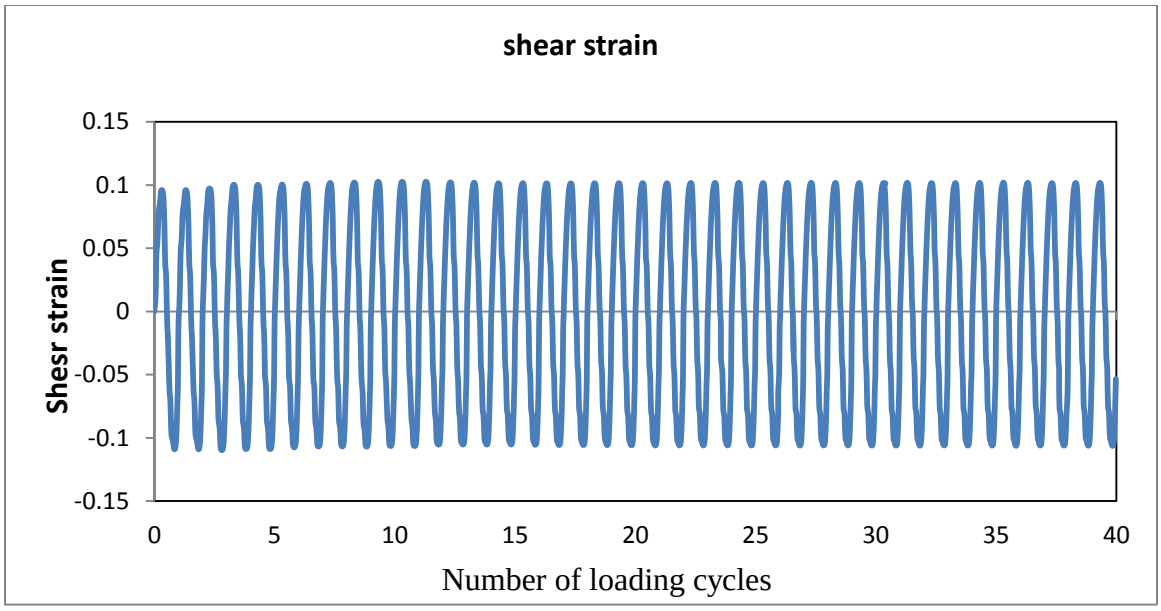

Figure C- 19: Shear strain vs number of loading cycles (γ = 5%, σ'_v =100 kPa) of TP2

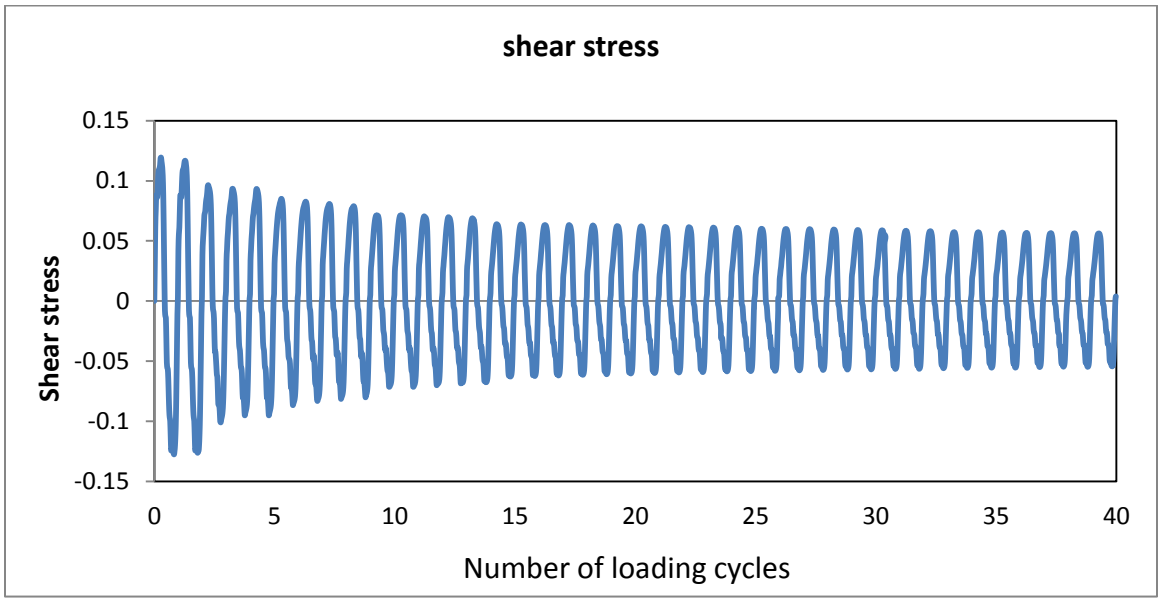

Figure C- 20: Shear stress vs number of loading cycles (γ= 5%, σ'_v =100 kPa) of TP2

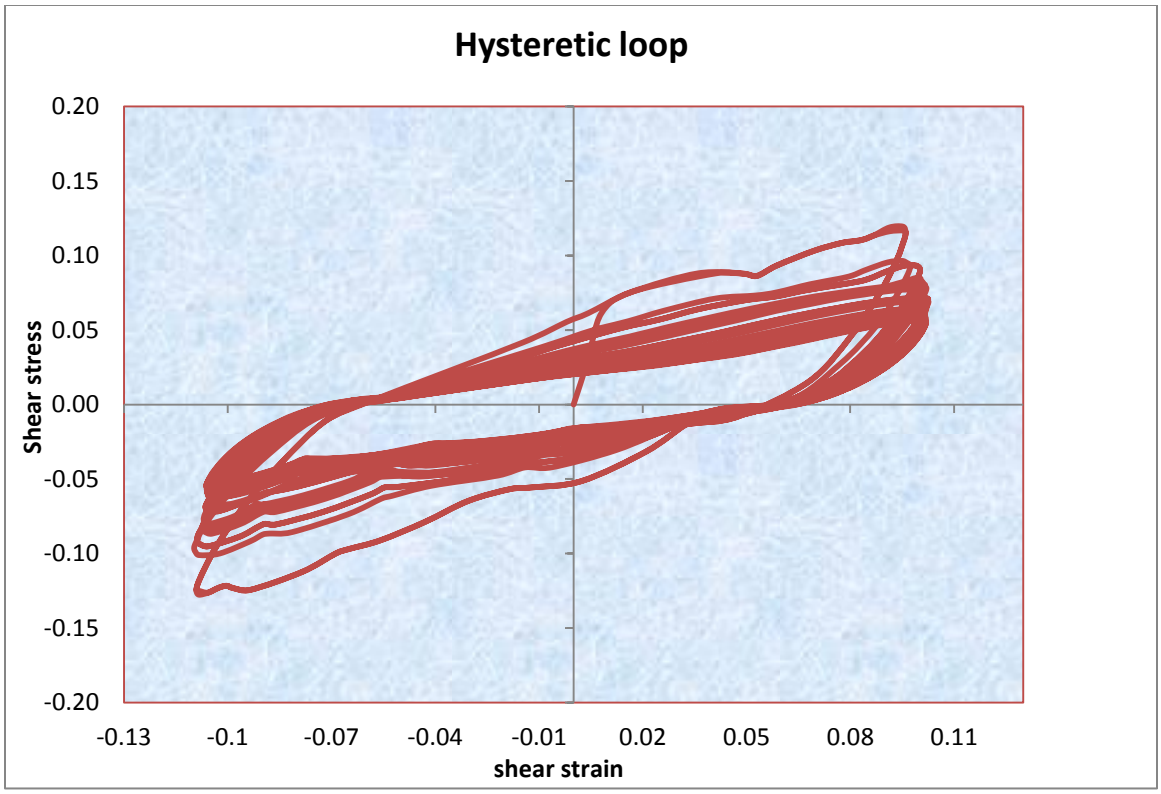

Figure C- 21: Shear stress vs shear strain (γ = 5%, σ'_v =100 kPa) of TP2

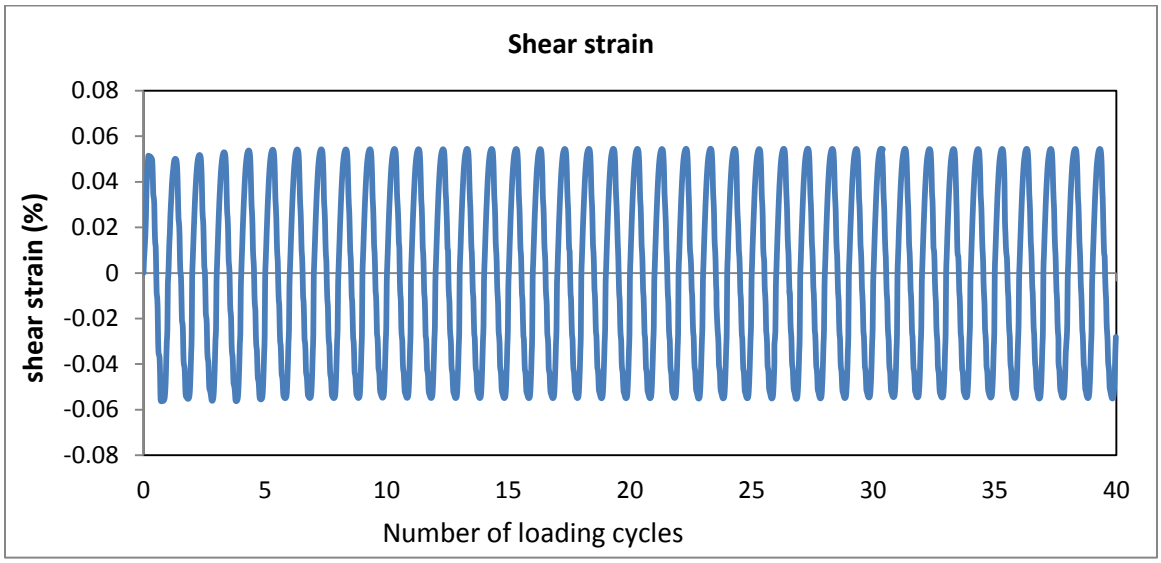

Figure C- 22: Shear strain vs number of loading cycles (γ = 5%, σ'_v =250 kPa) of TP1

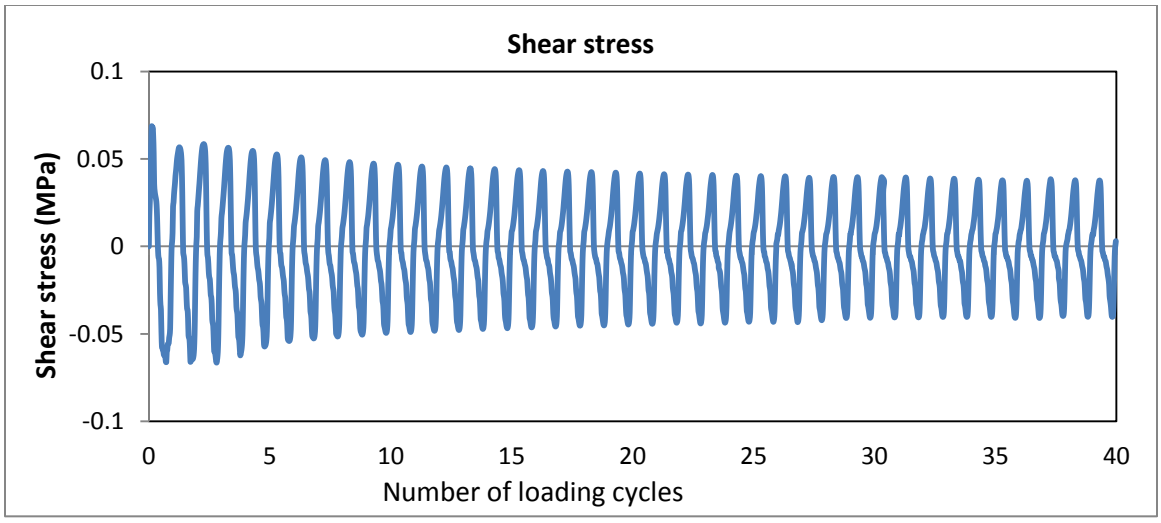

Figure C- 23: Shear stress vs number of loading cycles (γ= 5%, σ'_v =250 kPa) of TP1

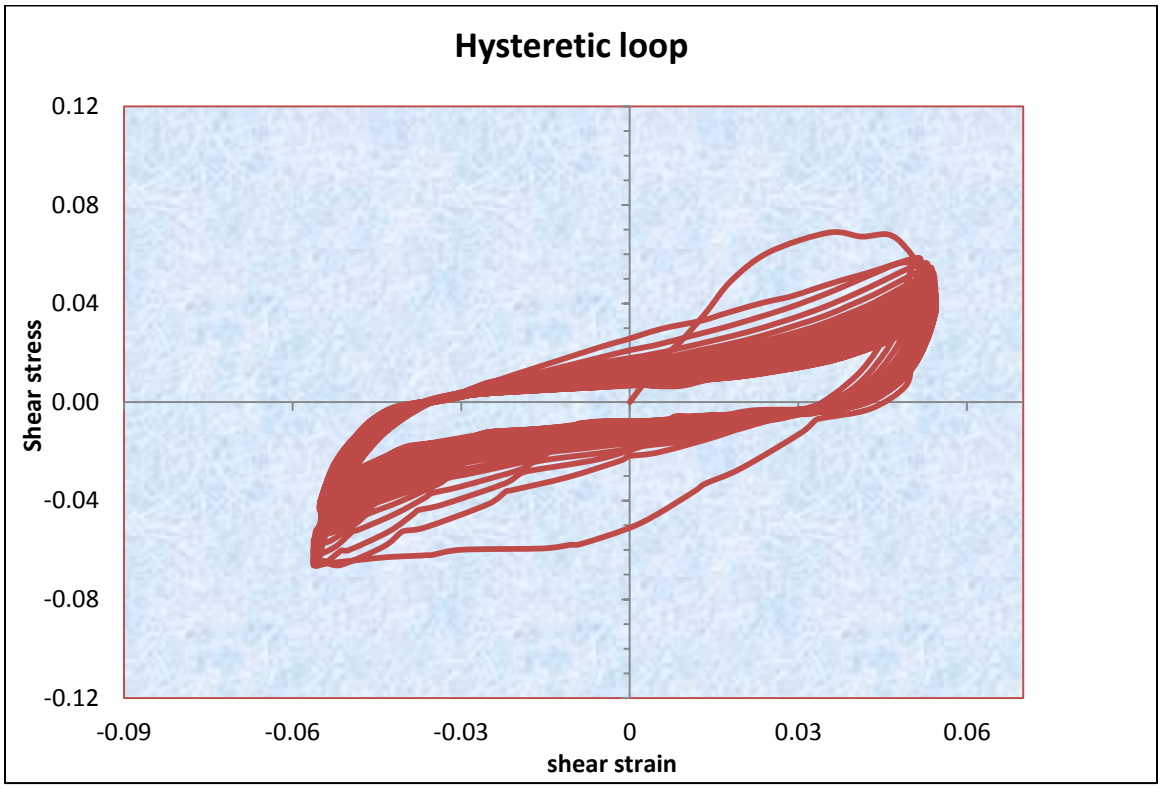

Figure C- 24: Shear stress vs shear strain (γ = 5%, σ'_v =250 kPa) of TP1

C.2 Shear modulus and damping ratio values of selected cycles

Table C- 1: Shear modulus and damping ratio values for TP1 at 100 kPa

Test pit 1 at axial load of 100 kPa										
Strain level	**0.01%**	**0.1%**	**1%**	**2.5%**	**5%**	**0.01%**	**0.1%**	**1%**	**2.5%**	**5%**
No loading cycles	**Shear modulus, G (Mpa)**					**Damping, D (%)**				
1	3.1935	2.4004	1.2037	0.9751	0.7347	6.0957	9.0953	13.8895	18.1595	22.9806
5	2.7737	2.2523	0.9215	0.7716	0.4905	5.5185	8.6181	12.0056	17.1198	21.1058
10	2.6479	2.1556	0.8761	0.6989	0.4094	5.1721	7.0865	10.7096	16.1804	20.5657
20	2.5250	2.0461	0.8025	0.6472	0.3685	4.9979	6.5554	9.7935	15.2013	20.1363
30	2.4545	1.9901	0.7718	0.6151	0.3353	4.8035	6.1754	9.4531	14.7097	19.6758
40	2.4143	1.9498	0.7498	0.5730	0.3284	4.6524	5.6992	9.0294	14.1081	19.2087

Table C- 2: Shear modulus and damping ratio values for TP1 at 400 kPa

Test pit 1 at axial load of 400 kPa										
Strain level	**0.01%**	**0.1%**	**1%**	**2.5%**	**5%**	**0.01%**	**0.1%**	**1%**	**2.5%**	**5%**
No loading cycles	**Shear modulus, G (Mpa)**					**Damping, D (%)**				
1	6.1865	4.7972	4.0558	2.9415	1.8910	3.1130	4.0564	7.5223	11.6092	16.4722
5	5.7797	3.8924	3.1240	2.0176	1.5185	2.8187	3.8373	7.0840	11.0237	15.1145
10	5.6771	3.5798	2.8673	1.7497	1.1656	2.5015	3.6045	6.0848	10.2768	14.1687
20	5.5499	3.2565	2.6105	1.5773	0.8931	2.3283	3.3627	5.5434	9.8393	13.5314
30	5.4773	3.0947	2.3264	1.4894	0.7797	2.2138	3.0765	5.2172	9.3539	13.1235
40	5.1509	2.9803	2.1584	1.4189	0.7253	2.0321	2.8676	5.0130	9.1028	12.5701

Table C- 3: Shear modulus and damping ratio values for TP2 at 100 kPa

Test pit 2 at axial load of 100 kPa										
Strain level	**0.01%**	**0.1%**	**1%**	**2.5%**	**5%**	**0.01%**	**0.1%**	**1%**	**2.5%**	**5%**
No loading cycles	**Shear modulus, G (Mpa)**					**Damping, D (%)**				
1	4.790	3.245	1.862	1.305	1.205	5.485	7.816	11.766	19.174	22.300
5	4.275	2.865	1.382	1.096	0.902	4.414	4.664	10.001	18.013	20.597
10	4.026	2.645	1.350	0.987	0.683	4.314	6.802	9.647	16.553	19.994
20	3.817	2.363	1.207	0.875	0.591	3.668	6.141	9.817	15.123	19.099
30	3.737	2.203	1.177	0.854	0.559	3.518	5.159	9.557	14.518	18.423
40	3.679	2.128	1.153	0.818	0.532	2.946	5.029	9.414	13.845	18.081

Table C- 4: Shear modulus and damping ratio values for TP2 at 250 kPa

Test pit 2 at axial load of 250 kPa										
Strain level	**0.01%**	**0.1%**	**1%**	**2.5%**	**5%**	**0.01%**	**0.1%**	**1%**	**2.5%**	**5%**
No loading cycles	**Shear modulus, G (Mpa)**					**Damping, D (%)**				
1	5.2940	3.4649	2.3098	1.8640	1.6635	4.3963	5.6546	11.3040	17.9907	21.4053
5	4.6214	3.0863	1.9943	1.7625	1.5470	4.0011	5.5740	10.1120	15.1611	20.6587
10	4.2547	2.9595	1.8773	1.6125	1.5148	3.9693	5.0766	9.4392	14.0312	18.6124
20	4.0404	2.7154	1.7511	1.5003	1.3116	3.5799	4.8949	8.9707	12.7278	17.4257
30	3.9222	2.6577	1.6466	1.4364	1.2158	3.2283	4.7205	8.4797	12.9924	16.1994
40	3.8057	2.5902	1.5853	1.3837	1.1521	2.8293	4.6188	8.0618	12.4454	15.8514

APPENDIX D

Shear modulus and Damping ratio curves which show dependency on different factors

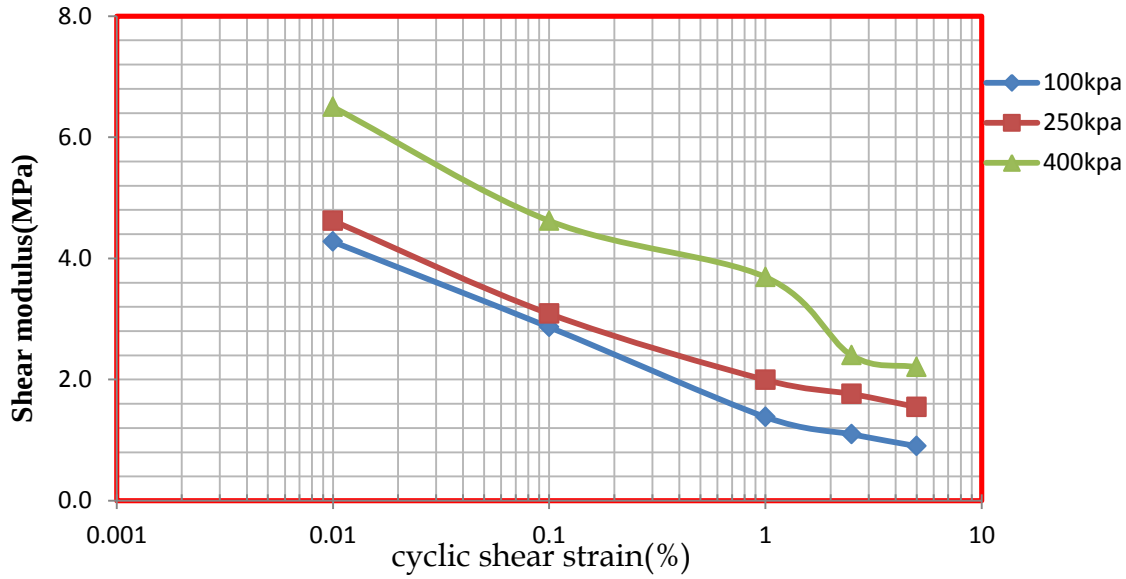

Figure D- 1: Effect of vertical stress on shear modulus under for TP2

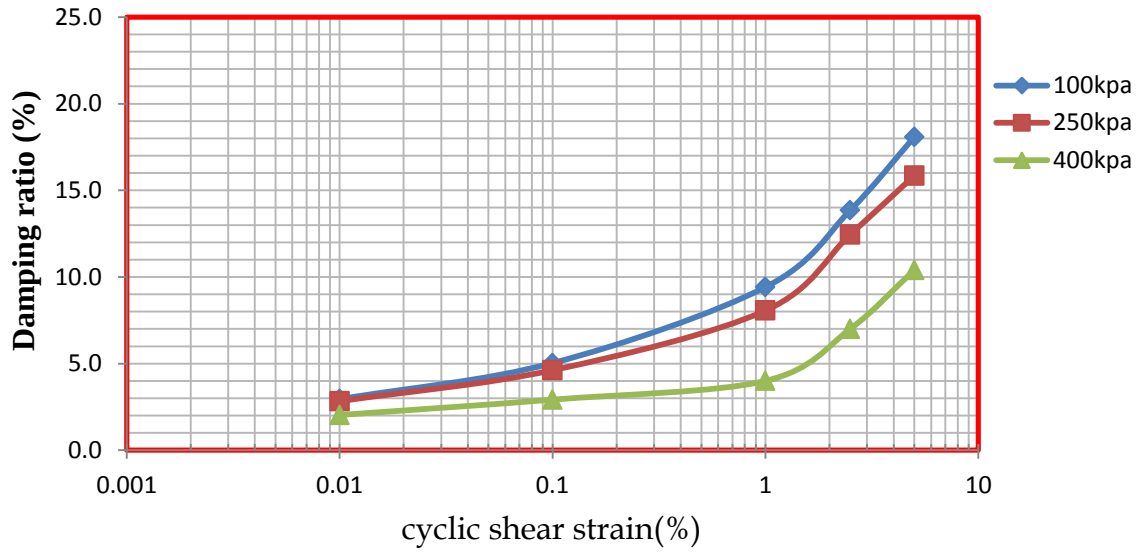

Figure D- 2: Effect of vertical stress on damping ratio forTP2

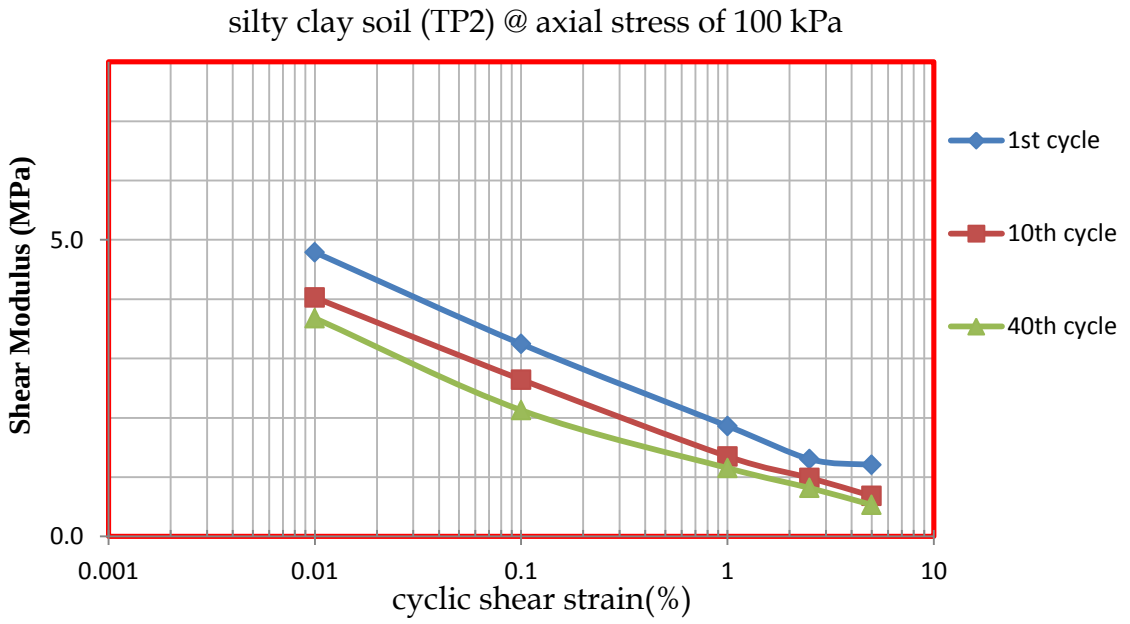

Figure D- 3: Effects of number of cyclic loading cycles on the value of shear modulus

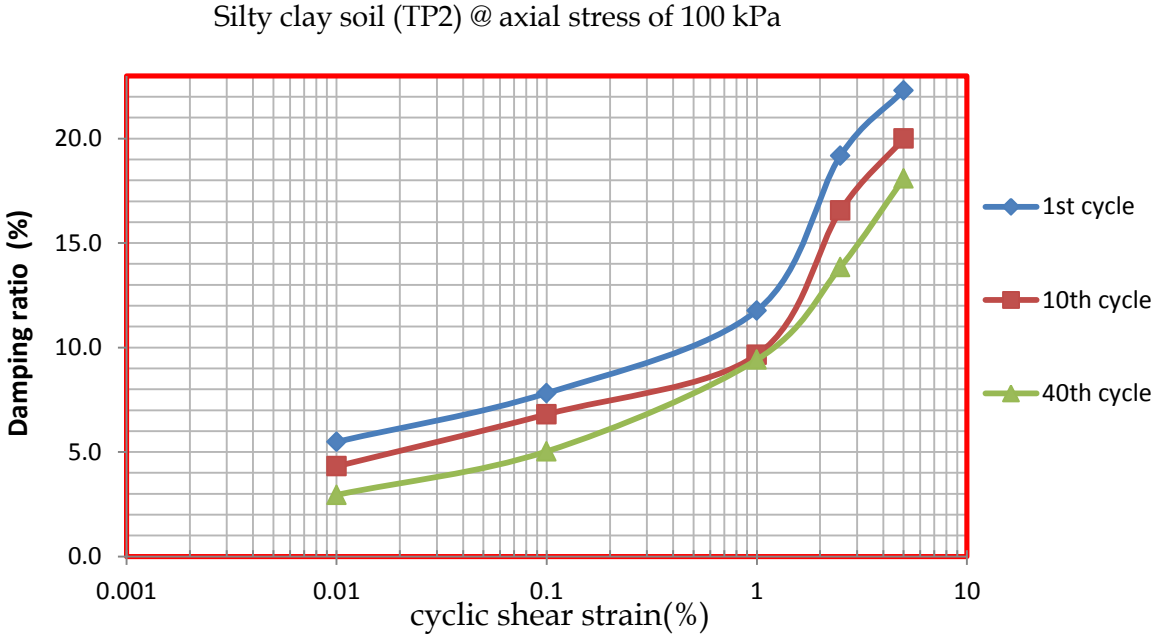

Figure D- 4: Effects of number of cyclic loading cycles on the value of damping ratio

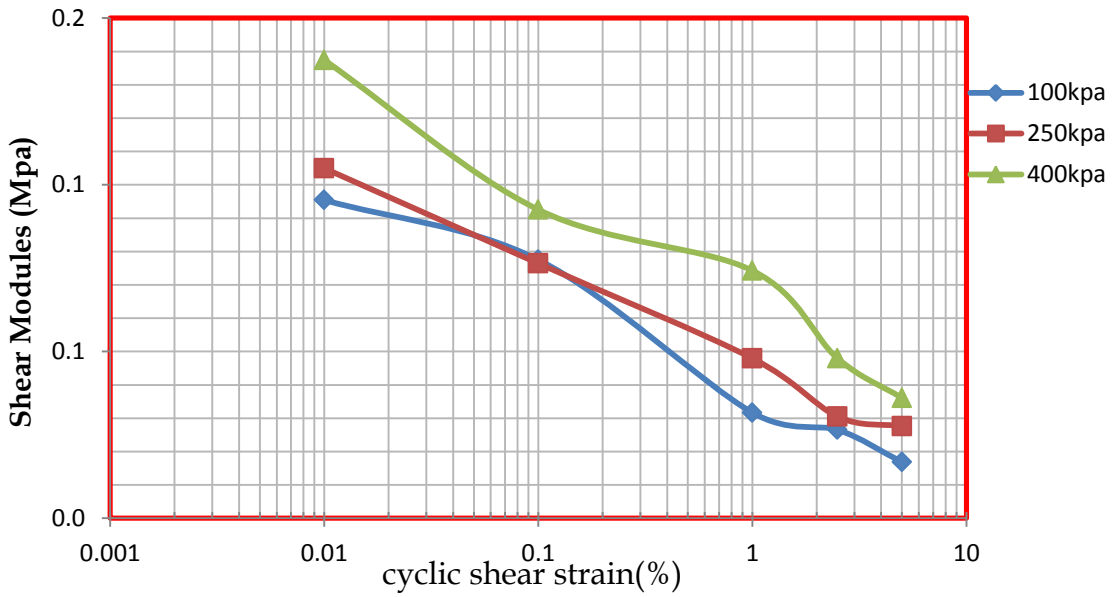

Figure D- 5: Effect of axial stress on normalized shear modulus (G/Gmax)

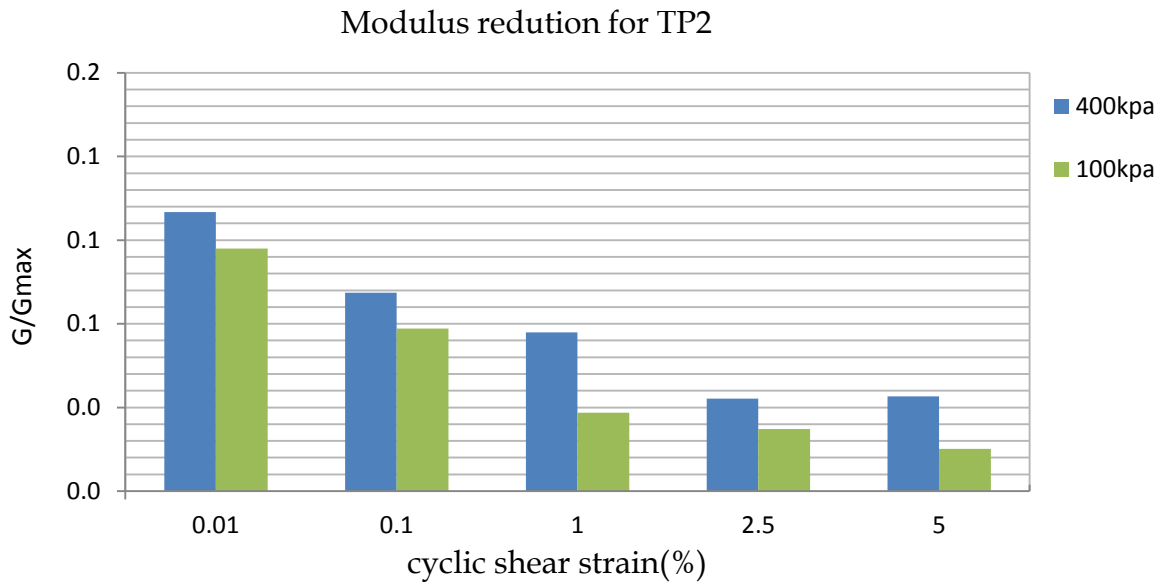

Figure D- 6: Effect of axial stress on normalized shear modulus (G/Gmax)

c